THE DISTRIBUTION AND SPECIATION OF IRON IN THE NORTHEAST SUBARCTIC PACIFIC

by

Marina Chong
B.Sc., University of British Columbia, 2003

A Thesis Submitted in Partial Fulfillment of the
Requirements for the Degree of

MASTER OF SCIENCE

in the School of Earth and Ocean Sciences

SUPERVISORY COMMITTEE

The Distribution and Speciation of Iron in the Northeast Subarctic Pacific

by

Marina Chong
B.Sc., University of British Columbia, 2003

Supervisory Committee

Supervisor

Dr. Jay T. Cullen
Departmental Member

Dr. Tom F. Pedersen
Departmental Member

Dr. Kevin Telmer
Outside Member

Dr. Alexander G. Brolo

Supervisory Committee

Supervisor

Dr. Jay T. Cullen

Departmental Member

Dr. Tom F. Pedersen

Departmental Memberr

Dr. Kevin Telmer

Outside Member

Dr. Alexander G. Brolo

ABSTRACT

The marine chemistry of dissolved iron (Fe) was examined in two studies conducted off the coast of British Columbia in the northeast Pacific. Dissolved (<0.4 μm) Fe was measured along inshore-offshore transects across the continental shelf in Queen Charlotte Sound. A benthic layer of high Fe, enriched due to exchange with shelf sediments, was found to extend across the shelf-slope break into offshore waters. Advection of these shelf waters may be a significant source of Fe to the nearby Fe-poor region of the northeast Pacific.

In this Fe-limited gyre, little is known about the chemical speciation and bioavailability of Fe. The fractionation of dissolved Fe into inorganic and organically bound species along Line P was established by competitive ligand equilibration coupled with cathodic stripping voltammetry (CLE-CSV), and the results confirm the presence of biogenic Fe-binding ligands at concentrations in excess of dissolved Fe with conditional stability constants between 8.3×10^{10} and 5.6×10^{12} for the Fe-ligand complexes. The temporal and spatial variations observed are consistent with either a biological source of

the ligands or an atmospheric source where greatest deposition occurs during the summer when stratification of the upper water column is most pronounced.

TABLE OF CONTENTS

Supervisory committee.....ii

Abstract.....iii-iv

Table of Contents.....v-viii

List of Figures.....ix

List of Tables.....x

Acknowledgements.....xi

1.0 CHAPTER 1. Introduction.....1-11

1.1 Iron in the marine environment.....2-4

1.2 The Iron Hypothesis and iron's role in biological productivity.....4-5

1.3 Advances in understanding the marine chemistry of iron and the major questions.....5-7

1.4 Thesis objective.....7-8

1.5 References.....9-11

2.0 CHAPTER 2. The Distribution of Dissolved Iron in Coastal Shelf and Slope Waters in Queen Charlotte Sound.....12-59

2.1.0 Abstract.....13

2.2.0 Introduction.....13-19

2.3.0 Methods.....20-24

2.3.1 *Study Site*.....20

2.3.2 *Sampling protocol*.....20-22

2.3.3 *Reagents*.....22-23

2.3.4 *Experimental methods*.....23-24

2.4.0 Results.....24-34

2.4.1 *Physical and nutrient data*.....24

2.4.2 *Dissolved (>0.4 μm) Fe profiles*.....25-34

2.5.0 Discussion.....34-51

2.5.1 *Vertical profiles*.....35-40

2.5.2 *Effect of the continental shelf*.....40-43

2.5.3 *Tidal currents in Queen Charlotte Sound*.....43-45

2.5.4 *Bottom boundary layer and near-bottom Ekman transport*.....45-47

2.5.5 *Upwelling and downwelling across the continental shelf*.....48-49

2.5.6 *Haida eddy formation*.....49-51

2.6.0 Conclusions.....51-52

2.7.0 References.....53-59

3.0 CHAPTER 3. The Complexation of Dissolved Iron by Organic Ligands along Line P in the Subarctic Northeast Pacific.....60-100

3.1.0 Abstract.....61

3.2.0 Introduction.....61-66

3.3.0 Methods.....66-71

3.3.1 *Sampling*.....66-67

3.3.2 *Instrumentation*.....67-68

3.3.3 *Reagents*.....68-69

3.3.4 *Titration of naturally occurring ligands*.....69-70

3.3.5 *Total dissolved Fe analysis*.....70-71

3.4.0 Results.....71-87

3.4.1 *Nutrient, chlorophyll, and CTD data*.....71-72

3.4.2 *Total dissolved iron (winter)*.....72-75

3.4.3 *Total dissolved iron (summer)*.....75

3.4.4 *CLE-CSV Theory*.....75-78

3.4.5 *Calibration of TAC*.....78-79

3.4.6 *Treatment of data*.....81

3.4.7 *CLE-CSV data*.....81-87

3.5.0 Discussion.....87-95

3.5.1 *Iron limitation in the oceans*.....87-90

3.5.2 *Results of CLE titrations*.....90-93

3.5.3 *Biological availability of iron along Line P*.....93-94

3.5.4 *Sources and sinks of naturally occurring ligands*.....94-95

3.6.0 Conclusions.....95-96

3.7.0 References.....97-100

4.0 CHAPTER 4. Concluding Remarks.....101-106

4.1 *Distribution of iron in Queen Charlotte Sound*.....102-103

4.2 *Iron speciation along Line P*.....103-104

4.3 *Future work*.....104-105

4.4 *References*.....106

APPENDICES

Appendix A. Line P nutrient data.....107-110

Appendix B. Titration data.....111-117

LIST OF FIGURES

Maps

Fig. 1 Geography of Queen Charlotte Sound.....17

Fig. 10 Map of Line P stations in the northeast Pacific.....65

Figures

Fig. 2 Water column profiles from station MB4.....26

Fig. 3 Water column profiles from station MB2.....27

Fig. 4 Water column profiles from station SS5.....28

Fig. 5 Water column profiles from station SS3.....29

Fig. 6 Water column profiles from station SS2.5.....30

Fig. 7 Water column profiles from station G4.....31

Fig. 8 Water column profiles from station G6.....32

Fig. 9 Dissolved iron profiles plotted against σ_T 37-39

Fig. 11 Chlorophyll concentrations along Line P.....73

Fig. 12 Total dissolved iron profiles along Line P (winter).....74

Fig. 13 Total dissolved iron profiles along Line P (summer).....76

Fig. 14 TAC calibration titration curve.....80

Fig. 15 Examples of typical CLE-CSV titration curve and transformations.....84

Fig. 16 Plots of L_T, NO_3, and Fe along Line P in summer and winter.....88-89

Fig. 17 Ratios of FeL to Fe′ along Line P.....92

LIST OF TABLES

Table 1 List of sampling locations in Queen Charlotte Sound.....21

Table 2 Total dissolved iron concentrations in Queen Charlotte Sound.....33

Table 3 CLE data from Line P.....82

Table 4 Titration data from 20 m at station P26.....83

Table 5 Organically bound and inorganic iron concentrations along Line P.....85

ACKNOWLEDGEMENTS

I would like to first thank my advisor, Jay Cullen, for his patience, guidance, and advice through all the challenges of both electrochemistry and setting up a new laboratory, and most of all I am grateful to him for being a wonderful teacher. I would also like to acknowledge: Keith Johnson and Nes Sutherland at IOS for their iron data, Debby Ianson for her input regarding physical process in Queen Charlotte Sound, the scientists, officers, and crew aboard the C.C.G.S. J.P. Tully, Kristina Brown for all her help and for being a great labmate, and an additional thanks to Keith Johnson for all his help in preparing for the Line P cruises without which these excursions would not have been nearly as successful. Ultimately, my experience as a graduate student would not have been possible without the love and encouragement from my parents whose support and confidence in me has been the greatest motivation and has allowed me to come this far. Finally, I am deeply grateful to Dennis Kramer for his enduring patience, his willingness to listen and give advice, and for all his empathy and support.

1.0 CHAPTER 1

Introduction

1.1 Iron in the marine environment

In spite of its abundance on land, the availability of iron (Fe) is severely limited in the oceans due to its complex chemistry in seawater. Iron is found in either the Fe(II) or Fe(III) redox state, the latter being the predominant form in seawater due to the presence of oxygen while reduced Fe (Fe(II)) is only found at comparable levels under suboxic or anoxic conditions. Iron has a tendency to form insoluble hydrolysis complexes in seawater and to become scavenged by particulate matter. Both processes result in operationally defined dissolved concentrations (passing through a 0.4 μm filter) of Fe that are at the picomolar level in open ocean surface waters. Another consequence of the reactive nature of Fe is a short residence time in seawater, estimated to be about 70-140 years (Bruland et al., 1994) compared to average ocean mixing times on the order of 10^3 years. This residence time is on the same order of magnitude as other reactive trace metals, like aluminum (Bruland et al., 1994), but despite similarities in their inorganic marine chemistry, the distribution of Fe between oceanic basins is very different from those of other particle-reactive elements (Johnson et al., 1997) because of its role as an essential micronutrient and its coordination chemistry with strong organic ligands.

In both terrestrial and marine plants, Fe is a necessary component for processes such as photosynthesis, respiration, and nitrogen fixation (Butler, 1998). Consequently, its typical vertical profile in the oceans resembles that of major algal nutrients. As stated earlier, dissolved Fe within the mixed layer, is found at very low levels, typically less than 0.1 nM in large open ocean gyres (Nishioka et al., 2001) and as a result, it is a challenge for phytoplankton to acquire sufficient Fe to accommodate their metabolic needs. Below the upper mixed layer of the water column where photosynthetic

organisms typically reside, remineralization of organic matter and low biological use allows for a significant increase in dissolved Fe. In regions of the ocean where upwelling occurs, these Fe-rich deep waters can provide a supply of Fe to the surface ocean.

The primary source of Fe to the open ocean is through the atmospheric transport of continental weathering products (Duce and Tindale, 1991). Duce and Tindale (1991) determined that about three times more Fe is supplied via atmospheric transport than is provided by rivers. The atmospheric transport of dust is episodic, however, and largely dependent on geography; for example, about eightfold more Fe is deposited in the northern hemisphere than the southern, as a result of there being more land north of the equator (Duce and Tindale, 1991). It was estimated by Duce and Tindale that 10-50% of the transported Fe dissolves upon deposition in the oceans but this solubility is highly variable and appears to be affected by the chemical composition of the aerosol particles. Recently, a study in Hawaiian waters presented evidence that a higher fraction of Fe is released from North Pacific aerosols compared to those that reach the North Atlantic (Boyle et al., 2004), suggesting that the geographical source and chemical reactions occurring during transport may have a role in regulating the bioavailability of Fe.

Another source of Fe to the oceans is found along continental margins, either by riverine input or by exchange with shelf sediments. Past work has shown that Fe measurements taken along transects extending from inshore to offshore waters show significant gradients in dissolved Fe (Johnson et al., 1997; Nishioka et al., 2001) with highest concentrations near the coast. The advection of these Fe-rich coastal waters into the open ocean, particularly in remote, Fe-depleted regimes, could partially alleviate the Fe-limitation experienced by native phytoplankton populations. Based on the findings of

studies in the North Pacific, it does not appear that these high coastal Fe concentrations penetrate far into the surface ocean (Johnson et al., 1997; Martin and Gordon, 1988). In near surface waters from a transect extending seaward of the central California coast, Johnson et al. (1997) calculated that dissolved Fe concentrations are reduced by about 98%, likely by particulate scavenging, over a distance of 64 km from the coast. The degree to which coastal sources affect the open ocean Fe inventory is likely limited to nearshore waters unless assisted by physical processes capable of enhancing offshore transport in Fe-rich coastal regions.

1.2 The Iron Hypothesis and iron's role in biological productivity

Much of the interest over recent years in the marine chemistry of Fe has arisen in response to John H. Martin's postulation that glacial-interglacial variations in CO_2 levels are a consequence of changes in Fe supply to the oceans (Martin, 1990). This theory, known as the Fe hypothesis, suggests that productivity in certain areas of the ocean is limited by extremely low supply of Fe. During glacial maxima, more atmospheric dust was supplied to these regions, initiating massive phytoplankton blooms and effecting a decrease in atmospheric CO_2 levels by about 80 ppm (Martin, 1990). Martin tested his theory first by performing Fe enrichment experiments on seawater from the northeast subarctic Pacific (Martin et al., 1989). This basin is characterized by excess nutrients (nitrate, phosphate, and silicate), and is recognized as a high nutrient low chlorophyll (HNLC) region. The results of bottle incubations spiked with Fe provided evidence the ambient Fe concentration was insufficient to allow phytoplankton to make use of all available macronutrients.

Several years later, a large-scale Fe enrichment experiment known as IronEx I took place in the equatorial Pacific Ocean, another HNLC area, where Fe was added to a 64 km^2 patch of water (Martin et al., 1994). In response to the fertilization, chlorophyll and productivity rates were both found to increase by 3-4 fold. Since then, several Fe fertilization projects have been implemented, including IronEx II, a follow up to Martin's work in the equatorial Pacific (Coale, 1996), SOIREE (Boyd et al., 2000) in the Southern Ocean, and SEEDS (Tsuda et al., 2003) in the subarctic northwest Pacific. It is evident that Fe has a significant role in regulating primary productivity and is closely tied to the cycling of both nitrate and carbon in the oceans.

1.3 Advances in understanding the marine chemistry of iron and the major questions

Much of what is known about Fe cycling to date is based upon studies conducted in the open ocean. It is in these waters that many of the questions about Fe have evolved, along with a realization that there are many regions in the world where Fe needs to be quantified in order to provide a complete picture of the global oceanic Fe budget. In particular, there is little data about Fe concentrations and distribution in coastal waters. In recent years, more attention has been addressed to the role of the continental margin in regulating coastal productivity and potential offshore transport of Fe, primarily in the Oregon and California upwelling regions (Bruland et al., 2001; Chase et al., 2005a; Elrod et al., 2004; Johnson et al., 1999). There is still little known about the influence of coastal Fe distribution on areas where there is limited atmospheric Fe deposition, such as the HNLC subarctic northeast Pacific.

Besides the current limits we have on understanding the distribution of Fe, there are still many questions about the chemistry of Fe in seawater. As mentioned earlier, Fe demonstrates a vertical profile characteristic of nutrients but does not show the inter-ocean fractionation that is observed in nitrate (Johnson et al., 1997). Based on the generalized "conveyer-belt" circulation of the world's ocean, nutrients are expected to accumulate in deep waters of the North Pacific, resulting in higher concentrations in the North Pacific compared to the North Atlantic, but the compilation of measurements from both the Pacific and Atlantic by Johnson et al. (1997) demonstrates a relatively constant deep water Fe concentration between the major oceanic basins. This is explained as either a consequence of limitations on Fe solubility in seawater or an effect of the presence of organic Fe-binding ligands that prevent the scavenging of dissolved Fe by particulate matter at concentrations less than 0.6 nM. Although there have been arguments against these ideas (Boyle, 1997), there have been several studies whose findings support the existence of natural chelators in seawater (Gledhill and van den Berg, 1994; Powell and Donat, 2001; Rue and Bruland, 1995; van den Berg, 1995; Witter et al., 2000; Wu and Luther III, 1995).

These studies all present evidence that there are organic ligands in seawater which bind Fe strongly and are always present in excess of the dissolved Fe concentration. These ligands may be similar to high affinity Fe chelators called siderophores which are produced by heterotrophic marine bacteria in order to increase the solubility of Fe (Gledhill et al., 2004; Tortell et al., 1996). There is only a small amount of data about the distribution of naturally occurring organic chelators as well as their structure and chemical properties. Additional research is needed to understand how they are produced,

the mechanisms involved in their uptake and which species are able to acquire organically complexed Fe.

1.4 Thesis objective

The studies presented in this thesis were motivated by a need to constrain the distribution of Fe in a coastal zone adjacent to an HNLC region and to explore variations in Fe speciation along a transect extending from inshore to offshore waters. The subarctic northeast Pacific was a natural choice for a study area as research cruises along the Line P transect conveniently set sail from Sidney, here on Vancouver Island, 3-4 times a year. As well, a cruise took place in August of 2004 to explore properties in Queen Charlotte Sound, off the northern tip of Vancouver Island.

In Chapter 2 of this thesis, dissolved Fe profiles are presented, the results of a study of the continental shelf region west of southern British Columbia. The goal of this project was to examine Fe levels within Queen Charlotte Sound, to assess the significance of shelf sediments as a source of Fe, and to estimate how these high dissolved Fe waters might be transported across the shelf slope. This area is of particular interest, not only due to its proximity to the HNLC northeast Pacific, but also because of its capacity for generating large scale eddies, known as Haida eddies, which have been found to carry significant amounts of coastal waters, and hence, dissolved Fe, into the Alaskan gyre (Crawford et al., 2002; Johnson et al., 2004).

Chapter 3 is an investigation into the organic complexation of dissolved Fe in the subarctic northeast Pacific. Since 1949, observations from the Line P transect, have served to provide one of the few sets of oceanographic time series measurements in the

world. As well, this line, extending from the west coast of Vancouver Island out to Ocean Station P, was the site for the WOCE and Canadian JGOFS program. Published literature on Fe analysis along Line P is very limited, however, and our study represents the first data set that establishes the presence of naturally occurring Fe chelators in this region. Variations in the thermodynamic properties and concentrations of the ligands with changes in ambient dissolved Fe levels are examined, as well seasonal changes in the marine chemistry of Fe at Station P.

1.5 References

Boyd, P.W. et al., 2000. A mesoscale phytoplankton bloom in the polar Southern Ocean stimulated by iron fertilization. Nature, 407: 695-702.

Boyle, E., 1997. What controls dissolved iron concentrations in the world ocean? -a comment. Marine Chemistry, 57: 163-167.

Boyle, E.A., Bergquist, B.A., Kayser, R.A. and Mahowald, N., 2004. Iron, manganese, and lead at Hawaii Ocean Time-series station ALOHA: Temporal variability and an intermediate water hydrothermal plume. Geochimica et Cosmochimica Acta, 69(4): 933-952.

Bruland, K.W., Orians, K.J. and Cowen, J., 1994. Reactive trace metals in the stratified central North Pacific. Geochimica et Cosmochimica Acta, 58: 3171-3182.

Bruland, K.W., Rue, E.L. and Smith, G.J., 2001. Iron and macronutrients in California coastal upwellling regimes: Implications for diatom blooms. Limnology and Oceanography, 46(7): 1661-1674.

Butler, A., 1998. Acquisition and utilization of transition metal ions by marine organisms. Science, 281: 207-210.

Chase, Z., Hales, B. and Cowles, T., 2005. Distribution and variability of iron input to Oregon coastal waters during the upwelling season. Journal of Geophysical Research, 110(C10S12).

Coale, K.H., et al., 1996. A massive phytoplankton bloom induced by an ecosystem-scale iron fertilization experiment in the equatorial Pacific Ocean. Nature, 383: 495-501.

Crawford, W.R., Cherniawsky, J.Y., Foreman, G.G. and Fower, J.F.R., 2002. Formation of the Haida-1998 oceanic eddy. Journal of Geophysical Research, 107(C7): 3069.

Duce, R.A. and Tindale, N.W., 1991. Atmospheric transport of iron and its deposition in the ocean. Limnology and Oceanography, 36(8): 1715-1726.

Elrod, V.A., Berelson, W.M., Coale, K. and Johnson, K.S., 2004. The flux of iron from continental shelf sediments: A missing source for global budgets. Geophysical Research Letters, 31(L12307).

Gledhill, M. et al., 2004. Production of siderophore type chelates by mixed bacterioplankton populations in nutrient enriched seawater incubations. Marine Chemistry, 88: 75-83.

Gledhill, M. and van den Berg, C.M.G., 1994. Determination of complexation of iron(III) with natural organic complexing ligands in seawater using cathodic stripping voltammetry. Marine Chemistry, 47: 41-54.

Johnson, K.S., Chavez, F.P. and Friederich, G.E., 1999. Continental-shelf sediment as a primary source of iron for coastal phytoplankton. Nature, 398: 697-700.

Johnson, K.S., Gordon, R.M. and Coale, K.H., 1997. What controls dissolved iron concentrations in the world ocean? Marine Chemistry, 57: 137-161.

Johnson, W.K., Miller, L.A., Sutherland, N.E. and Wong, C.S., 2004. Iron transport by mesoscale Haida eddies in the Gulf of Alaska. Deep-Sea Research Part II, 52(7-8): 933-953.

Martin, J.H., 1990. Glacial-interglacial CO2 change: The iron hypothesis. Paleoceanography, 5(1): 1-13.

Martin, J.H. et al., 1994. Testing the iron hypothesis in ecosystems of the equatorial Pacific Ocean. Nature, 371: 123-129.

Martin, J.H., Gordon, R.M., Fitzwater, S. and Broenkow, W.W., 1989. VERTEX: phytoplankton/iron studies in the Gulf of Alaska. Deep-Sea Research, 36(5): 649-680.

Nishioka, J., Takeda, S., Wong, C.S. and Johnson, W.K., 2001. Size-fractionated iron concentrations in the northeast Pacific Ocean: distribution of soluble and small colloidal iron. Marine Chemistry, 74: 157-179.

Powell, R.T. and Donat, J.R., 2001. Organic complexation and speciation of iron in the South and Equatorial Atlantic. Deep-Sea Research II, 48: 2877-2893.

Rue, E.L. and Bruland, K.W., 1995. Complexation of iron(III) by natural organic ligands in the Central North Pacific as determined by a new competitive ligand equiligration/adsorptive cathodic stripping voltammetric method. Marine Chemistry, 50: 117-138.

Tortell, P.D., Maldonado, M.T. and Price, N.M., 1996. The role of heterotrophic bacteria in iron-limited ocean ecosystems. Nature, 383: 330-332.

Tsuda, A. et al., 2003. A mesoscale iron enrichment in the western subarctic Pacific induces a large centric diatom bloom. Science, 300: 958-961.

van den Berg, C.M.G., 1995. Evidence for organic complexation of iron in seawater. Marine Chemistry, 50: 139-157.

Witter, A.E., Lewis, B.L. and Luther, G.W.I., 2000. Iron speciation in the Arabian Sea. Deep-Sea Research II, 47: 1517-1539.

Wu, J. and Luther III, G.W., 1995. Complexation of Fe(III) by natural organic ligands in the Northwest Atlantic Ocean by a competitive ligand equilibration method and a kinetic approach. Marine Chemistry, 50: 159-177.

2.0 CHAPTER 2

The Distribution of Dissolved Fe in Coastal Shelf and Slope Waters in Queen Charlotte Sound

2.1.0 Abstract

The distribution of total dissolved (<0.4 μm) iron (Fe) across the continental slope of Queen Charlotte Sound was examined as a means of assessing the potential of these waters as a source of Fe to the Fe-limited waters of the subarctic northeast Pacific. Iron profiles, obtained in shelf, slope, and offshore waters demonstrate decreasing concentrations of Fe with distance from the continent as well as the presence of an Fe-rich benthic boundary layer which penetrates across the shelf-slope break. Four different physical mechanisms that may aid in the cross-shelf advection of these Fe-replete waters are considered: tidal currents, Ekman transport of the bottom boundary layer, coastal upwelling/downwelling, and the formation of Haida eddies.

2.2.0 Introduction

Iron (Fe) is an essential micronutrient for all living organisms owing largely to the importance of Fe and Fe-sulfur proteins in photosynthetic and respiratory electron transfer reactions (Oda et al., 2005). In oxygenated seawater Fe is only sparingly soluble (0.2 nM at pH 8.1) (Millero, 1998) and its low concentration in surface waters of remote, high nutrient-low chlorophyll (HNLC) regions limits photosynthetic carbon fixation and nutrient utilization by resident phytoplankton (de Baar et al., 2005) and the carbon use efficiencies of heterotrophic marine bacteria (Tortell et al., 1996). As a consequence of its regulatory role on primary productivity in the open ocean, the marine cycling of Fe is closely linked to that of carbon and nitrogen.

The vertical and horizontal distribution of Fe in seawater is regulated by the balance between input and removal processes and underlying biological, chemical and

physical transformations of Fe species in the ocean's interior (Johnson et al., 1997). There exists a pronounced onshore-offshore gradient in surface water dissolved Fe concentrations, with dissolvable Fe concentrations 1-2 orders of magnitude greater nearshore (Johnson et al., 1999) that is driven primarily by the proximity of coastal waters to terrestrial, fluvial and sedimentary Fe sources. This gradient is enhanced in regions where Fe-rich deep waters are brought up to the surface, further contributing to the high productivity often observed at the continental margins.

In the northeast Pacific, several studies have been conducted over recent years that have investigated the distribution of Fe in coastal regimes. Seasonal upwelling events in coastal waters off central California occur during the spring season, resulting in a large pulse of Fe into surface waters (Johnson et al., 2001). Consequently, in the following months, low Fe levels and excess nitrate were observed at the offshore stations which contrasted with the high Fe and low nitrate found at the inshore station. Fe availability was observed to affect phytoplankton community structure with diatoms dominating in Fe-rich upwelling waters and picoplankton dominating in low-Fe waters. The relationships between Fe and the biological parameters measured by Johnson et al. (2001) illustrate the importance of Fe in controlling productivity and species composition of the microbial communities in dynamic, coastal upwelling environments.

Although coastal upwelling zones are normally highly productive regions, phytoplankton off central California are observed to experience varying degrees of Fe limitation (Hutchins et al., 1998). Variability in seawater Fe concentrations and the degree of phytoplankton community Fe stress reflects the heterogeneity in fluvial Fe inputs along the central California coastline. In addition, the width of the continental

shelf plays large part in dictating the supply of Fe to overlying waters. The Monterey Bay region of central California experiences significant riverine input compared to other regions of the central coast, flowing into waters over a continental shelf that extends 20 to 50 km offshore (Bruland et al., 2001). In contrast, the Big Sur coastline south of Monterey Bay has negligible freshwater input from rivers and the continental shelf in this region is only a few kilometers wide. Bruland et al. (2001) demonstrated Fe-replete conditions supporting large diatom biomass off Monterey Bay but observed excess macronutrients and low Fe concentrations along with low diatom abundance off the Big Sur coastline. A broad shelf has the effect of "trapping" sediments during periods of high fluvial outflow which then undergo resuspension during upwelling events, significantly enriching coastal waters during the spring season when upwelling is most intense. In contrast, where continental shelves are narrow, Fe-limitation can sometimes be observed when Fe-deplete subsurface waters experience only limited contact with Fe-rich sediments before shoaling near the coast.

Along the Oregon coast, shelf sediments and discharge from the Columbia River are the two main sources of Fe to the nearshore waters (Chase et al., 2002). Chase et al. (2002) found that there are multiple physical processes involved in introducing terrestrially derived Fe into nearby waters and these processes ultimately control the distribution of phytoplankton. One such process is the interaction between the river plume and tidal flow within the Columbia River estuary. Measurements of river water revealed that the Columbia River contains relatively low levels of Fe (14-30 nM) in comparison to other large rivers (Lohan and Bruland, 2005). In the river plume, however, dissolved Fe and especially nitrate concentrations were elevated during flood

tide, resulting from entrainment of nutrient-rich subsurface waters, and dropped off significantly during ebb tide. The change in chemical characteristics of the river plume according to tidal cycle also regulated phytoplankton biomass as shown by chlorophyll *a* distribution which were lower during flood tide and increased an order of magnitude on the ebb. These different factors regulating Fe supply to nearshore waters off California and Oregon demonstrate the importance of bathymetry, freshwater input of particulate matter, and physical forcing in maintaining the elevated concentrations of Fe observed at ocean margins.

Mechanisms that can lead to transport of these Fe-rich coastal waters to the ocean interior are only poorly understood. In this study we investigated dissolved Fe distributions in the shelf and slope waters of Queen Charlotte Sound in the subarctic northeast Pacific (Fig.1). The continental shelf here is extensive, ranging from 100-150 km (Fig. 1), and there are three deep troughs of glacial origin extending seaward across the shelf. This region is particularly interesting given its proximity to the HNLC Gulf of Alaska, where excess nutrients, low surface Fe concentrations, and Fe-limited phytoplankton communities have been observed (Martin et al., 1989). To what degree Fe-rich waters from the Sound might contribute to the Fe inventory of the HNLC basin and thereby help to alleviate the chronic Fe-limitation of phytoplankton growth in the basin is as yet unknown.

A recently discovered transport mechanism important to the northeast Pacific is the formation of westward moving anticyclonic coastal eddies. Called Haida eddies after the nearby Haida Gwaii, they form off the southern tip of the Queen Charlotte Islands in late winter and track westward into the subarctic northeast Pacific

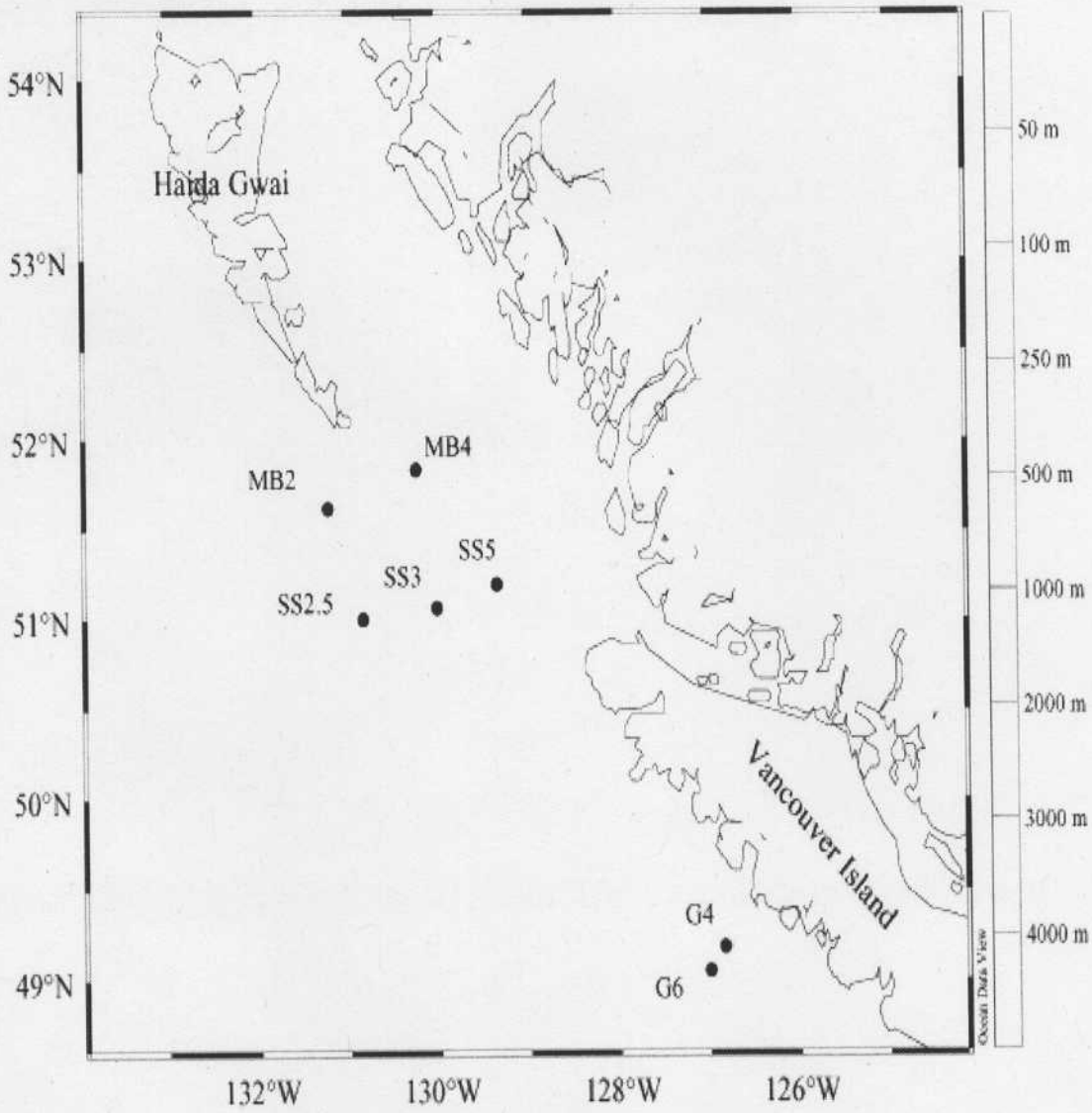

Figure 1. Map of Queen Charlotte Sound and stations.

(Crawford et al., 2002). Haida eddies are detectable by unusually high sea surface height via satellite altimetry. Recent work has found that these eddies transport from 3000 to 6000 km^3 of water up to 1000 km west into the Gulf of Alaska, where iron limitation of primary productivity occurs (Whitney and Robert, 2002). In the first study detailed study of the biogeochemistry of these eddies, a Haida eddy that formed in the winter of 2000 was followed for 20 months and sampled repeatedly for nutrient dynamics (Peterson et al., 2005). Dissolved Fe concentrations within the eddy were measured at levels nearly two orders of magnitude higher than what is typically observed at Ocean Station P (50°N, 145°W), a well characterized HNLC environment (Johnson et al., 2005). The Fe concentration in the eddy that was surveyed the longest decreased quickly over the first year but after 16 months still contained 1.5 to 2 times more Fe than surrounding waters (ie. 0.3 nM outside the eddy versus 0.55 nM inside the eddy at 150 m depth). Johnson et al. (2005) estimated that in the southeastern Gulf of Alaska, 5-50% of the dissolved Fe is transported to this area each year by the formation and passage of Haida eddies. This indicates that these eddies may provide a means for the HNLC northeast Pacific to be naturally fertilized on an annual basis.

The role of upwelling in supplying the open ocean with significant amounts of Fe is probably negligible in Queen Charlotte Sound. Similar to the Oregon and California coasts, upwelling begins in spring along the west coast of Vancouver Island and continues into the early fall (Bakun et al., 1974). The upwelling in this region is weak, however, compared to the California and Oregon coasts due to seasonal warming (Bakun et al., 1974). Although upwelling forces the shoaling of Fe-rich subsurface waters, the iron is quickly lost to biological uptake and particulate settling. Off the Oregon coast,

phytoplankton have been found to respond to artificial Fe additions even after a period of upwelling over a wide continental shelf (Chase et al., 2005b). In the Queen Charlotte region, the combination of relatively weak upwelling (Bakun et al., 1974) and losses to biological and chemical activity results in very low projection of Fe-replete waters beyond the shelf break.

The goal of our study was to investigate the importance of cross-shelf advection in transporting Fe rich shelf waters into the northeast subarctic Pacific. We present the first set of dissolved Fe profiles from Queen Charlotte Sound, representative of stations situated over the continental shelf, over the shelf slope, and seaward of the shelf-slope break. Sampling took place during the summer season, a time when winds are generally weak and occasionally favorable for upwelling along the coast of British Columbia. The geography of Queen Charlotte Sound allows this basin to experience physical processes that are unique and isolated from the circulation that typically occurs along an eastern boundary region. Tidal currents have been established to have a strong influence on current flow and water column turbulence over shelf areas (Bowers et al., 2005; Xing and Davies, 2002) and may be a crucial source of energy for mixing within the benthic layer in the sound. The generation of a seaward flux of this water may be accomplished through Ekman transport within the bottom boundary layer, episodes of coastal upwelling and downwelling, and, as aforementioned, the formation of westward circulating Haida eddies. A discussion of these four physical mechanisms will be given, as well as evaluations of their contributions towards establishing the observed dissolved Fe distributions obtained in this study.

2.3.0 METHODS

2.3.1 Study Site

Three onshore-offshore transects were sampled, two within Queen Charlotte Sound across the shelf break (MB and SS) and the third (G) along the west coast of Vancouver Island (Fig.1) during the period of Aug.13-19, 2004 aboard the C.C.G.S. J.P. Tully. The Middle Bank (MB) line crossed the Moresby Trough, a steep submarine canyon transecting the continental shelf. The SS line followed the Goose Island Trough, to the south of the MB line. The G line, by Estevan Point on Vancouver Island, was sampled to provide a comparison from a region with a narrow shelf.

2.3.2 Sampling protocol

Water column profiles were collected at stations MB2, MB4, SS2.5, SS3, SS5, G6, and G4 in Queen Charlotte Sound. The locations and approximate depths sampled are given in Table 1. Seawater was collected using Teflon® coated 10 or 12 L Go-Flo bottles (General Oceanics) deployed on a Kevlar line and tripped at depth with Teflon® messengers (Bruland and Franks, 1979). On board, in the ship's wet lab, the bottles were overpressured with high purity nitrogen gas. Acid-washed Teflon® tubing connected the Go-Flo bottles to in-line acid-cleaned acrylic filtration units (Geofilter®) that were contained in a Class 100 laminar flow bench. The seawater samples were filtered through acid-washed 147 mm diameter 0.4 μm polycarbonate membranes (Isopore) into 500 mL acid-cleaned low-density polyethylene bottles. The sample bottles were double-bagged, kept in the cooler through the duration of the cruise, and then acidified to pH 2 with 12 N HCl (Seastar™) upon return to the laboratory.

Table 1. List of sampling locations.

Station	Latitude	Longitude	Sampling date	Bottom depth (m)
MB2	51:26.00N	131:12.97W	8/13/2004	2200
MB4	51:49.96N	130:14.01W	8/13/2004	200
SS2.5	51:00.03N	130:50.02W	8/15/2004	2200
SS3	51:03.82N	130:00.59W	8/15/2004	1400
SS5	51:11.67N	129:20.41W	8/15/2004	280
G4	49:10.93N	126:50.06W	8/17/2004	200
G6	49:03.01N	126:59.97W	8/17/2004	900

Temperature, salinity, dissolved oxygen, and fluorescence through the water column were measured by CTD and nutrient samples were collected by a rosette and analyzed by researchers at the Institute of Ocean Sciences.

2.3.3 Reagents

Seastar™ Baseline® trace-metal pure hydrochloric acid and ammonia were used to acidify seawater samples and subsequently to raise the pH back to 8 before analysis. Milli-Q water (>18 MΩ cm) was used for all rinsing and sample preparation.

The Fe-binding ligand, 2,3-dihydroxynaphthalene (DHN) (Acros Organics) was dissolved in Milli-Q water by heating in the microwave for 10 s at a time until fully dissolved. Ammonia was added (final concentration of 1%) and then organic contaminants were removed from the solution by shaking with 5 mL of chloroform for 3 minutes. The solution was allowed to settle and separate and the DHN in the aqueous phase was extracted with a pipette into another container and cleaned with chloroform a second time. The DHN was then pipetted into a 30 mL Teflon® PFA bottle and diluted 10-15 fold (depending on concentration) with distilled methanol.

A combined catalytic oxidant and buffer solution was prepared and purified (protocol courtesy of Constant van den Berg) as follows: the 0.45 M catalytic oxidant bromate was prepared using potassium bromate (Fluka) dissolved in Milli-Q water. To remove any trace metals in the reagent, 100 μM of MnO_2 was added and the solution was stirred a minimum of two hours. The buffer, piperazine-1,4-bis(2-hydroxypropanesulfonic acid) (POPSO), was made up to 1 M in a 1 M ammonia solution (pH 8). The POPSO was cleaned with MnO_2 as well. The purified bromate was then

filtered through an acid-rinsed 0.2 μm sterile filter (Sarstedt) and an appropriate volume of POPSO was filtered and added to the solution. A final cleaning with MnO_2 was performed before the bromate/POPSO solution was used for analysis.

MnO_2 was prepared by mixing 0.02 M $KMnO_4$ with 0.03 M $MnCl_2$ and stirred while adding 0.1 M NaOH until the pH reached 7-8.5 (C. van den Berg, pers.comm.). The solution was centrifuged, the supernatant discard, and the process was repeated three times. The final precipitate was suspended in Milli-Q water at a final concentration of 0.05 M.

2.3.4 Experimental methods

Standard trace metal clean techniques were applied in performing Fe analysis by adsorptive cathodic stripping voltammetry (CSV). Total dissolved Fe concentrations were determined following a method developed by (Obata and van den Berg, 2001) using a Metrohm 663 VA stand hanging mercury drop electrode connected to a μAutolab III potentiostat. For each analysis, 10 mL of acidified seawater was pipetted into the voltammetric cell cup and ammonia was added to the sample until the pH reached 8. Then 0.2 M of the catalytic oxidant, bromate, 0.01 M POPSO to buffer the solution to pH 8, and 20 μM of the Fe-binding ligand, DHN, were added to the cell cup and the solution was purged while stirring for 3 minutes with 0.2 μm filtered high purity nitrogen gas. After deaeration, a new mercury drop was extruded and the deposition potential was held at -0.1 V while stirring for 15 to 180 s depending on the concentration of Fe in the sample to concentrate the Fe-DHN complex at the working electrode. The stirrer was then turned off and the potential was scanned from -0.1 to -0.9 V at a scan rate of 24 mV/s

using the sampled dc mode. The concentration of Fe in each sample was determined by standard additions of 0.5 to 2 nM of Fe (III). The blank was measured to be 50 pM and the detection limit, calculated as 3 times the standard deviation of the concentration in low-Fe seawater, was 25 pM based on a 60 s deposition.

2.4.0 RESULTS

2.4.1 Physical and nutrient data

Vertical profiles of temperature, salinity, dissolved oxygen, nutrients and fluorescence are given in Figs. 2(a-c) to 8(a-c). Surface waters in Queen Charlotte Sound are characterized by high chlorophyll, high oxygen, and depleted nutrients as well as warm temperatures and low salinities in comparison to values at depth (below 300m). Higher near surface temperatures and lower surface salinities are observed at stations along the southern G line. Note that surface nutrient concentrations at MB2 (Fig. 3b) are unusually high, possibly due to contamination. In general, steady increases in salinity and decreases in temperature occur through the upper 200 m and become more constant with depth below 200 m. Phytoplankton biomass, as determined by fluorescence, drops off almost to 0 immediately below 100 m at all stations. Over the shelf, the benthic layer below 180 m is nutrient-rich and depleted in oxygen while temperature and salinity remain constant as shown in Figs. 2a and 4a. At the shelf-slope break (Figs. 5a and 8a), oxygen concentrations between 180-200 m are higher in comparison to the shelf stations (Figs. 2a,4a, and 7a) and increase at these depths at the offshore stations (Figs. 3a and 6a). Nutrient levels do not exhibit significant variations across the shelf but are elevated south of Queen Charlotte Sound, along the G line (Figs.7b and 8b).

2.4.2 Dissolved (>0.4 μm) Fe profiles

Total dissolved Fe profiles are presented in Figs. 2d to 8d and the values along with calculated standard deviations, based on n=2 or 3, are given in Table 2.

MB Line

The dissolved Fe profiles (Figs.2d and 3d) along the MB line roughly resemble the typical vertical distribution of nutrients, showing some amount of depletion near the surface and increasing with depth. Dissolved Fe at MB4 was measured to be 0.43±0.05 nM on average from 10m down to 50m, exhibiting a subsurface maximum at 100m of 2.16±0.04 nM and increasing to 3.50±0.6 nM at 195 m. The concentrations throughout the MB4 profile consistently exceed the Fe levels measured at MB2. At this station, there is an average of 0.36±0.04 nM Fe in the upper 35 m of the water column which increases to 0.791±0.006 nM at 100m. Below 100m Fe concentration drops to 0.56±0.02 nM and then increases to a deep water concentration of 1.56±0.09 nM.

SS Line

From 10m down to 150m, dissolved Fe does not vary significantly at SS5, averaging 0.56±0.09 nM (Fig. 4d). Similar to the MB4 profile, a dramatic increase in concentration takes place through the bottom 100m of the sampled water column, resulting in 5.3±0.3 nM of Fe at 250m depth. Surface concentrations down to 75m at SS3 (Fig. 5d) are lower than at SS5, varying between 0.23±0.05 to 0.31±0.02 nM except at 50m where Fe drops to 0.0926±0.0008 nM. There is a maximum of 5.1±0.7 nM at

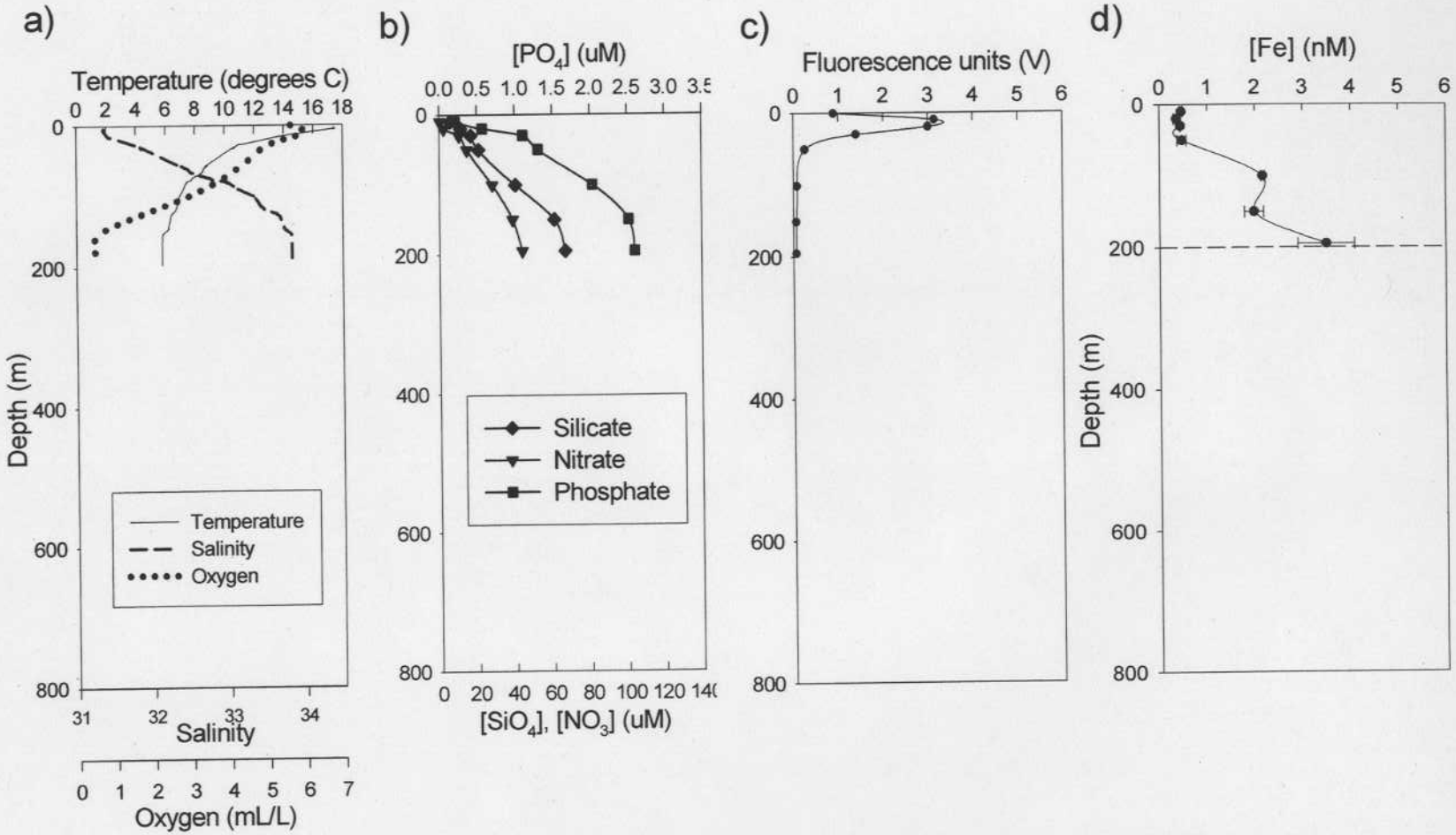

Fig. 2. Water column profiles from station MB4 (shelf station) of a) temperature, salinity, and dissolved O_2, b) dissolved nutrient concentrations, c) fluorescence as a proxy for phytoplankton biomass, and d) dissolved (<0.4μm) Fe. Dashed line indicates seafloor.

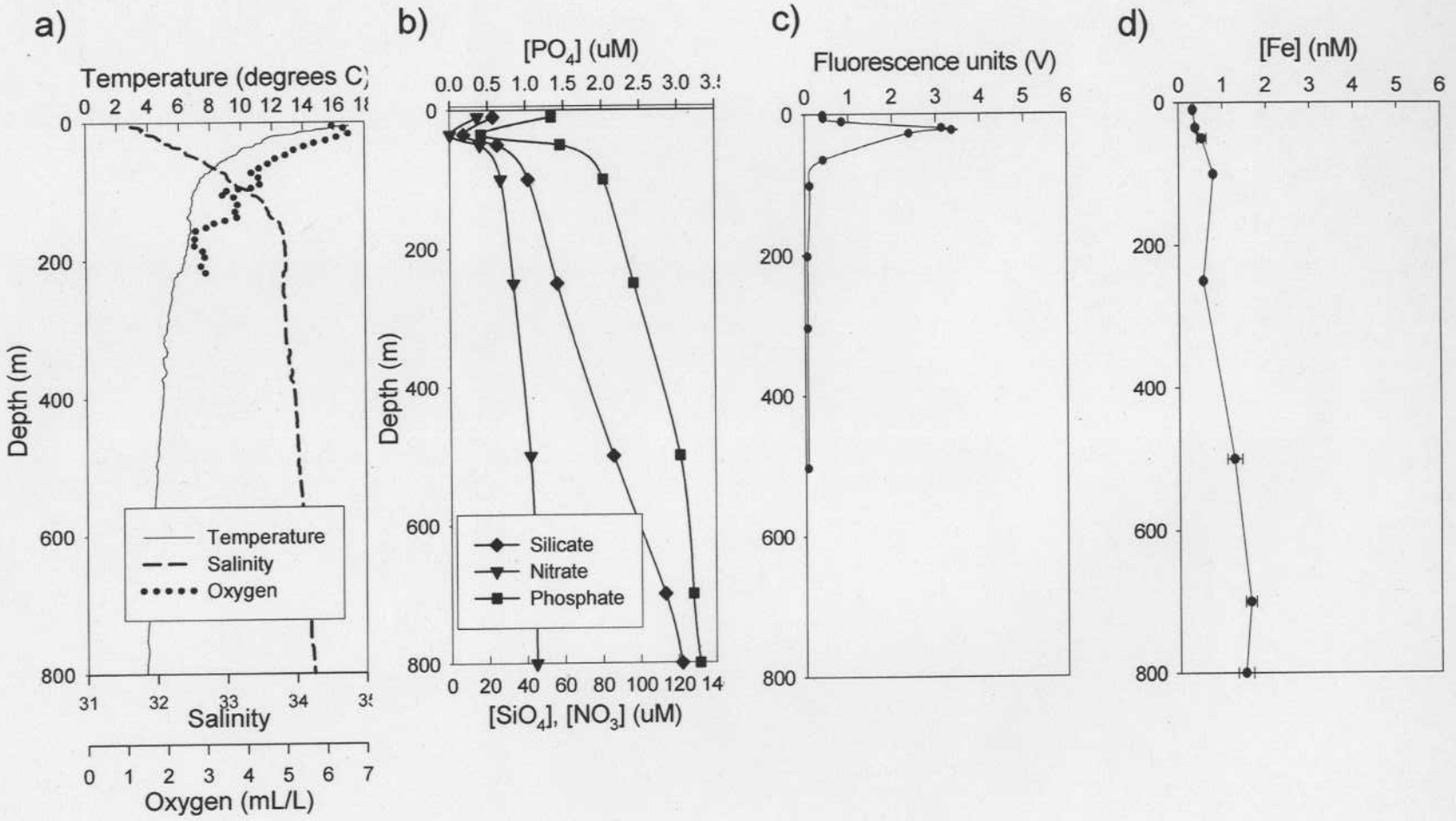

Fig. 3. Same as Fig. 2 but for station MB2 (offshore station).

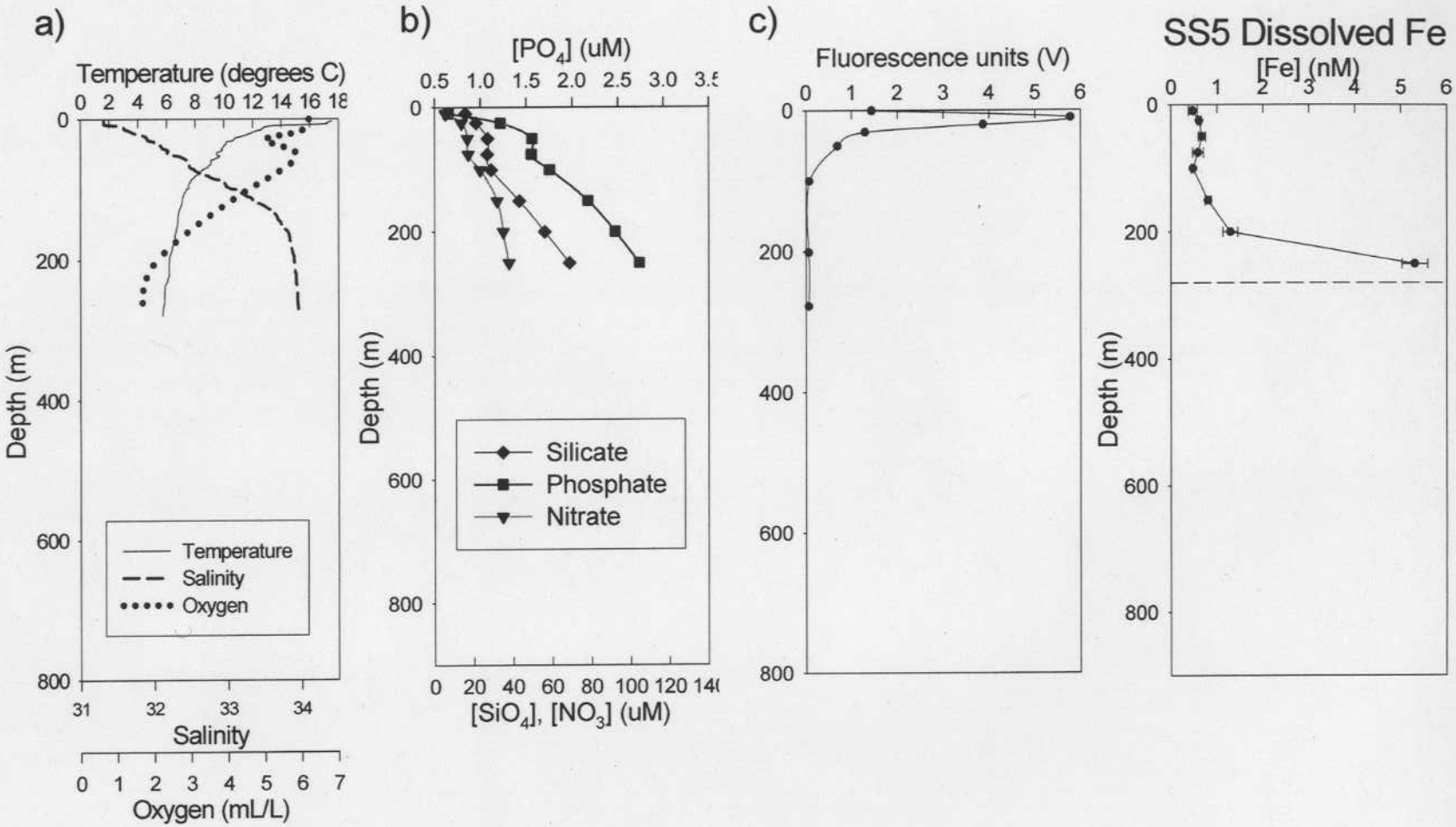

Fig. 4. Same as Fig. 2 but for station SS5 (shelf station).

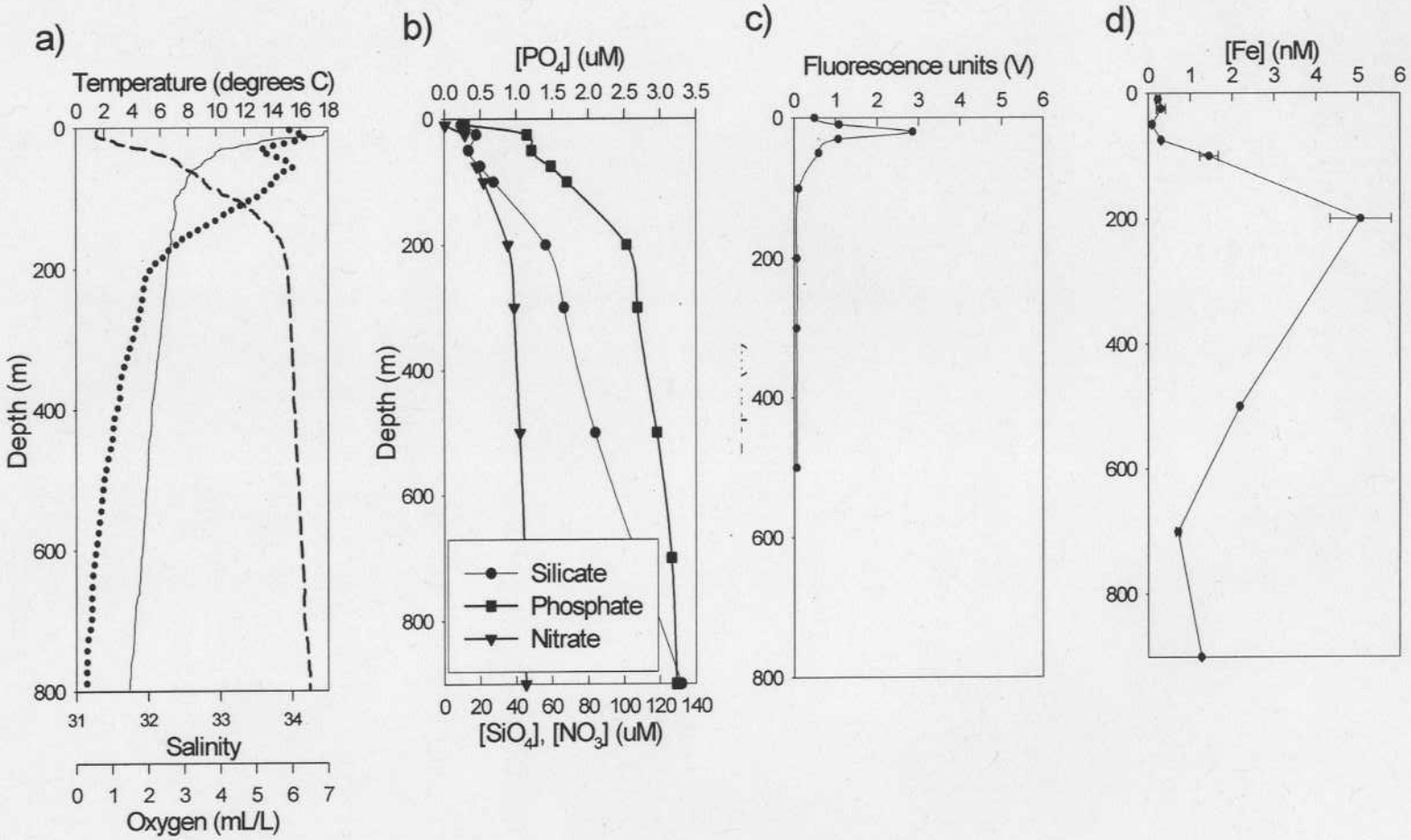

Fig. 5. Same as Fig. 2 but for station SS3 (shelf-slope station).

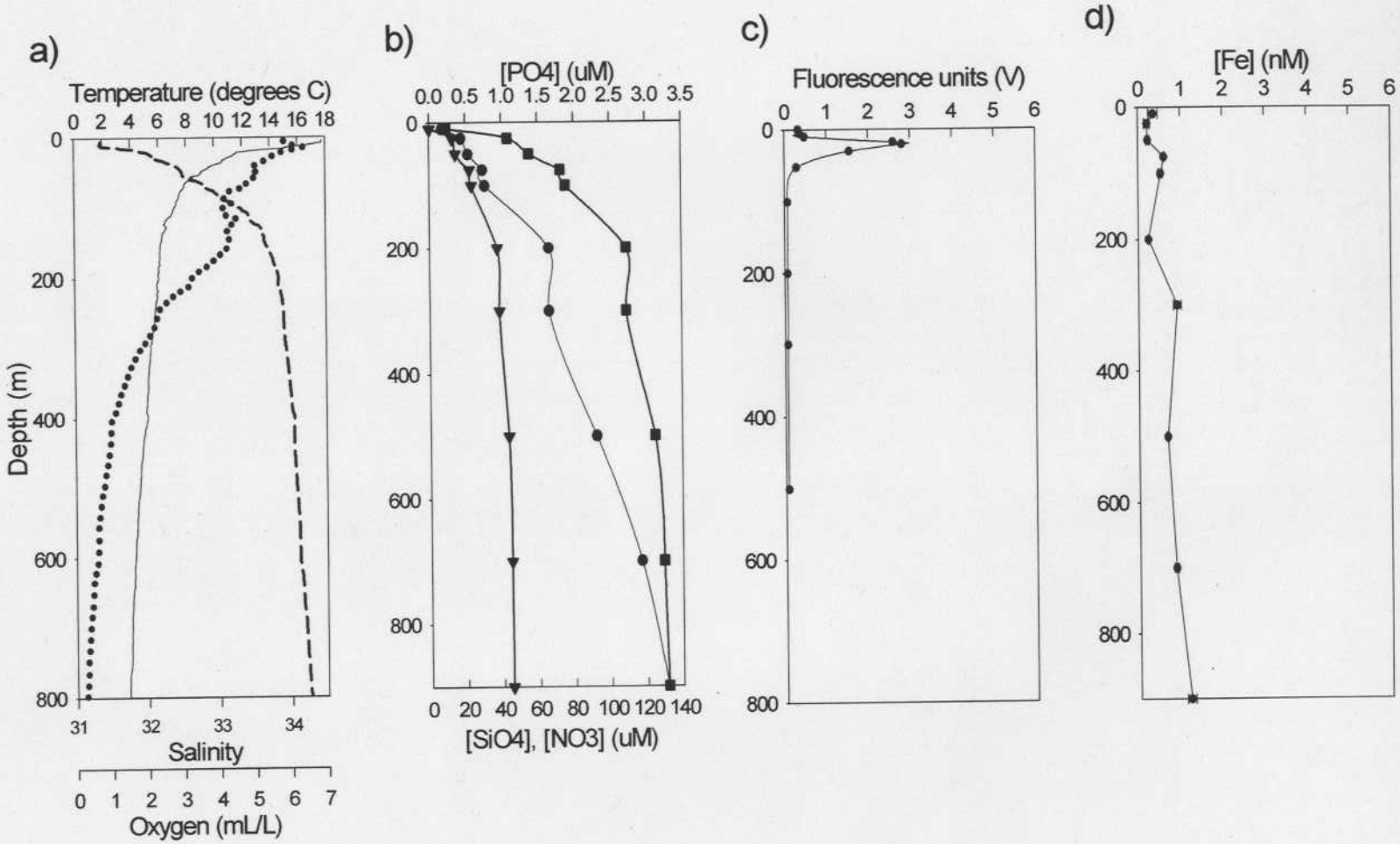

Fig. 6. Same as Fig. 2 but for station SS2.5 (offshore station).

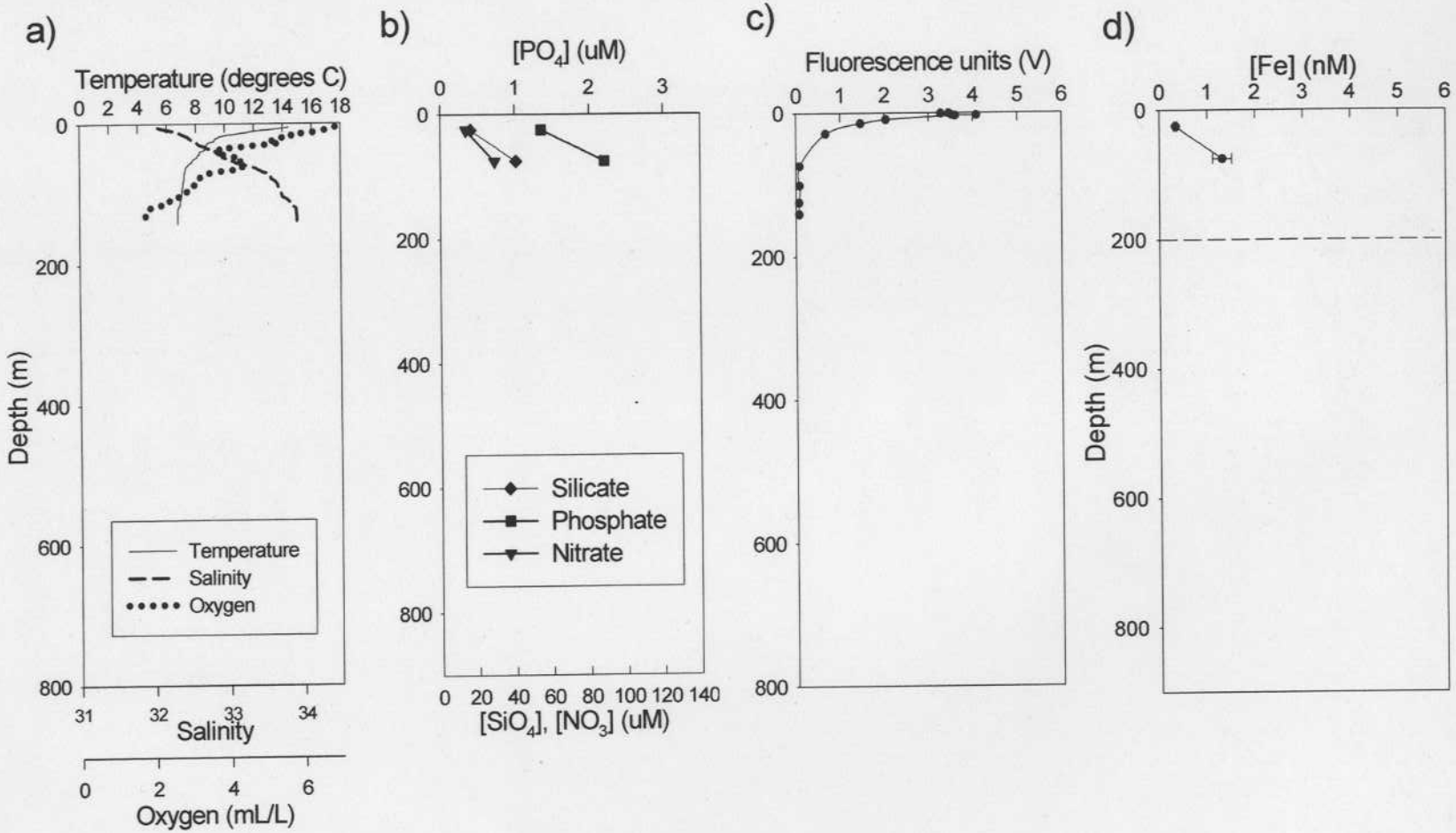

Fig. 7. Same as Fig. 2 but for station G4 (shelf station).

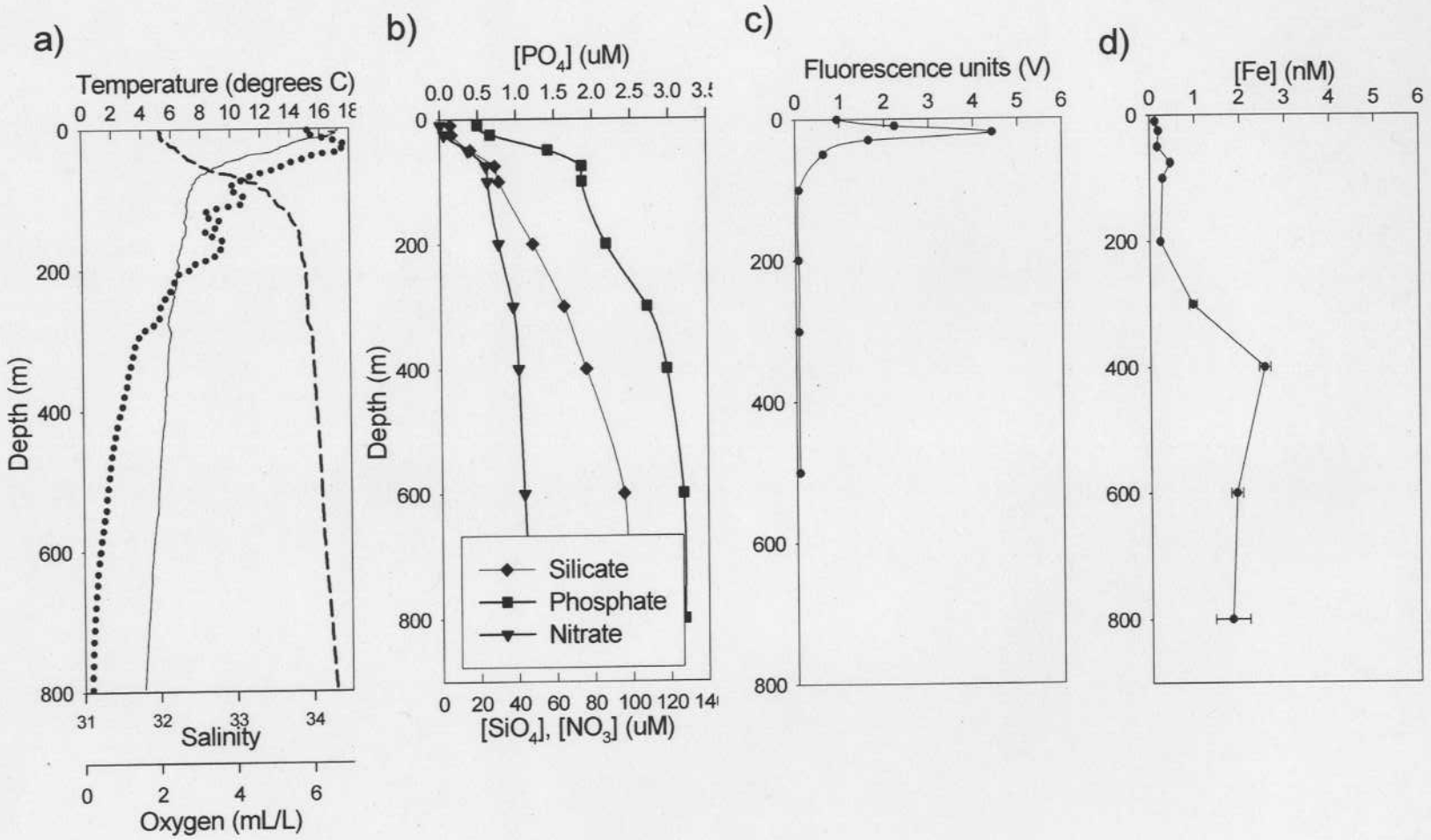

Fig. 8. Same as Fig. 2 but for station G6 (shelf-slope station).

Table 2. Total dissolved iron concentrations in Queen Charlotte Sound.

Station	Depth (m)	[Fe] (nM)	Standard deviation	Station	Depth (m)	[Fe] (nM)	Standard deviation
MB2	10	0.33	0.03	**G6**	10	0.126	0.001
	35	0.388	0.005		25	0.202	0.003
	50	0.53	0.10		50	0.18	0.01
	100	0.79	0.01		75	0.47	0.02
	250	0.56	0.02		100	0.289	0.002
	500	1.26	0.17		200	0.238	0.002
	700	1.62	0.12		300	0.96	0.09
	800	1.50	0.18		400	2.54	0.12
MB4	10	0.46	0.03		600	1.91	0.13
	20	0.36	0.06		800	1.80	0.39
	30	0.44	0.00	**G4**	25	0.34	0.03
	50	0.47	0.09		75	1.32	0.20
	100	2.16	0.04				
	150	1.98	0.20				
	195	3.50	0.59				
SS2.5	10	0.37	0.11				
	25	0.22	0.07				
	50	0.24	0.04				
	75	0.619	0.004				
	100	0.54	0.05				
	200	0.24	0.01				
	300	0.92	0.09				
	500	0.68	0.02				
	700	0.86	0.05				
	900	1.20	0.10				
SS3	10	0.23	0.05				
	25	0.31	0.10				
	50	0.093	0.001				
	75	0.31	0.02				
	100	1.45	0.22				
	200	5.07	0.74				
	500	2.20	0.01				
	700	0.71	0.06				
	900	1.275	0.004				
SS5	10	0.48	0.10				
	25	0.62	0.04				
	50	0.68	0.08				
	75	0.59	0.11				
	100	0.48	0.03				
	150	0.81	0.07				
	200	1.29	0.16				
	250	5.31	0.28				

200m, which exceeds even the deep water Fe concentration, and Fe then drops down to 2.196±0.006 nM at 500 m. Below 700m, Fe is lower, reaching 1.275±0.004 nM at the deepest sampled depth.

The dissolved Fe profile at SS2.5 (Fig. 6d) does not exhibit the same dramatic variations with depths as seen at the shelf and shelf-slope stations. Upper water column values range from 0.22±0.07 to a small subsurface maximum at 75m of 0.619±0.004 nM. Another maximum in dissolved Fe is present at 300m where the concentration reaches 0.92±0.09 nM and further down in the profile, the deep water contains 1.2±0.1 nM of Fe. The overall ranges of Fe concentrations measured at the offshore stations SS2.5 and MB2 are quite comparable.

G Line

Total dissolved Fe data are only available for 25 and 75m at station G4 (Fig. 7d). Within this interval, Fe increases rapidly, from 0.34±0.03 to 1.3±0.2 nM. The only other station to exhibit such a sharp elevation in Fe concentration within surface waters is MB4. Station G6 (Fig. 8d) also demonstrates a only a slight increase at 75m but a more substantial subsurface maximum is observed at 400m where Fe increases to 2.5±0.1 nM and drops to 1.4±0.1 nM by 800m.

2.5.0 Discussion

It is apparent from the physical and nutrient data that waters were stratified in Queen Charlotte Sound during the sampling period. The lack of significant variations in temperature and salinity across the shelf supports the relaxation of upwelling or

downwelling circulation at this time and indicates that there was little influence from coastal runoff. Although the research conducted previously over the California and Oregon shelf regions examined the effect of summer upwelling in regulating iron distributions in the coastal region, Queen Charlotte Sound is not known to be an area of significant upwelling (Bakun et al., 1974). Furthermore, while brief pulses of upwelling during the summer may succeed in enhancing primary productivity in the near vicinity of the coast by bringing up nutrient-rich waters, rapid biological consumption, as evident in the vertical profiles, may prevent the offshore transport of Fe in surface waters. Consequently, our interest lies with the dissolved Fe associated with the benthic layer over the continental shelf in which concentrations are distinctly elevated.

2.5.1 Vertical profiles

The benthic layer containing high levels of dissolved Fe that can be seen in the vertical profiles from shelf stations supports previous findings that pointed to the presence of a broad continental shelf and reducing sediments as major sources of Fe to overlying waters (Johnson et al., 1999; Elrod et al., 2004). Although surface Fe concentrations were depleted relative to subsurface waters at all stations, likely from biological uptake, an onshore-offshore dissolved Fe gradient is evident in the mid-depth and near-bottom waters of stations from both the MB and SS lines. This trend across the shelf slope probably reflects a similar gradient in total (dissolved and particulate) Fe, a trend that has been reported in studies off the California (Johnson et al., 2001) and Oregon (Chase et al., 2002; Chase et al., 2005a) coasts. Although upwelling has a greater role along these coasts, likely resulting in much higher dissolved Fe at the surface at

stations closest to the shore, and measurements in these studies were based on unfiltered seawater samples, the much higher concentrations of Fe found at the coastal stations compared to offshore sites is consistent with the idea that continental margins are a significant source of Fe, regardless of the method of supply.

We hypothesize that advection of a near-bottom layer across the shelf at depth is a critical process that results in the seaward transport of Fe-rich shelf waters across the shelf-slope break while limiting losses of Fe to biological uptake or particle surface scavenging, processes that are heightened in productive surface waters. To illustrate the movement of waters within the benthic layer, the dissolved Fe concentrations are plotted against σ_T and presented in Fig.9.

The most striking feature emerging from the density plots shown in Fig.9 is the presence of a layer of elevated Fe at σ_T values between 26 and 27, probably originating from waters in contact with sediments in stations situated over the continental shelf. Less dense waters show relatively low Fe concentrations with little variation across the shelf but in the most dense shelf waters, the increase in dissolved Fe is dramatic. In the northern end of the sound where the MB line lies, this layer is observed between 75-150 m depth both over the shelf and offshore. South of this transect, a similar feature is visible along the SS line where dissolved Fe is very high below 250 m over the shelf, shoals slightly to 200 m over the shelf-slope break and then sinks to 300 m offshore. Unfortunately, there is insufficient data from station G4 to determine if the same process is taking place along the west coast of Vancouver Island but the similarity between the G6 and SS3 Fe profiles suggests that this may be the case. This trend in dissolved Fe distribution across the continental shelf is highly suggestive of some means of cross-shelf

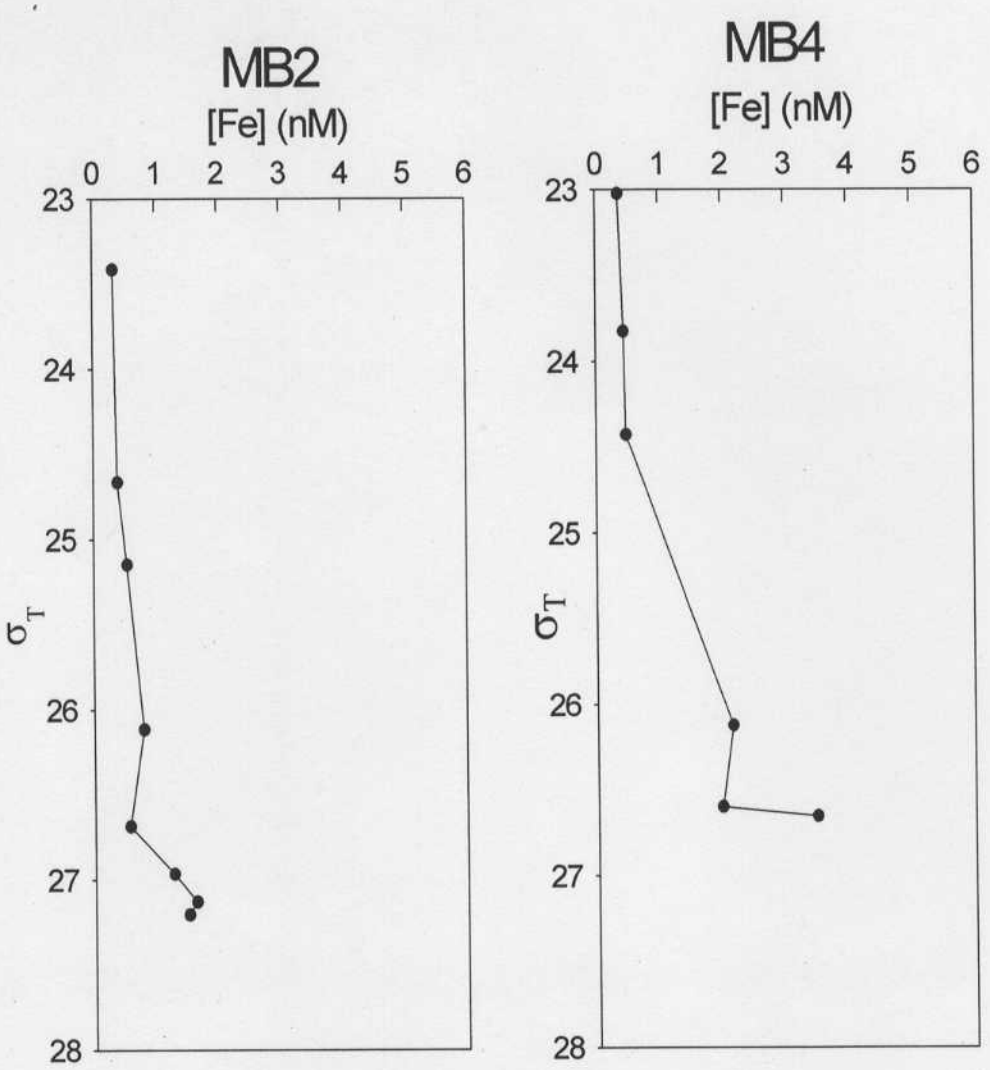

Fig. 9. Dissolved Fe concentrations plotted against σ_T. Stations on the left are the most offshore and stations on the right are the most inshore.

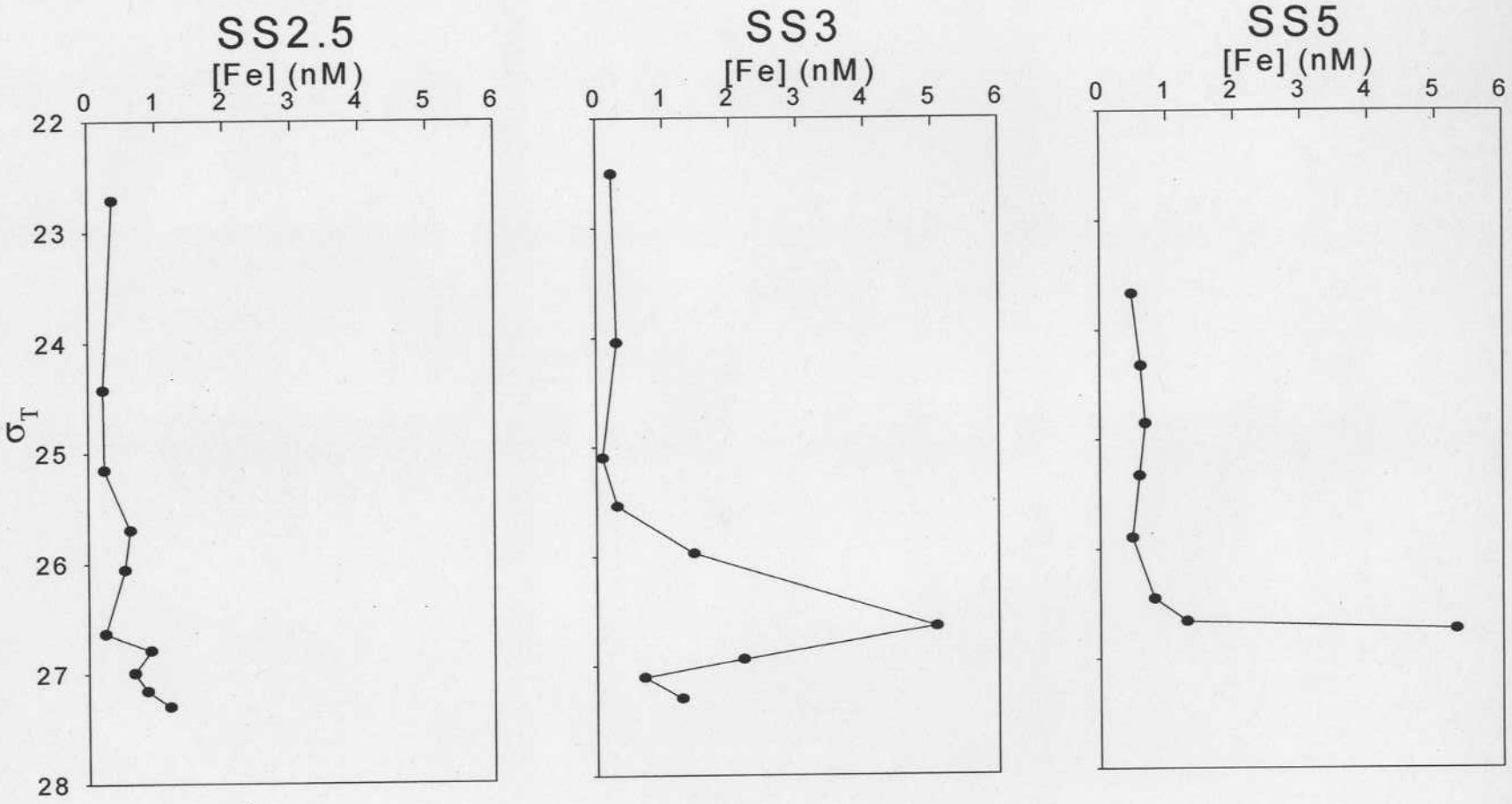

Fig. 9. continued.

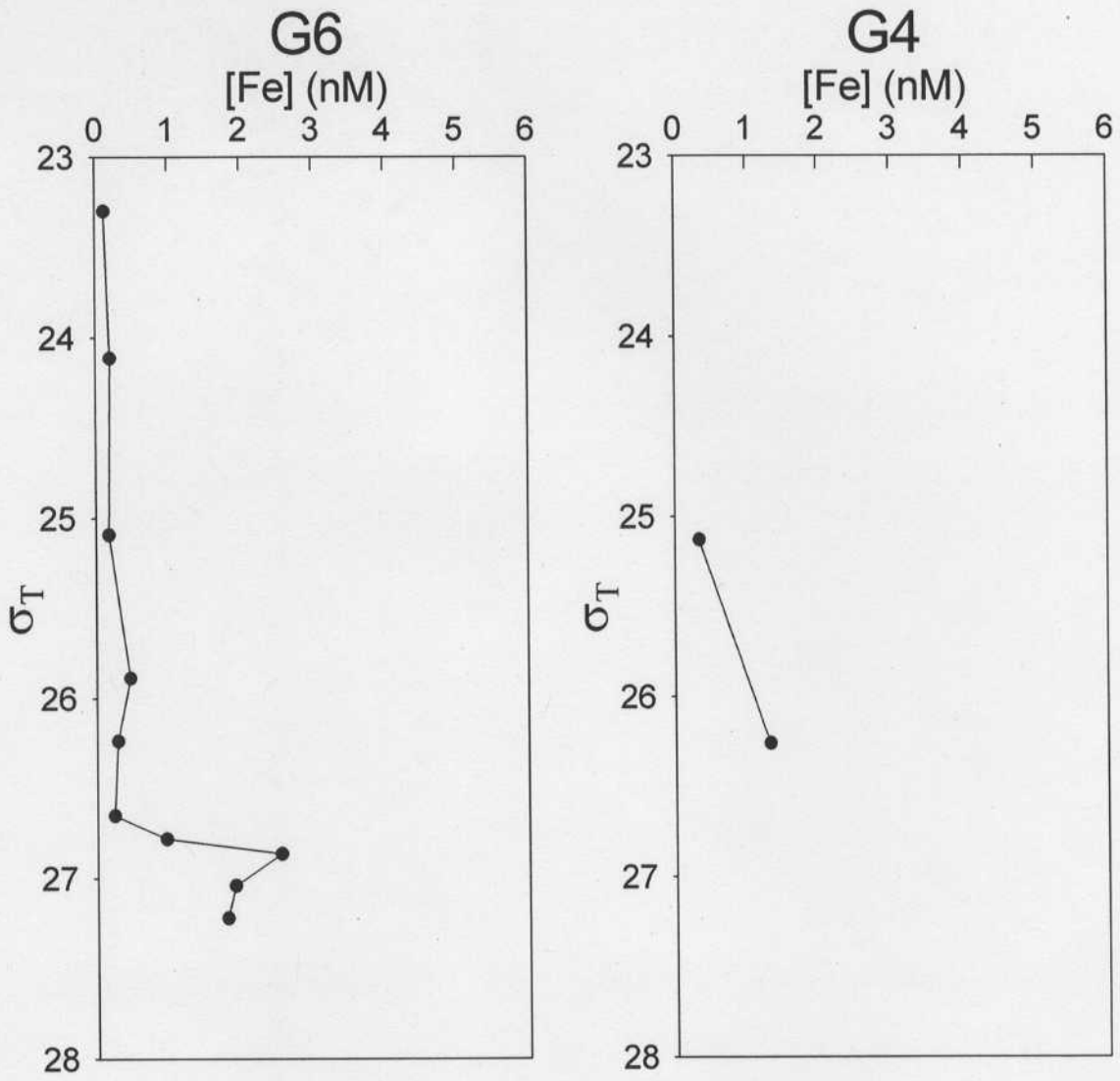

Fig. 9. continued.

advection of high Fe waters. By the time the water originating from the shelf is transported to the offshore stations, however, only 50 to 80% of the dissolved Fe present on the shelf remains in the waters beyond the shelf break. One possible reason for this loss of Fe is through increased Fe oxide formation and chemical scavenging as the shelf waters move into more oxygenated waters, effectively removing dissolved Fe from the water column. For example, along the MB line, the Fe-rich water mass found between depths of 100-150 m is associated with 1.8-3.2 mL/L of dissolved O_2 at the shelf station MB4 and associated with O_2 concentrations of 3-3.8 mL/L at the offshore station, MB2. Another factor that may have a significant impact on how much Fe reaches offshore waters is the circulation within the Queen Charlotte Sound, a system that is known to be complex and confused during the summer season (Crawford et al., 1985).

From the CTD data, it appears that there are different physical mechanisms taking place in waters west of the shelf break. The density plots given in Fig. 9 verify that Fe-enriched water orginates on the continental shelf. Furthermore, the presence of mid-depth variations in offshore Fe profiles is highly indicative of some means of lateral transport of near-bottom shelf waters. In the following discussion we will first examine the role of the continental shelf as the prominent source of Fe to Queen Charlotte Sound. We will then evaluate the potential of four physical mechanisms towards transporting dissolved Fe across the shelf break: tidal currents, upwelling/downwelling, bottom Ekman flux, and Haida eddies. These well-documented processes have all been shown to have a strong influence on circulation in coastal waters.

2.5.2 Effect of the continental shelf

One of the initial studies of sediments as a source of Fe to coastal waters was carried out off the Peruvian coast about two decades ago (Hong and Kester, 1986). Profiles of Fe(II) showed high concentrations (up to 40 nM) at depth over the continental shelf that decreased rapidly up through the water column and offshore. Since this early study, more attention has been given to the role of shelf sediments in regulating coastal productivity. Subsequent work included measurements of Fe in transects across the California Current System (Johnson et al., 1999) and the resulting data demonstrated dissolvable Fe concentrations approximately 20-fold higher during typical upwelling condidtions than levels observed during an El Niño year where upwelling was minimal and river flow was high. These results implied that the sediment contribution outweighed the amount of Fe derived from fluvial input.

Along continental margins, waters are Fe replete, relative to the Fe requirements of eukaryotic phytoplankton, largely due to resuspension of bottom sediments (Martin, 1990). Fe in sedimentary material exists as Fe-oxides, generally thought to be biologically unavailable, but the oxygen depletion associated with sediments allows for high concentrations of Fe(II) to be present within pore waters close to the sediment-water interface (Morford et al., 2005). Iron in the pore waters does not appear to diffuse into overlying waters, however, quickly becoming oxidized at the sediment-water interface and reprecipitating (Morford et al., 2005). A recent study of the sponge reefs along the western Canadian continental shelf (Whitney et al., 2005) found that once winter downwelling ceases, deep waters are able to well up across the shelf. The deep water is high in nutrients and very low in oxygen due to remineralization and in spring, the high coastal productivity in Queen Charlotte Sound would further diminish dissolved oxygen

at depth. As this water crosses the shelf, it may provide an environment that is sufficiently depleted in oxygen to allow a diffusion of Fe(II) from pore waters into the benthic layer, without precipitation back to the sediments. The coastal productivity in the spring associated with waters in Queen Charlotte Sound would further deplete bottom waters of oxygen by raining out organic matter at high rates.

Besides the diffusion of inorganic Fe(II) from pore waters, there may be a significant source of dissolved Fe originating from decaying organic materials in shelf sediments. The oxidation of settling organic matter results in the depletion of dissolved oxygen in the benthic layer and the combination of low oxygen and low pH (resulting from release of CO_2 from decomposing organic matter) in these waters allows for the mobilization of Fe from sediment pore waters by reduction to Fe(II). Another recent study (Elrod et al., 2004) examined the flux of Fe and inorganic carbon derived from the oxidation of organic matter from shelf sediments into the overlying water column. The authors found a strong correlation between these two variables, supported by models of sediment diagenesis which suggest that the oxidation of organic carbon regulates Fe reduction (Van Cappellen and Wang, 1996). Elrod et al. (2004) estimate, Elrod et al. (2004) estimated, based on a globally averaged carbon oxidation rate of organic matter accumulated in shelf sediments, that continental shelves contribute to a global dissolved Fe input of 8.9×10^{10} mol/yr, more than the global soluble atmospheric input of 1-10×10^{9} mol/yr (Fung et al., 2000). Although such studies are not numerous, they provide compelling evidence that these sediments are a significant source of Fe to coastal waters.

Research in coastal waters of Peru and California have highlighted the importance of shelf width on the flux of Fe from sediments and the resulting concentration of Fe in

waters.within 5-10 m of the shelf bottom. The continental shelf of central Peru is roughly 150 km wide and total dissolved Fe concentrations approach values of 118 nM at 60 m depth, 5 m above the shelf bottom, under suboxic conditions, a value noted by the authors to be the highest concentration of dissolved Fe observed in any eastern boundary region (Bruland et al., 2005). In southern Peru however, the shelf is only about 10 km wide and here near-bottom (within 5-10 of the bottom) dissolved Fe is found to be between 1.4-4.6 nM. Similar results have emerged from studies of surface waters off central California (Bruland et al., 2001; Chase et al., 2005a; Chase et al., 2005b). In these cases, total dissolved Fe in surface waters over the wider shelf in Monterey Bay was significantly higher than Fe in waters south of Monterey Bay where the shelf is only a few kilometres wide. In our study, the region of the continental shelf where the MB and SS lines are situated is broader than the shelf areas off California and Oregon, and more similar to Peru at a width of approximately 150 km. In comparison, the shelf off the west coast of Vancouver Island where the G line lies is about 40 km wide and station G6 is associated with a mid-depth dissolved Fe concentration that is half of what is observed at station SS3. This difference may be a result of the much broader shelf area in Queen Charlotte Sound, allowing benthic waters to be in contact with a larger deposit of Fe-rich sediments.

2.5.3 Tidal currents in Queen Charlotte Sound

Along the west coast of B.C., tides are predominantly semidiurnal (Cummins and Oey, 1997) and large diurnal currents have been observed in Queen Charlotte Sound with especially strong flows over the Middle, Goose Island, and Cook Banks (see Fig.1)

(Foreman et al., 2000). Strong tidal forcing can have significant impact on the circulation within shelf regions. For example, at the southern end of Vancouver Island, tidal currents are also strong and when these currents interact with the topography in the Juan de Fuca Strait entrance, diurnal continental shelf waves are created that propagate north (Foreman and Thomson, 1997). These shelf waves lose energy by the time they reach Brooks Peninsula, however, and are an unlikely source of tidal energy to Queen Charlotte Sound; thus tidal forcing must transmit from across the open ocean boundary (Foreman and Thomson, 1997).

Tidal energy can effectively transport particulate matter and solutes in coastal regions (Bowers et al., 2005; Ommundsen, 2002; Pereira et al., 2005). As mentioned previously, tidal currents along the continental shelf of Queen Charlotte Sound are strong. In the Irish Sea, satellite imagery has shown that areas with fast tidal currents are associated with enhanced turbidity (Bowers et al., 2005). As well, tidal flow aids in maintaining well-mixed conditions throughout the water column in shelf edge regions (Xing and Davies, 2002). The model used by Xing and Davies (2002) also demonstrates that in the absence of wind and fixed stratification, tidal forcing results in a weak on-shelf current and a slightly stronger off-shèlf current over the seabed. In eastern Brazilian coastal waters, the interaction between tides and topography consisting of two shallow banks across a shelf may provide a significant flux of nutrients to the subsurface ocean (Pereira et al., 2005). The presence of canyons across shelf breaks induces meanders in subsurface flows and the formation of eddies (Foreman et al., 2000). The results of such simulation studies offer strong evidence that the combination of tidal forcing and topographic features such as banks and troughs produce enough turbulent energy to allow

Fe-rich shelf sediments and pore waters to be mixed up and possibly advected seaward across the continental shelf.

At the shelf edge, summer tides produce an internal tide which strongly influences tidal currents within Queen Charlotte Sound by generating large tidal current ellipses over Middle, Goose, and Cook Banks (Cummins and Oey, 1997). The internal tide is reflected off the continental slope and radiates offshore (Cummins and Oey, 1997), a process that can potentially erode the sediment surface and prevent fine-grained sediment from settling (Cacchione et al., 2002). In addition, it has been noted that the energy associated with internal tides is not sufficient to account for total dissipation of tidal energy (Cummins and Oey, 1997), and the remaining energy is thought to be dispelled through bottom friction, form drag, or vertical motions (Klymak and Gregg, 2004), all of which would contribute turbulence and further mixing of shelf waters near to the water-sediment interface. Klymak and Gregg (2004) suggest that these internal tides may drive mixing in the deep ocean and in the Queen Charlotte Sound, we propose that they serve to mix Fe-replete shelf and shelf slope waters with offshore waters.

2.5.4 Bottom boundary layer and near-bottom Ekman transport

There have been a small number of measurements and modeling studies performed on shelf waters off the Oregon and northern California coasts with a focus on dynamics of the bottom boundary layer (Lentz and Trowbridge, 1991; Perlin et al., 2005). In the vicinity of the coast of British Columbia, however, the subsurface current direction parallel to the shelf edge and the near bottom flow within Queen Charlotte Sound has yet to be constrained. Assuming dynamics in shelf waters along the British Columbia coast

are similar to those of Oregon and northern California, we can nevertheless put forth some ideas about what the circulation over the shelf may resemble.

Lentz and Trowbridge (1991) describe the bottom boundary layer over the northern California shelf as "the region in which the flow is directly modified by the presence of the bottom" and note its importance in contributing to cross-shelf exchange. Here, turbulence is high due to strong shears, resulting in the emergence of a bottom mixed-layer whose height is regulated by the direction and magnitude of flow along the shelf edge as well as the interior stratification (Lentz and Trowbridge, 1991). For a water column of about 200 m depth, comparable to our shelf stations, the bottom mixed-layer height ranges from 0-30 m, encompassing the apparent mixed-layer height of about 20 m observable in the dissolved Fe and CTD profiles from stations MB4 and SS5 (Lentz and Trowbridge, their Figs. 9 and 14). In order to accommodate a bottom mixed-layer of 20 m, the along-shelf flow ranges from 0-20 cm/s, depending on direction, which compares well with observed summer currents off the western continental margin of Vancouver Island of between 0.4±6.0 to 18.8±7.2 cm/s (Foreman et al., 2000). Using an average velocity of 10 cm/s, the Ekman boundary layer is 1-3 m at a latitude of 50°N resulting in a flux across the shelf of 0.05-0.15 m^2/s. Solutions for net boundary layer transport (equation 5-11, Cushman-Roisin, 1994) are derived from the Navier Stokes equations that include friction with assumptions given in the text (equations 5-3 to 5-5, Cushman-Roisin, 1994). The average Fe concentration near the bottom at stations MB4 and SS5 is 4±1 nM and we estimate the width of Queen Charlotte Sound to be 200 km. The resulting Fe transport out of Queen Charlotte Sound within the bottom Ekman boundary layer is then $1.3 - 3.8 \times 10^6$ mol Fe/yr, an order of magnitude lower than the annual supply

of Fe via atmospheric deposition to the subarctic Northeast Pacific of $2.5\text{-}5.0\times10^{7}$ mol (Johnson et al., 2005). There is, however, a large uncertainty associated with the assumed eddy viscosity used in the calculation of bottom boundary transport.

Several studies on the bottom boundary layer over shelf areas have come to a consensus with respect to the dependency of the dynamics of this layer on the direction of subsurface current flow along the shelf break (Lentz and Trowbridge, 1991; Middleton and Ramsden, 1996; Perlin et al., 2005). The application of Ekman transport to alongshore current in the interior results in either offshore flow within the bottom boundary layer associated with a poleward current, or onshore flow across the shelf if the current is equatorward. With respect to Queen Charlotte Sound, a major question that that needs to be answered in order to constrain cross-shelf flow is how far north the California Undercurrent extends. It has been demonstrated that the poleward flowing California Undercurrent does range as far north as southern Vancouver Island but this appears to be the northern limit (Freeland and Denman, 1982; Reed and Halpern, 1976) and there is no evidence that this current reaches Queen Charlotte Sound. . If the California Undercurrent were to extend beyond the northern tip of Vancouver Island and produce a considerable offshore Ekman effect, the waters rich in Fe due to turbulent mixing over the shelf would be transported downslope, possibly via the glacial troughs that intersect the shelf bed. These bathymetric features have been shown to act as channels that contain elevated levels of nutrients. Upwelling through these canyons helps to sustain large sponge reef colonies along the west coast of Canada (Whitney et al., 2005).

2.5.5 Upwelling and downwelling across the continental shelf

There have been a handful of modeling studies of the currents and the upwelling/downwelling system in the Sound (Crawford et al., 1985; Crawford et al., 1995; Hannah et al., 1991). The effect of upwelling/downwelling over the continental shelf is thought to impact productivity significantly in the Gulf of Alaska. In winter, winds are typically from the southeast, promoting downwelling along the coast (Hannah et al., 1991). In summer, the southeasterlies relax and the upwelling climatological upwelling index is near zero, although short periods of upwelling do occur (Ladd et al., 2005). Off the southern end of Vancouver Island, an upwelling event was observed in the Juan de Fuca Strait through a major submarine canyon known as the Juan de Fuca Canyon and nicknamed the "Spur Canyon" (Freeland and Denman, 1982). The dense water that shoals up through the canyon is depleted in dissolved oxygen and rich in nutrients and originates from the California Undercurrent. The authors concluded that the presence of the Spur Canyon allows water to be brought up from greater depths than would be expected from typical coastal upwelling scenarios. More than a decade later, an analogous process was detected in Hecate Strait, immediately north of Queen Charlotte Sound (Whitney et al., 2005).

Observations of up-canyon intrusions of bottom waters across Moresby Trough during episodes of weak upwelling revealed the transport of waters enriched in nutrients (Whitney et al., 2005). When these waters flow up-shelf, they are steered into the canyons and become depleted in dissolved oxygen due to the remineralization of organic matter. Upon crossing the shelf, the high nutrient, low oxygen water in the troughs

undergoes tidal mixing (Ladd et al., 2005), enhancing the concentration of dissolved Fe through exchange with waters in contact with the shelf sediments.

Upwelling/downwelling processes are closely tied to mixing of near bottom waters over continental shelves. During a cycle involving a period of upwelling followed by relaxation of upwelling winds, waters in the bottom boundary layer flow up and down the shelf slope (Perlin et al., 2005). The thickness of the bottom boundary layer and the turbulence experienced at this depth is greatest during upwelling relaxation (Perlin et al., 2005). We suggest that in Queen Charlotte Sound, short pulses of upwelling during the summer allow water to flow upslope through the glacial troughs in this region. The termination of spring blooms results in a high rain of organic debris which, upon sinking into waters contained in the troughs, diminishes the concentration of dissolved oxygen. When this low oxygen water comes into contact with waters over the banks, the presence of a thick bottom mixed layer, along with tidally driven mixing enriches the water with Fe. As soon as relaxation of upwelling favorable winds takes place, waters are further mixed within the boundary layer and then slump back down the shelf, following isopycnal surfaces as they move offshore. The downwelling of this water mass limits the loss of dissolved Fe to biological uptake or scavenging and depending on how far offshore this water penetrates, could provide a coastal source of Fe to nearby Fe-limited regions.

2.5.6 Haida eddy formation

Anticylonic, mesoscale eddies in the Gulf of Alaska can affect cross-shelf transport by entraining shelf water into their cores and then propagating away from the

coast (Ladd et al., 2005), introducing Fe-rich coastal waters into this HNLC region. These eddies are generated off the tip of Cape St. James, where warmer, fresher water from Hecate Strait flows over the colder, more saline waters of Queen Charlotte Sound (Di Lorenzo et al., 2005). The resultant buoyant flow forms plumes which spin off as small anticyclonic eddies and when the flow is strong, these small eddies merge to become Haida eddies (Di Lorenzo et al., 2005). Haida eddies are observed to convey water, nutrients, and biota characteristic of the Hecate Strait, Queen Charlotte Sound, and West Coast Queen Charlottes area, westward into the Gulf of Alaska as far out as Station P (Mackas and Galbraith, 2005; Whitney and Robert, 2002). In the winter when these eddies are produced, primary productivity is minimal and surface concentrations of dissolved Fe and nutrients are presumably much higher compared to the values detected during our sampling period. Calculations based on observations of the especially large 1998 Haida eddy show that these eddies can transport up to 5000-6000 km^3 of Fe- and nutrient-replete coastal water every year (Whitney and Robert, 2002).

Johnson et al. (2005) also provide an estimate of the amount of iron transported offshore by Haida eddies. Using a volume of 3100 km^3 for a typical newly formed eddy, the Haida-2001 eddy was calculated to contain about 4.8×10^7 mol of total (particulate and dissolved) Fe. Since at least two eddies are formed annually, the yearly export of Fe to offshore waters is then double this amount. In comparison, based on an atmospheric deposition rate of 0.08-0.16 $\mu mol/(m^2/d)$ (Duce, 1986), Johnson et al. (2005) calculate that over the oceanic area that is affected by Haida eddies, the annual atmospheric flux of Fe is $2.5\text{-}5.0\times10^7$ mol, the same order of magnitude as Fe transport by one eddy. Thus,

Haida eddies are as important as atmospheric deposition, a mode that has traditionally been thought to be the principal source of Fe to this remote region.

The impact of Haida eddies on offshore waters has been observed along Line P, a transect intersecting the west coast of Vancouver Island and Station P in the Gulf of Alaska. Mid-way along Line P, at station P16, the Haida-1998 eddy increased Fe concentration in the upper water column by nearly an order of magnitude (Whitney and Robert, 2002). The studies that have been conducted on Haida eddies so far all verify that the formation of these eddies serve as annual episodes of natural fertilization of HNLC waters of the northeast Pacific. Their effect can persist for extended periods of time and their westward propagation allows coastal waters carrying elevated levels of Fe to reach Fe-depleted areas. The realization of the formation and effect of these eddies has only come over recent years and although our understanding of their potential influence is currently limited, future studies will no doubt continue to elucidate their role in the marine environment.

2.6.0 Conclusions

Dissolved Fe concentrations in waters over the continental shelf of Queen Charlotte Sound are high, especially within the bottom 20-50 m of the water column. As surface nutrients in general show depletion at all stations, waters appear to be Fe-replete and highly productive in this region. At depth, dissolved Fe concentrations decrease significantly across the shelf slope and plots of Fe versus density suggest that this exceptionally Fe-rich bottom layer in shelf waters flows offshore across the slope following isopycnal surfaces. The broad continental shelf in this area has an important

role as the primary source of iron to overlying waters through the resuspension of sediments and benthic fluxes. There are four possible mechanisms that may contribute to the offshore, downslope advection of this Fe-replete layer: tidal currents, Ekman transport within the bottom boundary layer, upwelling/downwelling along the shelf break, and the formation of Haida eddies. Future work quantifying the effect of these physical processes on Fe distribution is needed in order to gain a more empirical understanding of their potential.

2.7.0 References

Anderson, M.A. and Morel, F.M.M., 1982. The influence of aqueous iron chemistry on the uptake of iron by the coastal diatom *Thalassiosira weissflogii*. Limnology and Oceanography, 27(5): 789-813.

Bakun, A., McLain, D.R. and Mayo, F.V., 1974. The mean annual cycle of coastal upwelling off western North America as observed from surface measurements. Fishery Bulletin, 72(3): 843-844.

Borer, P.M., Sulzberger, B., Reichard, P. and Kraemer, S.M., 2005. Effect of siderophores on the light-induced dissolution of colloidal iron (III) hydroxides. Marine Chemistry, 93(2-4): 179-193.

Bowers, D.G., Ellis, K.M. and Jones, S.E., 2005. Isolated turbidity maxima in shelf seas. Continental Shelf Research, 25: 1071-1080.

Boyd, P.W. et al., 2000. A mesoscale phytoplankton bloom in the polar Southern Ocean stimulated by iron fertilization. Nature, 407: 695-702.

Boye, M. and van den Berg, C.M.G., 2000. Iron availability and the release of iron-complexing ligands by Emiliania huxleyi. Marine Chemistry, 70: 277-287.

Boyle, E., 1997. What controls dissolved iron concentrations in the world ocean? -a comment. Marine Chemistry, 57: 163-167.

Boyle, E.A., Bergquist, B.A., Kayser, R.A. and Mahowald, N., 2004. Iron, manganese, and lead at Hawaii Ocean Time-series station ALOHA: Temporal variability and an intermediate water hydrothermal plume. Geochimica et Cosmochimica Acta, 69(4): 933-952.

Bruland, K.W., 1989. Complexation of zinc by natural organic ligands in the central North Pacific. Limnology and Oceanography, 34(2): 269-285.

Bruland, K.W., 1992. Complexation of cadmium by natural organic ligands in the central North Pacific. Limnology and Oceanography, 37(5): 1008-1017.

Bruland, K.W. and Franks, R.P., 1979. Sampling and analytical methods for the determination of copper, cadmium, zinc, and nickel at the nanogram per liter level in sea water. Analytica Chimica Acta, 105: 223-245.

Bruland, K.W., Orians, K.J. and Cowen, J., 1994. Reactive trace metals in the stratified central North Pacific. Geochimica et Cosmochimica Acta, 58: 3171-3182.

Bruland, K.W., Rue, E.L. and Smith, G.J., 2001. Iron and macronutrients in California coastal upwellling regimes: Implications for diatom blooms. Limnology and Oceanography, 46(7): 1661-1674.

Bruland, K.W., Rue, E.L., Smith, G.J. and DiTullio, G.R., 2005. Iron, macronutrients and diatom blooms in the Peru upwelling regime: brown and blue waters of Peru. Marine Chemistry, 93(2-4): 81-103.

Butler, A., 1998. Acquisition and utilization of transition metal ions by marine organisms. Science, 281: 207-210.

Cacchione, D.A., Pratson, L.F. and Ogston, A.S., 2002. The shaping of continental slopes by internal tides. Science, 296: 724-727.

Chase, Z., Hales, B. and Cowles, T., 2005a. Distribution and variability of iron input to Oregon coastal waters during the upwelling season. Journal of Geophysical Research, 110(C10S12).

Chase, Z. et al., 2005b. Manganese and iron distributions off central California influenced by upwelling and shelf width. Marine Chemistry, 95: 235-254.

Chase, Z., van Geen, A., Kosro, P.M., Marra, J. and Wheeler, P.A., 2002. Iron, nutrient, and phytoplankton distributions in Oregon coastal waters. Journal of Geophysical Research, 107(C10)(3174): 38-1-38-17.

Coale, K.H. and Bruland, K.W., 1988. Copper complexation in the Northeast Pacific. Limnology and Oceanography, 33(5): 1084-1101.

Coale, K.H., et al., 1996. A massive phytoplankton bloom induced by an ecosystem-scale iron fertilization experiment in the equatorial Pacific Ocean. Nature, 383: 495-501.

Crawford, W., Huggett, W.S., Woodward, M.J. and Daniel, P.E., 1985. Summer circulation of the waters in Queen Charlotte Sound. Atmosphere-Ocean, 23(4): 393-413.

Crawford, W., Woodward, M.J., Foreman, M.G.G. and Thomson, R.E., 1995. Oceanographic features of Hecate Strait and Queen Charlotte Sound in summer. Atmosphere-Ocean, 33(4): 639-681.

Crawford, W.R., Cherniawsky, J.Y., Foreman, G.G. and Fower, J.F.R., 2002. Formation of the Haida-1998 oceanic eddy. Journal of Geophysical Research, 107(C7): 3069.

Croot, P.L. and Johansson, M., 2000. Determination of iron speciation by cathodic stripping voltammetry in seawater using the competing ligand 2-(2-Thiazolylazo)-p-cresol (TAC). Electroanalysis, 12(8): 565-576.

Cullen, J.T., Bergquist, B.A. and Moffett, J.W., 2005. Thermodynamic characterization of the partitioning of iron between soluble and colloidal species in the Atlantic Ocean. Marine Chemistry, 98(2-4).

Cummins, P.F. and Oey, L.-Y., 1997. Simulation of barotropic and baroclinic tides off northern British Columbia. Journal of Physical Oceanography, 27: 762-781.

Cushman-Roisin, B., 1994. Introduction to Geophysical Fluid Dynamics. Prentice Hall, Englewood Cliffs, N.J., 320 pp.

de Baar, H.J.W. et al., 2005. Synthesis of iron fertilization experiments: From the Iron Age in the Age of Enlightenment. Journal of Geophysical Research, 110(C9).

Di Lorenzo, E., Foreman, M.G.G. and Crawford, W.R., 2005. Modelling the generation of Haida Eddies. Deep-Sea Research II, 52(7-8): 853-873.

Duce, R.A., 1986. The impact of atmospheric nitrogen, phosphorous, and iron species on marine biological productivity. In: P. Buat-Menard (Editor), The Role of Air-Sea exchange in Geochemical Cycling. Dordrecht, pp. 497-529.

Duce, R.A. and Tindale, N.W., 1991. Atmospheric transport of iron and its deposition in the ocean. Limnology and Oceanography, 36(8): 1715-1726.

Elrod, V.A., Berelson, W.M., Coale, K. and Johnson, K.S., 2004. The flux of iron from continental shelf sediments: A missing source for global budgets. Geophysical Research Letters, 31(L12307).

Foreman, M.G.G. and Thomson, R.E., 1997. Three-dimensional model simulations of tides and buoyancy currents along the west coast of Vancouver Island. Journal of Physical Oceanography, 27: 1300-1325.

Foreman, M.G.G., Thomson, R.E. and Smith, C.L., 2000. Seasonal current simulations for the western continental margin of Vancouver Island. Journal of Geophysical Research, 105(C8): 19,665-19,698.

Freeland, H.J. and Denman, K.L., 1982. A topographically controlled upwelling center off southern Vancouver Island. Journal of Marine Research, 40: 1069-1093.

Fung, I.Y. et al., 2000. Iron supply and demand in the upper ocean. Global Biogeochemical Cycles, 14(1): 281-295.

Gledhill, M. et al., 2004. Production of siderophore type chelates by mixed bacterioplankton populations in nutrient enriched seawater incubations. Marine Chemistry, 88: 75-83.

Gledhill, M. and van den Berg, C.M.G., 1994. Determination of complexation of iron(III) with natural organic complexing ligands in seawater using cathodic stripping voltammetry. Marine Chemistry, 47: 41-54.

Hannah, C.G., LeBlond, P.H., Crawford, W.R. and Budgell, W.P., 1991. Wind-driven depth-averaged circulation in Queen Charlotte Sound and Hecate Strait. Atmosphere-Ocean, 29(4): 712-736.

Hong, H. and Kester, D.R., 1986. Redox state of iron in the offshore waters of Peru. Limnology and Oceanography, 31(3): 512-524.

Hutchins, D.A., DiTullio, G.R., Zhang, Y. and Bruland, K.W., 1998. An iron limitation mosaic in the California upwelling regime. Limnology and Oceanography, 43(6): 1037-1054.

Hutchins, D.A., Franck, V.M., Brzezinski, M.A. and Bruland, K.W., 1999a. Inducing phytoplankton iron limitation in iron-replete coastal waters with a strong chelating ligand. Limnology and Oceanography, 44: 1009-1018.

Hutchins, D.A., Witter, A.E., Butler, A. and Luther, G.W.I., 1999b. Competition among marine phytoplankton for different chelated iron species. Nature, 400: 858-861.

Johnson, K.S. et al., 2001. The annual cycle of iron and the biological response in central California coastal waters. Geophysical Research Letters, 28(7): 1247-1250.

Johnson, K.S., Chavez, F.P. and Friederich, G.E., 1999. Continental-shelf sediment as a primary source of iron for coastal phytoplankton. Nature, 398: 697-700.

Johnson, K.S., Gordon, R.M. and Coale, K.H., 1997. What controls dissolved iron concentrations in the world ocean? Marine Chemistry, 57: 137-161.

Johnson, W.K., Miller, L.A., Sutherland, N.E. and Wong, C.S., 2004. Iron transport by mesoscale Haida eddies in the Gulf of Alaska. Deep-Sea Research Part II, 52(7-8): 933-953.

Johnson, W.K., Miller, L.A., Sutherland, N.E. and Wong, C.S., 2005. Iron transport by mesoscale Haida eddies in the Gulf of Alaska. Deep-Sea Research Part II, 52(7-8): 933-953.

Klymak, J.M. and Gregg, M.C., 2004. Tidally generated turbulence over the Knight Inlet sill. Journal of Physical Oceanography, 34: 1135-1151.

Kuma, K., Nishioka, J. and Matsunaga, K., 1996. Controls on iron (III) hydroxide solubility in seawater: The influence of pH and natural organic chelators. Limnology and Oceanography, 41(3): 396-407.

Ladd, C., Stabeno, P. and Cokelet, E.D., 2005. A note on cross-shelf exchange in the northern Gulf of Alaska. Deep-Sea Research II, 52: 667-679.

Lentz, S.J. and Trowbridge, J.H., 1991. The bottom boundary layer over the northern California shelf. Journal of Physical Oceanography, 21: 1186-1201.

Lohan, M.C. and Bruland, K.W., 2005. Importance of vertical mixing for additional sources of nitrate and iron to surface waters of the Columbia River plume: Implications for biology. Marine Chemistry, in press.

Mackas, D.L. and Galbraith, M.D., 2005. Zooplankton distribution and dynamics in a North Pacific eddy of coastal origin: I. Transport and loss of continental margin species. Journal of Oceanography, 58: 725-738.

Martin, J.H., 1990. Glacial-interglacial CO2 change: The iron hypothesis. Paleoceanography, 5(1): 1-13.

Martin, J.H. et al., 1994. Testing the iron hypothesis in ecosystems of the equatorial Pacific Ocean. Nature, 371: 123-129.

Martin, J.H. and Gordon, R.M., 1988. Northeast Pacific iron distributions in relation to phytoplankton productivity. Deep-Sea Research, 35(2): 177-196.

Martin, J.H., Gordon, R.M., Fitzwater, S. and Broenkow, W.W., 1989. VERTEX: phytoplankton/iron studies in the Gulf of Alaska. Deep-Sea Research, 36(5): 649-680.

Middleton, J.F. and Ramsden, D., 1996. The evolution of the bottom boundary layer on the sloping continental shelf: A numerical study. Journal of Geophysical Research, 101(C8): 18,061-18,077.

Millero, F.J., 1998. Solubility of Fe(III) in seawater. Earth and Planetary Science Letters, 154: 323-329.

Moffett, J.W., 2001. Transformations among different forms of iron in the ocean. In: D.R. Turner and K.A. Hunter (Editors), The Biogeochemistry of Iron in Seawater. John Wiley & Sons Ltd., pp. 343-369.

Morford, J.L., Emerson, S.R., Breckel, E.J. and Kim, S.H., 2005. Diagenesis of oxyanions (V, U, Re, and Mo) in pore waters and sediments from a continental margin. Geochimica et Cosmochimica Acta, 69(21): 5021-5032.

Nishioka, J., Takeda, S., Wong, C.S. and Johnson, W.K., 2001. Size-fractionated iron concentrations in the northeast Pacific Ocean: distribution of soluble and small colloidal iron. Marine Chemistry, 74: 157-179.

Obata, H. and van den Berg, C.M.G., 2001. Determination of picomolar levels of iron in seawater using catalytic cathodic stripping voltammetry. Analytical Chemistry, 73: 2522-2528.

Oda, T., Nagao, h., Sugiyama, A. and Wada, K., 2005. Electronic structure and magnetism at the active site in ferredoxin: Ab initio approach to $(Fe_2S_2)^{2+}$ complex with the 1st peptide shell. Polyhedron, 24(16-17): 2550-2556.

Ommundsen, A., 2002. Models of cross shelf transport introduced by the Lofoten Maelstrom. Continental Shelf Research, 22: 93-113.

Pereira, A.F., Belem, A.L., Belmiro, M.C. and Geremias, R., 2005. Tide-topography interaction along the eastern Brazilian shelf. Continental Shelf Research, 25: 1521-1539.

Perlin, A., Moum, J.N. and Klymak, J.M., 2005. Response of the bottom boundary layer over a sloping shelf to variations in alongshore wind. Journal of Geophysical Research, 110(C10S09).

Peterson, T.D., Whitney, F.A. and Harrison, P.J., 2005. Macronutrient dynamics in an anticyclonic mesoscale eddy in the Gulf of Alaska. Deep-Sea Research II, 52(7-8): 909-932.

Powell, R.T. and Donat, J.R., 2001. Organic complexation and speciation of iron in the South and Equatorial Atlantic. Deep-Sea Research II, 48: 2877-2893.

Reed, R.K. and Halpern, D., 1976. Observations of the California undercurrent off Washington and Vancouver Island. Limnology and Oceanography, 21(3): 389-398.

Reid, R.T. and Butler, A., 1991. Investigation of the mechanism of iron acquisition by the marine bacterium Alteromonas luteoviolaceus: Characterization of siderophore production. Limnology and Oceanography, 36(8): 1783-1792.

Rich, H.W. and Morel, F.M.M., 1990. Availability of well-defined iron colloids to the marine diatom.

Rue, E.L. and Bruland, K.W., 1995. Complexation of iron(III) by natural organic ligands in the Central North Pacific as determined by a new competitive ligand equiligration/adsorptive cathodic stripping voltammetric method. Marine Chemistry, 50: 117-138.

Tortell, P.D., Maldonado, M.T. and Price, N.M., 1996. The role of heterotrophic bacteria in iron-limited ocean ecosystems. Nature, 383: 330-332.

Trick, C.G., Anderson, R.J., Price, N.M., Gillam, A. and Harrison, P.J., 1983. Examination of hydroxamate-siderophore production by neritic eukaryotic marine phytoplankton. Marine Biology, 75: 9-17.

Tsuda, A. et al., 2003. A mesoscale iron enrichment in the western subarctic Pacific induces a large centric diatom bloom. Science, 300: 958-961.

Van Cappellen, P. and Wang, Y., 1996. Cycling of iron and manganese in surface sediments: A general theory for the coupled transport and reaction of carbon, oxygen, nitrogen, sulfur, iron, and manganese. American Journal of Science, 296: 197-243.

van den Berg, C.M.G., 1995. Evidence for organic complexation of iron in seawater. Marine Chemistry, 50: 139-157.

Whitney, F.A. et al., 2005. Oceanographic habitat of sponge reefs on the Western Canadian Continental Shelf. Continental Shelf Research, 25: 211-226.

Whitney, F.A. and Robert, M., 2002. Structure of Haida eddies and their transport of nutrient from coastal margins into the NE Pacific Ocean. Journal of Oceanography, 58: 715-723.

Witter, A.E., Lewis, B.L. and Luther, G.W.I., 2000. Iron speciation in the Arabian Sea. Deep-Sea Research II, 47: 1517-1539.

Wu, J., Boyle, E., Sunda, W. and Wen, L.-S., 2001. Soluble and colloidal iron in the oligotrophic North Atlantic and North Pacific. Science, 293(5531): 847-849.

Wu, J. and Luther III, G.W., 1995. Complexation of Fe(III) by natural organic ligands in the Northwest Atlantic Ocean by a competitive ligand equilibration method and a kinetic approach. Marine Chemistry, 50: 159-177.

Xing, J. and Davies, A.M., 2002. Influence of wind direction, wind waves, and density straification upon sediment transport in shelf edge regions: The Iberian shelf. Journal of Geophysical Research, 107(C8): 3101.

3.0 CHAPTER 3

The Complexation of Dissolved Iron by Organic Ligands along Line P in the Subarctic Northeast Pacific

3.1.0 Abstract

In the subarctic northeast Pacific, the poor solubility of iron (Fe) in oxygenated seawater and distance from terrestrial sources of the metal ultimately leads to the limitation of primary productivity rates by Fe availability. The competitive ligand equilibration method, combined with adsorptive cathodic stripping voltammetry (CLE-CSV) was applied to seawater samples to examine the chemical speciation of dissolved Fe along the well-studied Line P transect, extending from the coastal margin of southern British Columbia to the Gulf of Alaska. The results of these experiments indicate the presence of high affinity Fe-binding ligands at concentrations in excess of the measured total dissolved Fe. The observed surface gradient in the ratio of organically bound to inorganic Fe across the transect suggests that phytoplankton may increase production of these organic ligands as they become more Fe-stressed as a mechanism to enhance the bioavailable Fe fraction.

3.2.0 Introduction

The first reliable datasets for dissolved (<0.4 μm) iron (Fe) demonstrated that its vertical profile was similar to that of nitrate in the northeast Pacific, indicating that the vertical distribution of Fe was controlled by active uptake by phytoplankton in surface waters (Martin and Gordon, 1988). Iron is now well-characterized as a metalloenzyme involved in the photosynthetic and respiratory cycles of marine heterotrophic bacteria and eukaryotic phytoplankton (Butler, 1998). The importance of Fe in regulating marine primary productivity has been further elucidated by the results of mesoscale Fe fertilization projects (Boyd et al., 2000; Coale, 1996; Martin et al., 1994) where additions

of Fe have been observed to enhance phytoplankton biomass in regions that are geographically isolated from terrestrial sources of the metal.

The biological accessibility of Fe is controlled by its aqueous chemistry (Anderson and Morel, 1982) and it is not the concentration so much as the chemical forms, or speciation, that determine whether Fe is available for uptake by the biota. In the presence of oxygen, Fe(III) predominates, although measurable levels of Fe(II) are found near the surface arising from photoreductive processes (Anderson and Morel, 1982). In natural waters, Fe(III) is found in a wide variety of complexes, the principal species being insoluble hydrolysis products involving ions as $Fe(OH)_2^+$ (Kuma et al., 1996). In fact, 50-90% of the iron in seawater has been found to exist in the particulate phase (Martin et al., 1989), a form that must undergo a dissolution process before it can be used by phytoplankton (Anderson and Morel, 1982). Consequently, research into the biogeochemistry of Fe has preferentially focused on the dissolved fraction (defined as <0.4 μm in diameter).

Although it is apparent that certain species within the dissolved Fe pool are readily taken up by phytoplankton, the chemistry of dissolved Fe in seawater may significantly decrease the bioavailable fraction (Hutchins et al., 1999a). The tendency of Fe to aggregate and form colloidal species is well known and as a result, colloids comprise a significant portion of the Fe measurements operationally define as dissolved (Wu et al., 2001). Compared to the concentration of dissolved Fe in the upper 500 m of the water column in Atlantic waters, "truly dissolved", or soluble, Fe (<0.02 μm) concentrations are lower by 20 to 40% with the majority being composed of a significant colloidal (0.2 to 0.4 μm) Fe class (Wu et al., 2001). Laboratory incubation experiments

with the marine diatom, *Thalassiosira weissflogii*, indicate that these phytoplankton cannot directly acquire synthetic colloidal Fe (Rich and Morel, 1990). In contrast, a study by Nishioka et al. (2001) demonstrates that the concentration of Fe in the small colloidal size class (0.03-0.1 μm) of subarctic Northeast Pacific waters exhibits depletion at the surface and increases at depths below 200 m. The similarity of this vertical distribution to nutrient-type profiles suggests that phytoplankton are able to acquire both soluble and colloidal Fe.

The use of competitive ligand equilibration in combination with adsorptive cathodic stripping voltammetry (CLE-CSV) has revealed the extensive complexation of dissolved Fe by naturally occurring organic ligands. The adaptation and application of this method to samples from various oceanic regions such as the western Mediterranean (van den Berg, 1995), the central north Pacific (Rue and Bruland, 1995), the west coast of Sweden (Croot and Johansson, 2000), the northwest Atlantic (Wu and Luther III, 1995), and the south and equatorial Atlantic (Powell and Donat, 2001), establish the ubiquitous presence of such chelators in seawater. Several trace metals, such as Zn, Cu, and Cd have been found to be almost entirely bound by organic compounds in seawater (Bruland, 1989; Bruland, 1992; Coale and Bruland, 1988) but whether these organically bound fractions are biologically accessible or not remains a topic of debate. Several studies have shown that more than 99% of dissolved Fe in the oceans is complexed by organic ligands (Gledhill and van den Berg, 1994; Rue and Bruland, 1995; van den Berg, 1995). These ligands may be released by marine micro-organisms (van den Berg, 1995) as a strategy to maintain Fe in a bioavailable form by mediating the dissolution of particulate Fe (Moffett, 2001).

If these organic ligands are actively produced by organisms, then it is likely that the ligands are similar to siderophores, low-molecular weight organic compounds that bind Fe specifically, or to porphyrins, which are found in intracellular materials (Hutchins et al., 1999b). The findings of several experiments demonstrate that marine bacteria and phytoplankton produce siderophores under Fe-limited conditions (Gledhill et al., 2004; Reid and Butler, 1991; Trick et al., 1983). Contrasting results arose from a study on the release of Fe-complexing ligands by the coccolithophore, *Emiliania huxleyi*, in which ligand production in this species was triggered by the addition of Fe to seawater (Boye and van den Berg, 2000) rather than Fe-depletion. There is also evidence that the interaction of siderophores and light is capable of significantly accelerating the dissolution of Fe oxides (Borer et al., 2005). Acquisition of organically bound Fe has been examined, revealing that uptake of these complexes can be accomplished by neritic eukaryotic phytoplankton and cyanobacteria (Hutchins et al., 1999b). Although our understanding of the identity, chemistry, and role of these naturally occurring Fe-chelators is far from complete, it is clear that these compounds are an important factor in regulating the bioavailability of this trace metal.

In our study, the CLE-CSV method was used with the ligand, 2-(2-Thiazolylazo)-*p*-cresol (TAC), to provide the first set of analyses of the speciation of Fe along a transect (Line P) extending from the west coast of Vancouver Island to Ocean Station P (P26) in the Gulf of Alaska (see Fig.10). Dissolved Fe profiles from the upper 1000 m of the water column were also measured to examine the spatial variations in Fe distribution with a change in regime from presumably more Fe-replete coastal waters to an offshore Fe deficient zone. This gyre in the northeast Pacific is one of the four major high nutrient

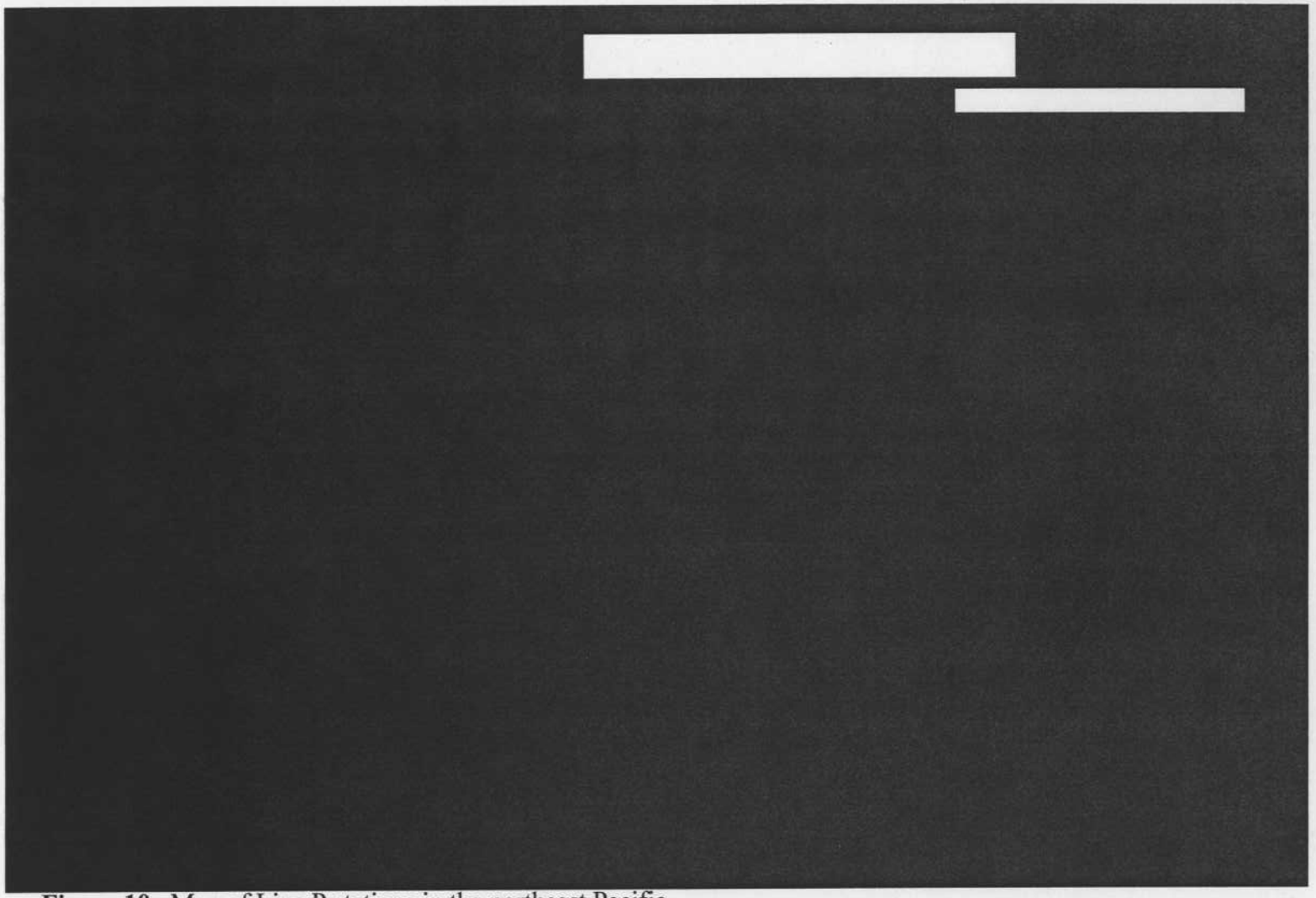

Figure 10. Map of Line P stations in the northeast Pacific

low chlorophyll (HNLC) regions in the world's oceans where limitation of phytoplankton growth rates and community composition by Fe availability is well-established (Martin et al., 1989). The main source of Fe to this area is the episodic transport of aerosols originating from the desert and loess regions of China (Duce and Tindale, 1991), an Fe supply that is insufficient to meet the metabolic needs of resident phytoplankton populations and results in a surface excess of nutrients such as nitrate (Martin et al., 1989). By understanding the chemical speciation of Fe along Line P we will gain insight into how phytoplankton respond to Fe-stress and how these organic Fe-binding ligands are cycled in the marine environment.

3.3.0 Methods

3.3.1 Sampling

Five stations along Line P (Fig. 10) were sampled onboard the C.C.G.S. J.P.Tully from Feb. 12-25, 2005 and again from Aug.16 to Sept. 2, 2005 following the protocol first used by the Ocean Chemistry group at the Institute of Ocean Sciences (IOS) (Johnson et al., 2004). During the winter cruise, samples from the upper 40 m were collected with a Teflon® pump and seawater was filtered through a pre-cleaned 0.22 μm cartridge filter (Opticap™ with Durapore® membrane by Millipore) contained within a PVC ULPA clean hood and connected to the pump with Teflon® tubing. Deeper samples were obtained with pre-cleaned Go-Flo® bottles sent down a Kevlar line and tripped with solid Teflon® messengers (Bruland and Frank, 1979). The Go-Flo® bottles were sampled within the ship's laboratory by connecting Teflon® tubing to valves on the bottles to which a cartridge filter and a plastic bell jar for protecting sample bottles were attached.

In August, samples from all depths were collected using Go-Flo® bottles, following the same procedures as in the previous cruise. Seawater samples for total dissolved Fe measurements were acidified to pH 1.7 with 12 N HCl (Seastar), double-bagged, and refrigerated until analysis. Samples for Fe speciation measurements were filtered into trace metal clean Teflon bottles and analyzed within 48 hours of collection.

3.3.2 Instrumentation

A Metrohm 663 VA hanging mercury drop electrode was used in conjunction with a μAutolab III voltammeter and potentiostat (Ecochemie). The counter electrode was a platinum wire and the reference electrode consisted of a double junction saturated Ag/AgCl unit with a 3 M KCl saltbridge contained within a glass electrolyte vessel. Stirring of sample solutions was done by a rotating Teflon rod and a Teflon voltammetric cell cup was used for all analyses. Triple distilled mercury (Bethlehem) and the largest drop size setting were used. The electrode and voltammeter/potentiostat were controlled with GPES 4.0 software (Ecochemie).

When not in use, the electrode and cell cup were stored in a 1% (vol/vol) HCl solution in Milli-Q (>18 MΩ cm) water. In between samples, the electrode and cell cup were rinsed with a 10% (vol/vol) HCl solution, HPLC grade methanol, and Milli-Q water. Seawater samples for total dissolved Fe were stored in 500 mL LDPE bottles which were sequentially cleaned by soaking in a detergent bath for 1 week, filled with 6 N HCl and placed in a 2N HCl bath for a minimum of 2 weeks, and then stored filled

with 1% (vol/vol) HNO_3 until use. CLE seawater samples were stored in acid-cleaned 1 L Teflon bottles and reagents were stored in 30 mL Teflon bottles which had been soaked for at a minimum of 24 hours in an 8 N nitric bath. All analyses and reagent preparation were carried out within a class 100 laminar-flow clean hood.

3.3.3 Reagents

For the CLE titrations, 2-(2-thiazolylazo)-*p*-cresol (TAC) (Aldrich) was dissolved in methanol distilled in the lab. During the February cruise, a borate solution was used to buffer the samples to pH 8. The borate was prepared from boric acid (Aldrich), dissolved in 1.0 M trace metal pure ammonia (Seastar) and cleaned by UV-oxidation for 2.5 hours, running through a column with Chelex-100 resin (BioRad), and finally UV-oxidizing an additional 2.5 hours. For the August cruise, the buffer piperazine-1,4-bis(2-hydroxypropanesulfonic acid) (POPSO) (Aldrich) was made up to 1.0 M in 1.0 M ammonia (Seastar) (pH 8) and purified by equilibration with 100 μM MnO_2 for several hours. The POPSO was filtered though a 0.2 μm acid-rinsed filter (Sarstedt) before use.

Total dissolved Fe, was measured using a method employing the electroactive ligand, 2,3-dihydroxynaphthalene (DHN) (Acros Organics) according to the method of Obata and van den Berg (2001). The DHN was added to Milli-Q water at a concentration 10 fold higher than the intended final concentration. The solution was heated using a microwave for 10 s at a time until fully dissolved and 1.0 % (vol/vol) ammonia was added immediately. In order to purify the solution, 5 mL of chloroform was slowly added to the hot solution and the mixture was shaken for 3 minutes. The solution was allowed to settle for at least 2 minutes and the DHN in the water phase was pipetted into

another clean container and extracted with another volume of chloroform. Purified DHN was pipetted into a 30 mL Teflon bottle and diluted 10 fold with distilled methanol. The analytical sensitivity of the DHN was found to remain constant upon repeated measurements of low Fe seawater with different batches of the purified ligand, indicating that any error associated with the DHN concentration had a negligible effect on the sensitivity. The catalytic oxidant, bromate, was prepared by dissolving enough potassium bromate (Fluka) into Milli-Q water to give a concentration of 0.45 M. The potassium bromate solution was purified by equilibration with MnO_2 and 1.0 M purified POPSO was added to the solution to give a concentration of 0.2 M in the mixture. The buffer/catalyst solution was then equilibrated a final time with MnO_2 and filtered before use.

The MnO_2 slurry was prepared by mixing 0.02 M $KMnO_4$ with 0.03 $MnCl_2$ and then stirring while 0.1 M NaOH was added until the pH reached 7-8.5 (C. van den Berg, pers.comm.). The solution was centrifuged, the supernatant discarded, and the process was repeated 3 times. The final precipitate was brought up to 0.05 M in Milli-Q water.

3.3.4 Titration of naturally occurring Fe-binding ligands

The CLE-CSV titrations were all performed within 48 hours of sample collection in order to minimize changes in chemical speciation due to biological or photochemical decomposition of the naturally occurring ligands. Subsamples (10 mL) of seawater were pipetted into 10 Teflon containers (15 mL) and 100 µL of 1 M POPSO added to buffer the seawater to pH 7.9, following the methods outlined by Croot and Johansson (2000) and Rue and Bruland (1995). Iron was added to the containers in concentrations ranging

from 0 to 8 nM and allowed to equilibrate for one hour (Cullen et al., 2005). A final concentration of 5 μM of TAC was then added and the subsamples were allowed to equilibrate for a minimum of 4 hours. For analysis by CSV, the samples were poured into the Teflon cell cup, deaerated for 2 minutes with high purity nitrogen gas, and adsorbed onto the Hg drop, while stirring, by depositing for 3-5 minutes, depending on ambient Fe concentration in the samples. At the end of the deposition period, the potential was scanned using the differential pulse mode from -0.35 to -0.9 V with a step potential of 0.003 V and a modulation amplitude of 49.95 mV.

To calibrate the conditional stability constant of the $Fe(TAC)_2$ complex, DTPA was added to UV-oxidized and Chelexed seawater and left to equilibrate with added iron (5 nM) overnight. TAC was added and allowed to equilibrate for at least 4 hours before running according to the procedure above. Results were similar to those of Croot and Johanssen (see comparison in Results section) and a β_{FeTAC} of $10^{12.7}$ was used for all speciation calculations.

3.3.5 Total dissolved Fe analysis

DHN-labile Fe was measured following a method developed by (Obata and van den Berg, 2001). Seawater samples were acidified down to pH 1.7 for a minimum of 24 hours before analysis. An aliquot of 10 mL of acidified seawater was pipetted into the cell cup and the pH was brought up to 8.0 with dilute ammonia. 500 μL of the POPSO/bromate mix was added and the solution purged for 4 minutes with N_2 gas. The Fe-DHN complex was deposited onto a fresh mercury drop while stirring for 15-240 s at a potential of -0.1 V. The stirrer was then turned off and allowed to equilibrate for 10 s

before scanning from -0.1 to -0.8 V using the sampled dc mode. Two standard additions of Fe(III) were made in order to calculate the Fe concentration by linear regression. A surface and deep seawater standard from the Fe intercomparison study, SAFe, was used to check the accuracy and precision of this method. Our value for the surface sample was somewhat lower at 0.07±0.01 nM than to the consensus value reached by participants of the SAFe cruise of 0.10±0.04 nM but our deep water concentration of 0.86±0.07 nM agrees well with the consensus value of 0.9±0.2 nM. The blank for this method was measured to be 20 pM and the detection limit, based on three times the standard deviation of Fe analysed in low iron seawater, was 25 pM for a 60 s deposition.

3.4.0 Results

3.4.1 Nutrient, chlorophyll and CTD data

The nitrate, phosphate, and silicate concentrations from each station are given in Appendix A (data from IOS). In the winter, surface nutrients are depleted relative to deep waters but are much higher at P4 and P26 than in the summer. During the August cruise, there is an increasing horizontal gradient in surface nitrate beginning with no detectable nitrate at P4 and ending with a concentration of 6.8 μM at P26. The change in phosphate and silicate along the line is less pronounced but exhibit the highest concentrations at P26 as well. This gradient, along with the decrease in dissolved iron towards P26, is indicative of a switch from a highly productive, nitrate-limited regime inshore to an iron-limited system offshore, where an excess in nutrients is observed.

Summer chlorophyll data provided by the Institute of Ocean Sciences for the upper 100 m is presented for each station (Fig. 11). The chlorophyll maxima generally

occur near the surface, between 15 to 40 m depths with the exception of P16 where the profile lacks a clearly defined maximum. P4 has the greatest algal biomass, reaching 2.7 μg/L of chlorophyll, a concentration that exceeds the range observed at this station by Maldonado and Price (1999) of 0.16 – 1.35 μg/L.

Temperature, salinity and density data (not shown) for Line P in August all indicate strong stratification. A thermocline is apparent across the transect at about 50 m depth, and a distinct halocline and pynocline at approximately 75 m inshore and deepening to 150 m at P26. In general, sea surface temperatures decrease seaward while salinity and density exhibit a decreasing gradient offshore. A signal from the presence of a Haida eddy situated southwest of P20 can be observed in the data by depressions at 1100 km offshore in the isothermal, isohaline, and isobath contours, characterizing the warmer, fresher and less dense coastal waters transported offshore by these eddies.

3.4.2 Total dissolved iron (winter)

Two dissolved Fe profiles were obtained during the February cruise at stations P4 and P26, the two end members of the transect (Fig. 12). The values obtained by flow injection analysis (FIA) (Keith Johnson and Nes Sutherland, IOS) are also given to provide a comparison of the two analytical methods. At P4, the profile does not follow a nutrient-type vertical distribution, exhibiting high concentrations (3.0±0.2 nM) at the surface. Below 100 m, the total dissolved Fe concentration drops down to 0.4±0.1 nM. The IOS profile follows a similar pattern of high Fe in the upper 100 m and then decreasing to 0.4 nM at 200 m.

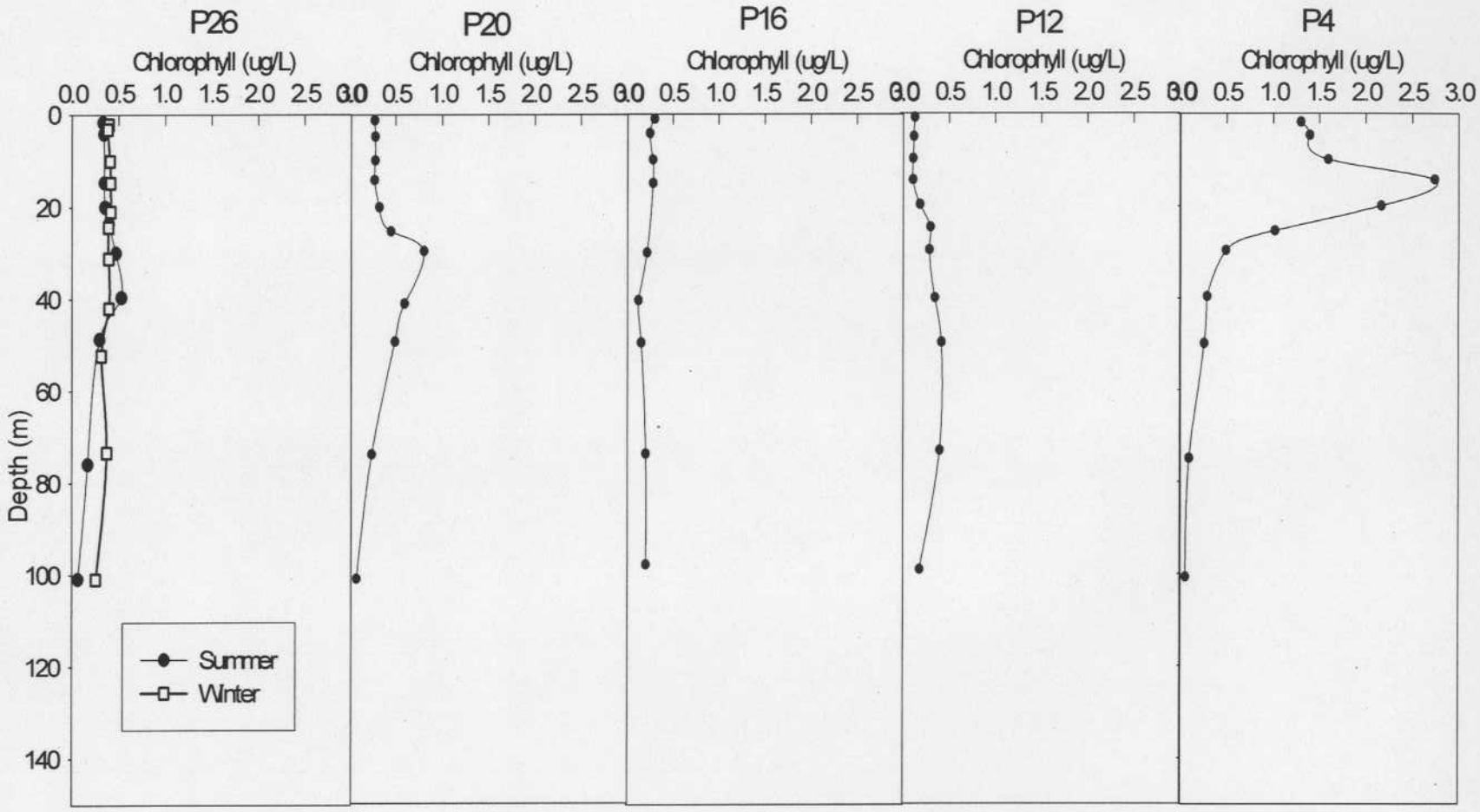

Fig. 11. Chlorophyll concentrations along Line P (data from IOS). P4 at the right end is the most coastal stations and P26 at the left end is the furthest offshore.

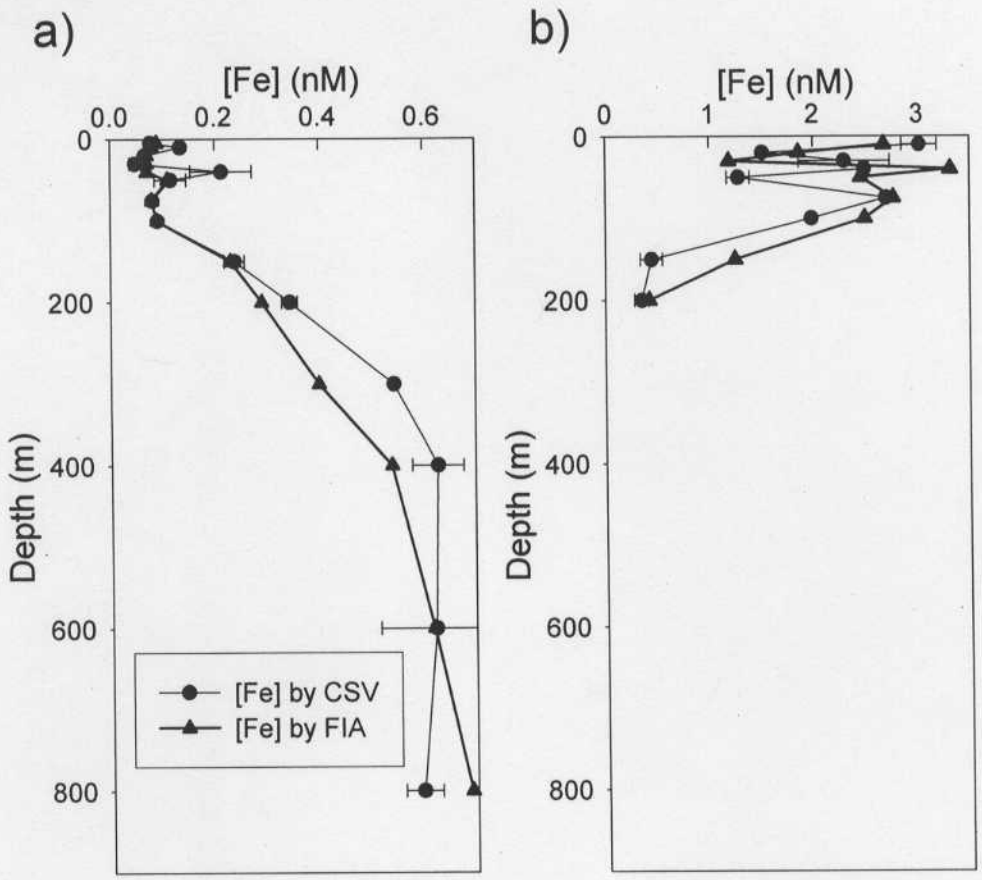

Fig. 12. Winter total dissolved Fe profiles from a) station P26, and b) station P4. Values obtained by FIA are also presented for comparison. Note the difference scales in the horizontal axis.

At P26, the data demonstrates a distribution much more representative of a typical oceanic, nutrient-type, profile. Iron levels are noticeably lower here, ranging from 0.077±0.006 nM to 0.134±0.007 nM within the upper 100 m. The dissolved Fe concentrations analyzed by IOS for this station once again follows a very similar distribution.

3.4.3 Total dissolved iron (summer)

During August, profiles down to 800 m were obtained for all 5 stations along the line (Fig. 13). The profile at P4 for the summer looks quite different from that of February. The concentration of Fe at the surface is high, reaching 3.2±0.2 nM, but drops rapidly to 0.11±0.01 nM by 30 m depth. Below 30 m, Fe levels increase but do not reach the high concentrations displayed in the winter profile. Moving offshore to P12, surface dissolved Fe concentrations decrease, with concentrations of 0.07±0.03 to 0.21±0.03 nM within the upper 100 m of the water column. Dissolved Fe increases with depth and a maximum is present at 300m of 0.64±0.07 nM. At P16, surface concentrations are once again low, from 0.09±0.02 to 0.200±0.006 nM, and increasing with depth up to 0.52±0.01 nM at 800 m. Surface Fe levels at P20 are also depleted, at concentrations of 0.022±0.008 to 0.14±0.02 nM and increase to 0.29±0.02 nM at 800 m. At 10 m depth at station P26, total dissolved Fe is high, at 0.30±0.02 nM and drops to concentrations of 0.05±0.02 to 0.16±0.02 immediately below. Dissolved Fe increases with depth and the highest concentration is seen at 600 m of 0.50±0.02 nM.

3.4.4 CLE-CSV Theory:

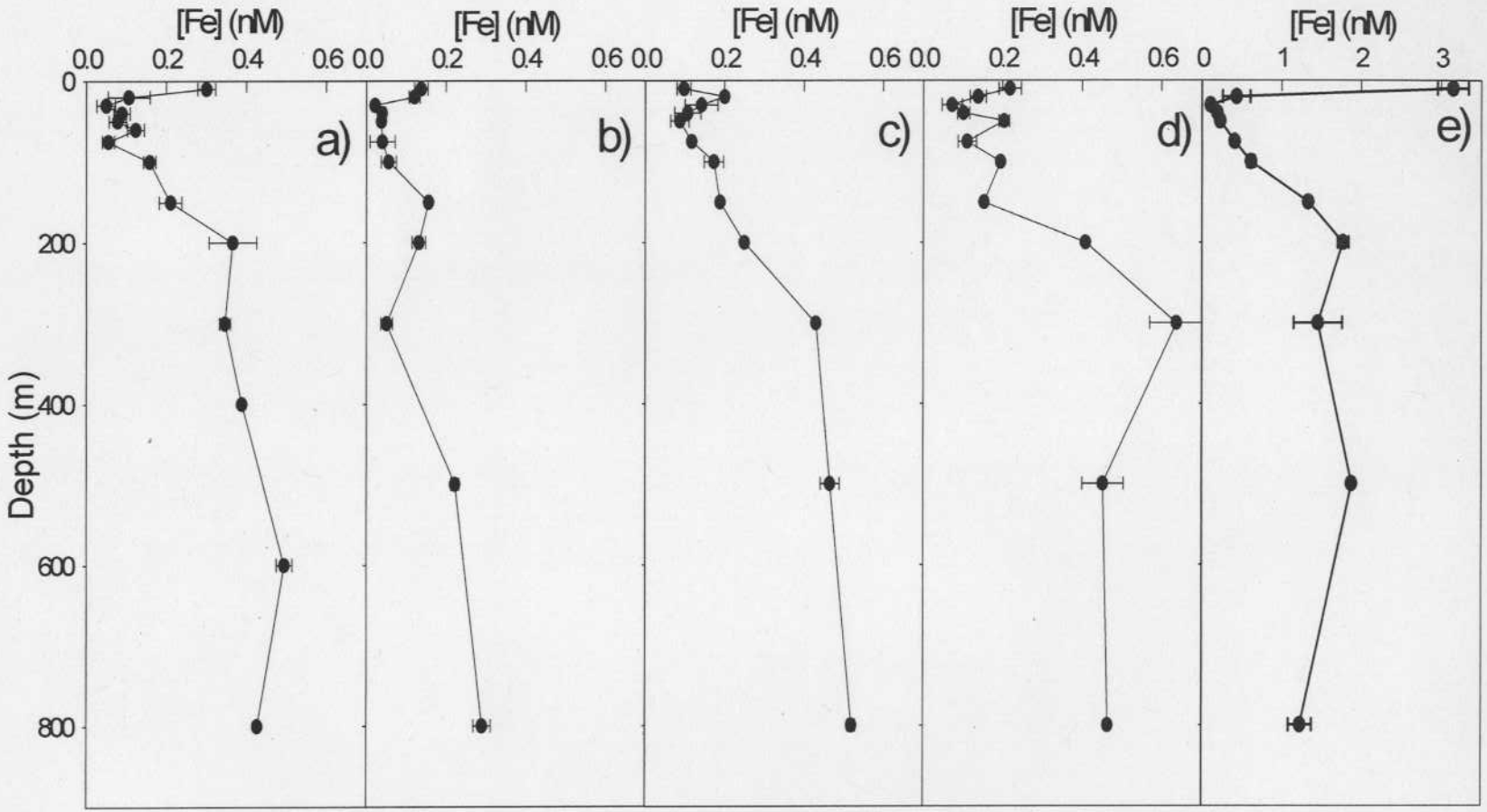

Fig. 13. Summer total dissolved Fe profiles from stations a)P26, b)P20, c)P16, d)P12, and e)P4. Note the different horizontal scale used in e). The distance from the coast increases from right to left.

In the study conducted by Croot and Johansson (2000), the application of electrospray mass spectroscopy to a solution of Fe(III) and TAC revealed the presence of both 1:1 and 1:2 complexes. For the purpose of our calculations we will assume all species exist as $Fe(TAC)_2$. Since the added TAC concentrations are always well in excess of the available dissolved Fe in the samples, this should not have a significant effect on the results.

The following theory for CLE applied to the speciation of Fe in seawater was first given by Rue and Bruland (1995) and van den Berg (1995) where salicylaldoxime was used as the competing ligand. The mass balance for Fe (where only Fe(III) is considered due to assumed oxidation of Fe(II)) in ambient seawater is:

$$[Fe_T] = [Fe'] + [FeL_i] \quad (1)$$

Here, $[Fe']$ represents all inorganic species and $[FeL_i]$ refers to iron bound by classes (L_i) of organic ligands. If only one class of binding ligand is considered, then the reaction is:

$$Fe' + L \Leftrightarrow FeL$$

and the conditional stability constant with respect to Fe′ at pH 8 is then,

$$K^{cond}_{Fe'L} = \frac{[FeL]}{[Fe'][L']} \quad (2)$$

The equilibrium is altered when the competing ligand TAC is added. The mass balance now becomes:

$$[Fe_T] = [Fe'] + [FeL_i] + [Fe(TAC)_2] \quad (3)$$

and the conditional stability constant for the complexation of Fe′ by TAC is:

$$B^{cond}_{Fe(TAC)_2} = \frac{[Fe(TAC)_2]}{[Fe'][TAC]^2} \quad (4)$$

The side reaction coefficient for $Fe(TAC)_2$ with respect to Fe′ is given as:

$$\alpha_{Fe(TAC)_2} = \frac{[Fe(TAC)_2]}{[Fe']} = B^{cond}_{Fe(TAC)_2}\ [TAC]^2 \quad (5)$$

$B^{cond}_{Fe(TAC)_2}$ is determined by calibration against the well-characterized ligand DTPA and the concentration of TAC is 5 μM.

The current, i_p, resulting from the "stripping" of the $Fe(TAC)_2$ complex from the mercury drop is related to the concentration of the complex by the following equation:

$$S = \frac{i_p}{[Fe(TAC)_2]} \quad (6)$$

S is the sensitivity determined by calculating the slope at the linear portion of the titration curve after naturally or added ligands have been completely titrated, which occurs at the high Fe end of the titration. Thus $[Fe(TAC)_2]$ can be evaluated, as well as $[Fe']$, by using the side reaction coefficient equation for $Fe(TAC)_2$ (5). From the mass balance (3), the $[FeL_i]$ is then computed using data obtained through CSV analysis of total dissolved iron.

3.4.5 Calibration of TAC:

The stability constant ($B^{cond}_{Fe(TAC)_2}$) of the $Fe(TAC)_2$ complex is first determined by establishing a competition between TAC and a model ligand, diethylenetriaminepentaacetic acid (DTPA). The mass balance for Fe with these two ligands is:

$$[Fe_T] = [Fe'] + [Fe(TAC)_2] + [FeDTPA] \quad (7)$$

The relationship between the reduction current arising from adsorption of the $Fe(TAC)_2$ complex and the concentration of the complex is:

$$i_{p/0} = S \cdot [Fe(TAC)_2] = (S \cdot [Fe_T] - [Fe']) \quad (8)$$

With the presence of DTPA, this becomes, by substituting with (7)

$$i_{p/i} = S \cdot ([Fe_T] - [Fe'] - [FeDTPA]) \quad (9)$$

and the ratio of the Fe reduction current with DTPA presence to that with its absence is:

$$X = \frac{i_{p/i}}{i_{p/0}} = \frac{B^{cond}_{Fe(TAC)_2} \cdot [TAC]^2}{(B^{cond}_{Fe(TAC)_2} \cdot [TAC]^2 + K^{comd}_{FeDTPA} \cdot [DTPA'])} \quad (10)$$

Here, $[DTPA']$ is the total amount of the ligand that is not bound to Fe, expressed as:

$$[DTPA'] = [DTPA_T] - (1 - X) \cdot [Fe_T]$$

$B^{cond}_{Fe(TAC)_2}$ is then equal to:

$$B^{cond}_{Fe(TAC)_2} = \frac{X \cdot K^{comd}_{FeDTPA} \cdot [DTPA']}{[TAC]^2 - X \cdot [TAC]^2} \quad (11)$$

The TAC-labile fraction of Fe (X) is plotted versus the concentration of DTPA added in Fig. 14. In calculating the conditional stability constant for the Fe-TAC complex, the side reaction of DTPA with major cations such as Mg^{2+}, Ca^{2+}, and H^+ was corrected for using a value of $\alpha_{DTPA'} = 10^{7.95}$ (Croot and Johansson, 2000). $B^{cond}_{Fe(TAC)_2}$ was found to be $10^{12.72 \pm 0.06}$, based on three trials, which is higher than Croot and Johansson's value of $10^{12.4 \pm 0.3}$ but still within agreement. $\alpha_{Fe(TAC)_2}$ was then calculated to be 125, which falls within the range of detection windows typically used in CLE studies.

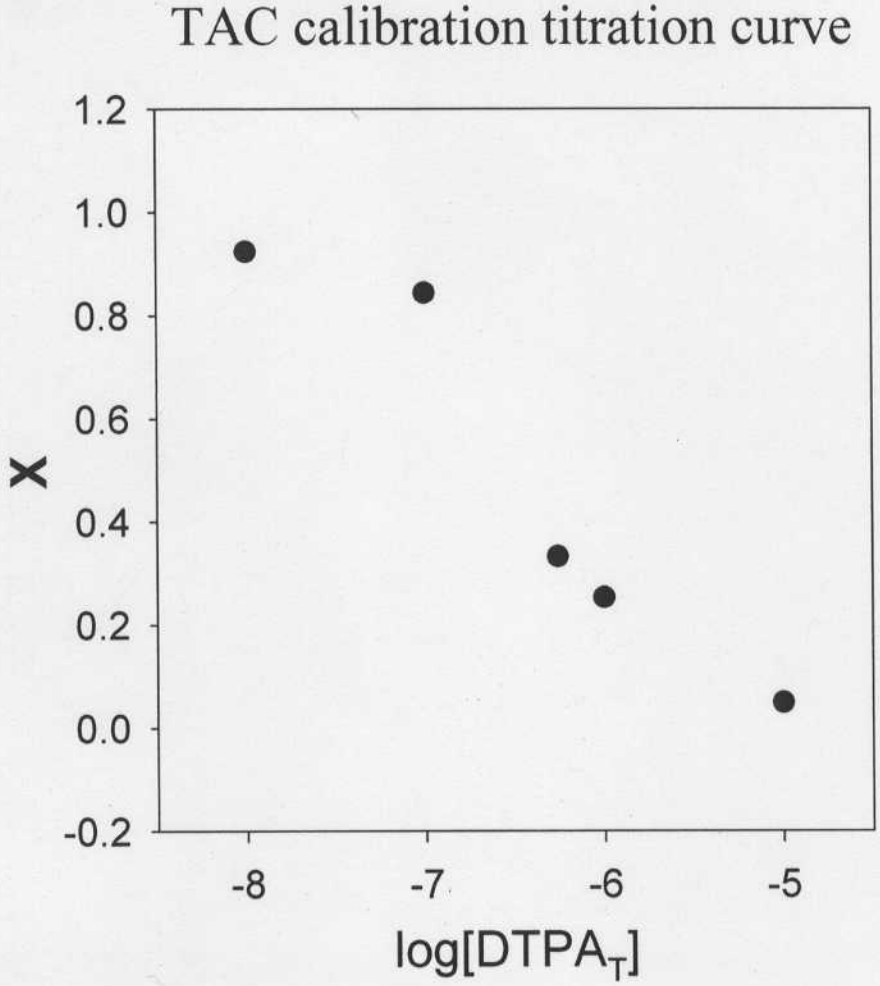

Fig. 14. Titration curve of TAC calibration experiment using DTPA as the model ligand. X is the ratio of the Fe reduction current with DTPA present to the current without DTPA.

3.4.6 Treatment of data:

From the titration curves, the conditional stability constants and the naturally occurring ligand concentrations, K_{FeL}^{comd} and $[L]_T$, were determined by Langmuir and Scatchard transformations (Ruzic, 1982; van den Berg and Kramer, 1979). An example of this data reduction is presented in Fig. 15. The Langmuir linearization is based on the relationship:

$$\frac{[Fe']}{[FeL]} = \frac{1}{K_{FeL}^{comd}} + \frac{[Fe']}{[L]_T} \qquad (12)$$

Plotting $[Fe']/[FeL]$ versus $[Fe']$ gives a straight line where the inverse of the slope is $[L]_T$ and K_{FeL}^{comd} is then calculated by the y-intercept of the line. If there is more than one class of ligands with different Fe-binding strengths, however, the transformation will be non-linear. The concentrations and conditional stability constants of each ligand class can be determined through Scatchard transformations. This is done by plotting $[FeL]/[Fe']$ against $[FeL]$, and assuming the formation of 1:1 complexes, the resulting line has a y-intercept equal to $K_{FeL}^{comd} \cdot [L]_T$ and an x-intercept equal to $[L]_T$. If there are two ligand classes, then there will be two linear regions in the plot which will each yield the K_{FeL}^{cond} and the $[L]_T$ of their respective ligand class.

3.4.7 CLE-CSV data:

Ligand concentrations and conditional stability constants, obtained through Langmuir and Scatchard transformations, are given in Table 3 for stations P12 to P26. The Fe titration data and transformations for the 20 m samples from P26 are presented in Table 4 and Fig. 15. A comparison of organically bound Fe versus inorganic

Table 3. CLE data from stations P12 to P26.

Station	Sample depth (m)	[Fe_T] (nM)	[L_T] (nM)	K'^{cond}_{FeL} (M^{-1})	[L_1] (nM)	$K'^{cond}_{FeL_1}$ (M^{-1})	[L_2] (nM)	$K'^{cond}_{FeL_2}$ (M^{-1})
August:								
P12	40	0.10	0.71	1.0×10^{12}				
	800	0.47	1.21	5.6×10^{12}				
P16	20	0.20	1.03	1.7×10^{11}	0.45	8.0×10^{11}	1.30	6.7×10^{10}
	75	0.12	0.43	1.0×10^{12}				
	200	0.25	0.89	1.1×10^{12}	0.49	3.0×10^{13}	1.00	3.5×10^{11}
P20	20	0.12	0.63	1.2×10^{12}				
	800	0.29	0.72	1.9×10^{11}				
P26	20	0.11	1.51	1.4×10^{11}	0.40	3.9×10^{13}	1.28	2.3×10^{11}
	50	0.08	1.18	1.2×10^{11}	0.69	3.6×10^{11}	2.60	3.4×10^{10}
	100	0.16	0.81	8.3×10^{10}	0.34	7.9×10^{11}	0.84	8.9×10^{10}
	200	0.37	0.59	1.5×10^{11}				
	800	0.43	0.57	6.6×10^{11}				
February:								
P26	40	0.07	0.72	1.0×10^{11}				
	100	0.09	1.13	3.9×10^{11}				
	200	0.29	1.62	1.1×10^{11}				
	600	0.62	1.09	1.8×10^{11}				

Table 4. Titration data from 20 m depth at station P26.

$[Fe_{Total}]$ (nM)	$[Fe_{added}]$ (nM)	Current (nA)	$[Fe(TAC)_2]$ (nM)	[Fe´] (nM)	[FeL] (nM)	[FeL]/[Fe´]	[Fe´]/[FeL]
0.11	0	0.43	0.0012	0.000009	0.11	11437	0.00009
0.61	0.5	3.4	0.21	0.0017	0.39	228	0.0044
1.11	1	7.9	0.54	0.0043	0.56	129	0.0077
1.61	1.5	11.8	0.83	0.0066	0.78	118	0.0085
2.11	2	16.8	1.19	0.0095	0.91	96	0.010
3.11	3	30.1	2.15	0.017	0.94	55	0.018
4.11	4	41.2	2.96	0.024	1.13	48	0.021
5.11	5	52.8	3.80	0.030	1.28	42	0.024
6.11	6	62.2	4.48	0.036	1.59	45	0.022
8.11	8	89.8	6.48	0.052	1.58	31	0.033

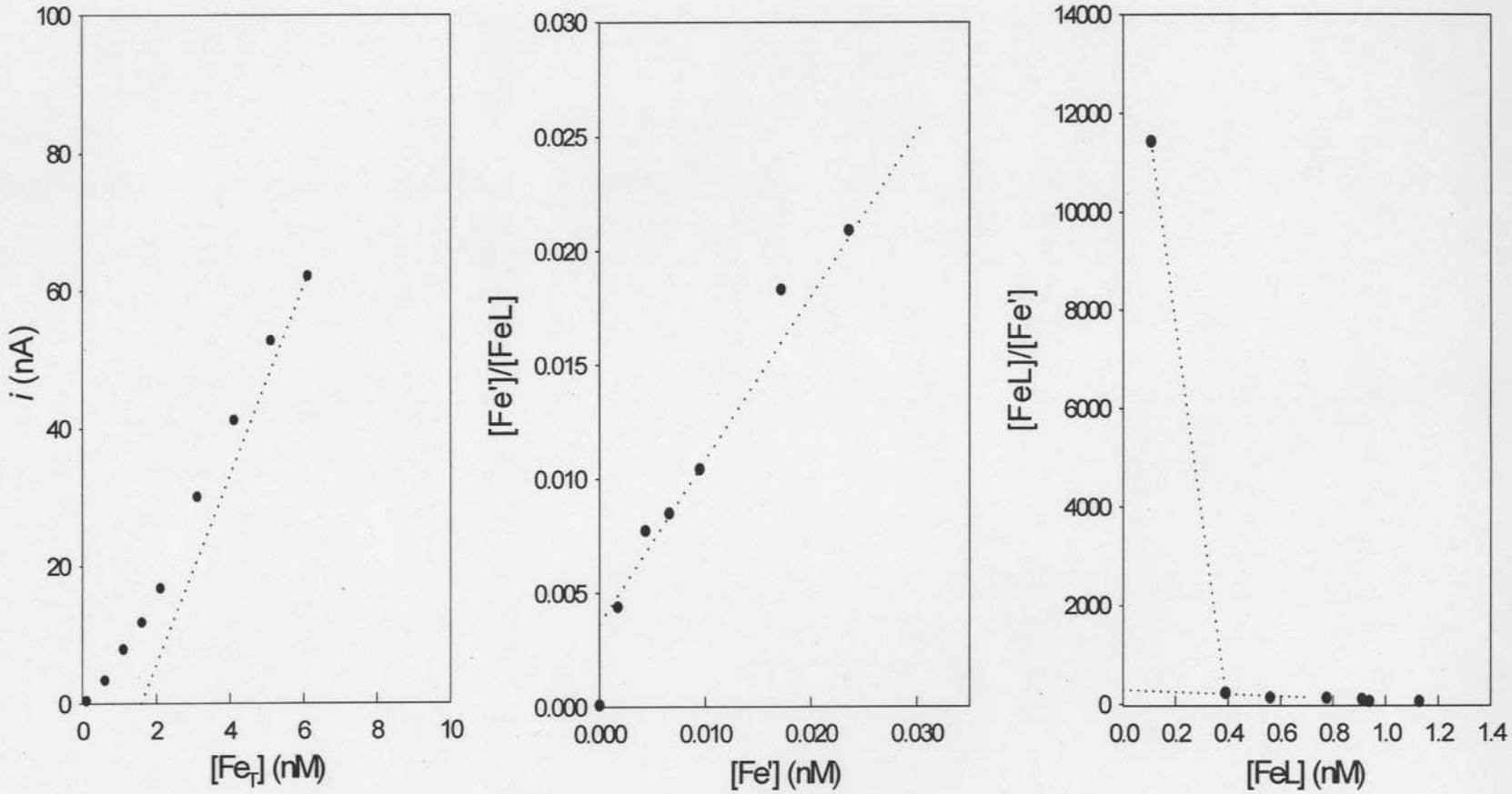

Fig. 15. a) CLE-CSV Fe titration of a 20 m surface sample from P26. Dashed line depicts slope used to calculate sensitivity. b) Langmuir transformation of the 20 m sample. The slope of the dashed line represents $1/[L_T]$. c) Scatchard transformation of the 20 m sample. The two dashed lines are the contributions from the strong and weak ligand classes.

Table 5. Organically bound and inorganic iron concentrations.

Station	Depth (m)	[FeL]/[Fe′]	[Fe′] (pM)	[FeL] (nM)
August:				
P12	40	120	0.41	0.05
	800	1170	0.36	0.42
P16	20	252	0.53	0.13
	75	16	1.1	0.02
	200	7349	0.03	0.25
P20	20	319	0.27	0.09
	800*	35	4.9	0.17
P26	20	11437	0.009	0.11
	50	2	0.61	0.001
	100*	75	3.3	0.246
	200	48	2.1	0.10
	800*	126	3.7	0.46
February:				
P26	40*	63	5.6	0.36
	200	1533	0.18	0.27
	600	14	4.4	0.06

Fe concentrations are given in Table 5. The depths marked with an asterisk in Table 5 indicate that the first titration point with no Fe added resulted in negative inorganic and organically bound Fe concentrations. The values from the first Fe addition were used for these depths and thus the $[FeL]/[Fe']$ may be underestimated by an order of magnitude, based on titration data from other depths. Upon examination of the variations in $[FeL]/[Fe']$ between the no-Fe added and first addition shows that often the order of magnitude for these two titration points are equivalent (see Appendix B). Although titrations were performed on samples from P4 during both the winter and summer cruises, the resulting curves exhibited excessive scatter which hindered the unambiguous calculations of concentrations and stability constants. Note that for the samples where more than one ligand class was detected, in most cases the sum of the concentrations of L_1 and L_2 was much higher than the corresponding $[L_T]$. This may be a result of the calculated $[L_T]$ being essentially an average of the two ligand classes as its concentration is always greater than $[L_1]$ but less than $[L_2]$.

The $[L_T]$ (Table 3) remains relatively constant along Line P in the summer, ranging from 0.43 to 1.51 nM. Conditional stability constants range from 8.3×10^{10} to 5.6×10^{12} and stronger ligands appear to be found closer to the coast. There is no consistent trend in how the concentration varies with depth. For surface samples (above 100 m), the highest total ligand concentration is seen at P26. At depths 100 m and below, ligand concentrations decrease with distance away from land, dropping from 1.21 nM at P12 (800 m), to 0.57 nM at P26.

At P26 in the winter, the total ligand concentration at 40m is lower than at depths 100 m and deeper. In the summer, the situation is reversed and the highest concentration

is found at 20m and a decrease with depth is evident. Deep water concentrations in the winter roughly double those of the summer while surface concentrations in the summer are about twofold greater than those of the winter. The conditional stability constants remain within the same order of magnitude for both winter and summer.

From the Scatchard transformations, L_1 is consistently lower in concentration and possesses a conditional stability constant at least an order of magnitude greater than L_2 (Table 3). The concentrations of the two ligand classes show little variation except at P26 at a depth of 50m where the amounts of both ligands are significantly higher.

3.5.0 Discussion

3.5.1 Iron limitation in the oceans

In coastal regions, primary productivity is typically limited by rapid depletion of nitrate during algal blooms during which the supply of macronutrients supply to surface waters is insufficient to match the biological demand. In regions such as the Southern, equatorial Pacific and northeast Pacific, a gradient in nitrate concentration exists, extending from inshore waters out to large-scale oceanic basins where excess nitrate can be observed in the surface waters of these HNLC regions. In the subarctic northeast Pacific, excess surface nitrate coincides with exceedingly low dissolved Fe concentrations (Fig. 16a) and shipboard incubation studies have revealed physiological adaptations within the resident phytoplankton community that support the hypothesis that the availability of dissolved Fe limits phytoplankton growth rates and controls the

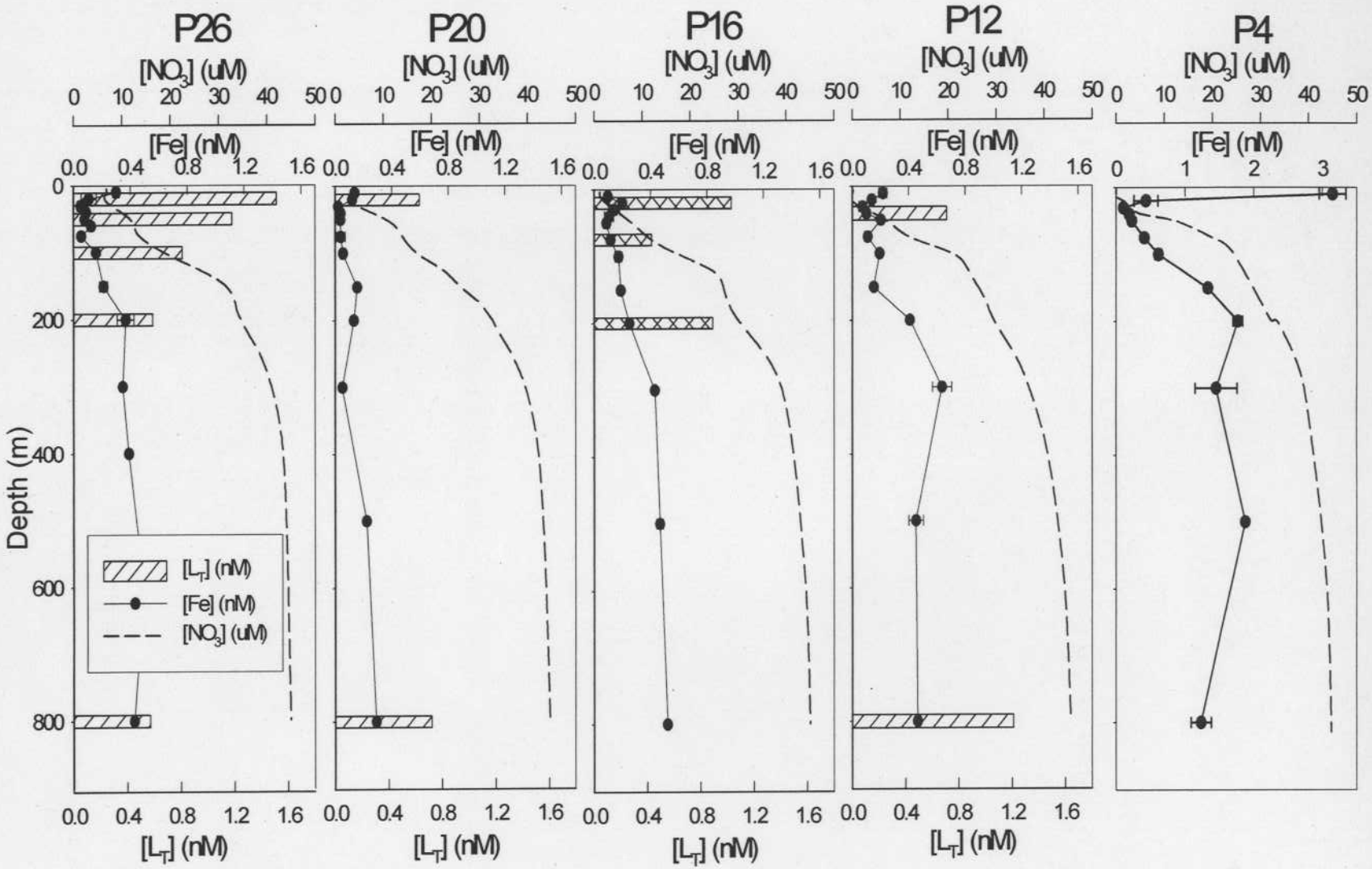

Figure 16a. Plots of total ligand concentration, dissolved nitrate, and total dissolved Fe along Line P. Distance from coast increases from right to left.

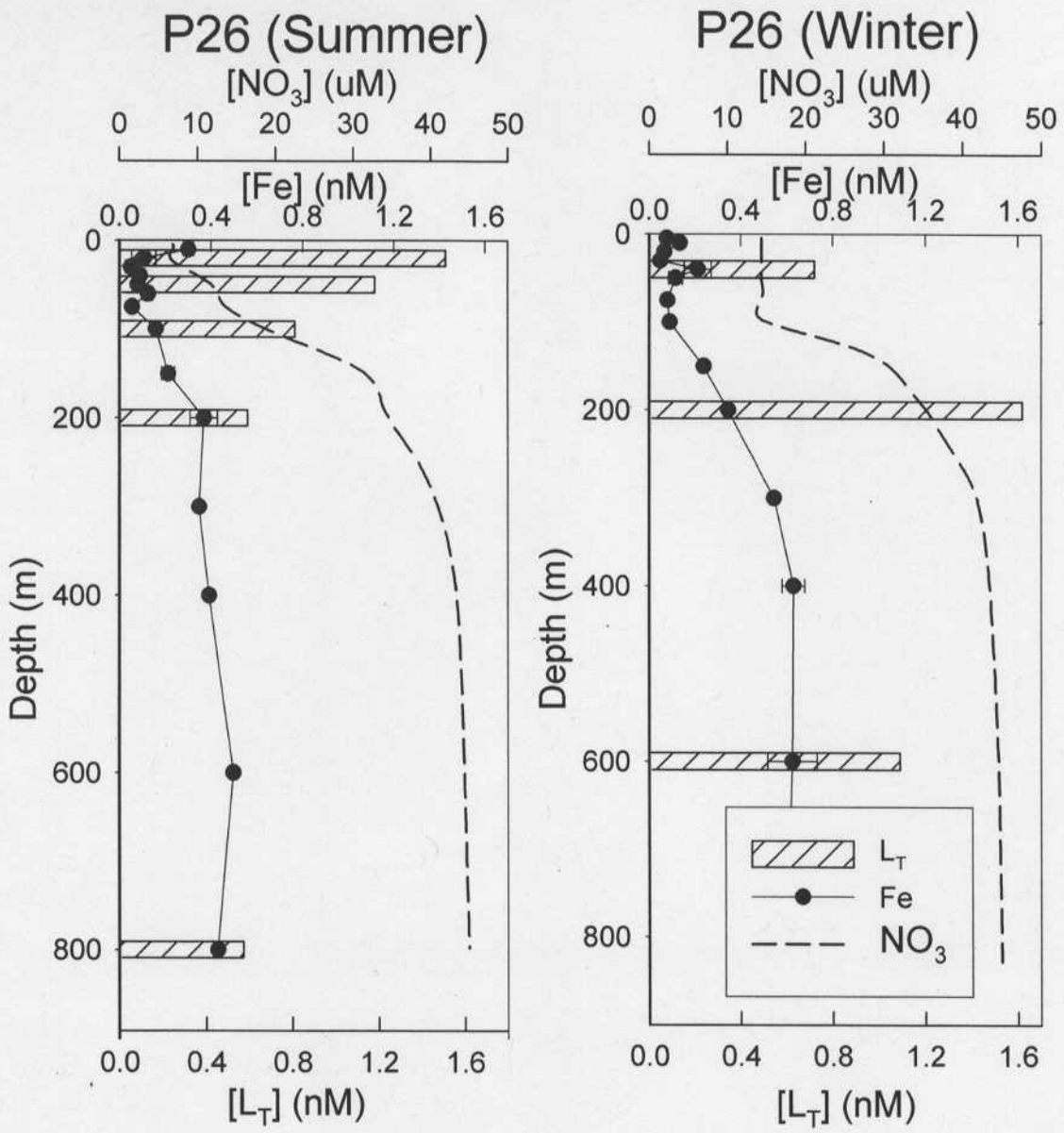

Figure 16b. Plots of total ligand concentration, dissolved nitrate, and total dissolved Fe at P26 during summer (left) and winter (right).

community composition of the primary producers (Maldonado and Price, 1999; LaRoche et al., 1996).

The results of various Fe fertilization experiments confirm that phytoplankton in HNLC waters respond to the *in situ* addition of Fe (Boyd et al., 2000; Coale, 1996; Martin et al., 1994; Tsuda et al., 2003). This biological response is dependent on the chemical speciation of Fe in seawater, rather than on Fe concentration, and it is the speciation of Fe that ultimately controls the structure of the phytoplankton community (Hutchins et al., 1999b). Although the exact function and fate of natural Fe chelators is uncertain, there is evidence that these ligands are both produced (Gledhill et al., 2004; Reid et al., 1993; Trick et al., 1983) and used by marine organisms (Maldonado and Price, 1999), suggesting a role in regulating the bioavailability of Fe. In this study, our goal was to investigate the distribution of dissolved Fe in waters of the northeast subarctic Pacific, and then to characterize Fe speciation from Fe-replete, nitrate-limited coastal waters, out to an Fe-limited HNLC area.

3.5.2 Results of CLE Titrations

Organic, Fe-complexing ligands are found throughout the water column, consistently at concentrations greater than the total dissolved Fe concentrations as illustrated in Fig. 16. As well, the presence of more than one ligand class can only be distinguished within the upper 200 m of the water profile (Table 3). This may be a consequence of the analytical limit of detection or a restriction of the stronger Fe-binding classes to the mixed layer. Below the mixed layer, there may still be more than one class

of ligand but either the ligands are too weak or too low in concentration to be measured by this method.

Profiles of dissolved nitrate, total dissolved Fe, and total dissolved ligand have been plotted together for comparison in Fig. 16. In surface waters along Line P during the summer, with the exception of P20, it appears that there is an increase in total ligand concentration with distance from shore with significantly higher concentrations at P26 (Fig. 16a). The location of the nearby Haida Eddy potentially transporting a large volume of coastal water into the Gulf of Alaska (Whitney and Robert, 2002) may be the cause behind the low surface ligand concentration at P20. In February, total ligand concentration at 40 m depth is lower than summer levels which (Fig. 16b), along with lower chlorophyll levels in winter, implies a biological origin for these Fe-binding ligands. Coincident with the high surface total ligand concentrations at P26 is a ratio of organically bound to total inorganic Fe at 20 m depth that is two orders of magnitude greater than surface [FeL]/[Fe′] at any other station. Data from Table 5 have been graphically illustrated in Fig. 17 and it can be observed that total dissolved inorganic Fe is very low at P26, at a concentration of 0.009 pM at 20 m, much lower than [Fe′] at the preceding stations. This form of Fe is generally considered labile and is preferentially taken up by phytoplankton (Maldonado and Price, 1999) and the decrease in [Fe′] seawards is indicative of increasing levels of Fe-limitation leading to the increasingly inefficient utilization of surface water nitrate from P4 to P26. In winter, surface [Fe′] at P26 is the highest, suggesting a greater supply of inorganic Fe possibly by greater wind mixing of Fe-rich waters from the nutricline or from increased atmospheric deposition. In comparison to [Fe′], the variation in [FeL] along Line P is much less significant,

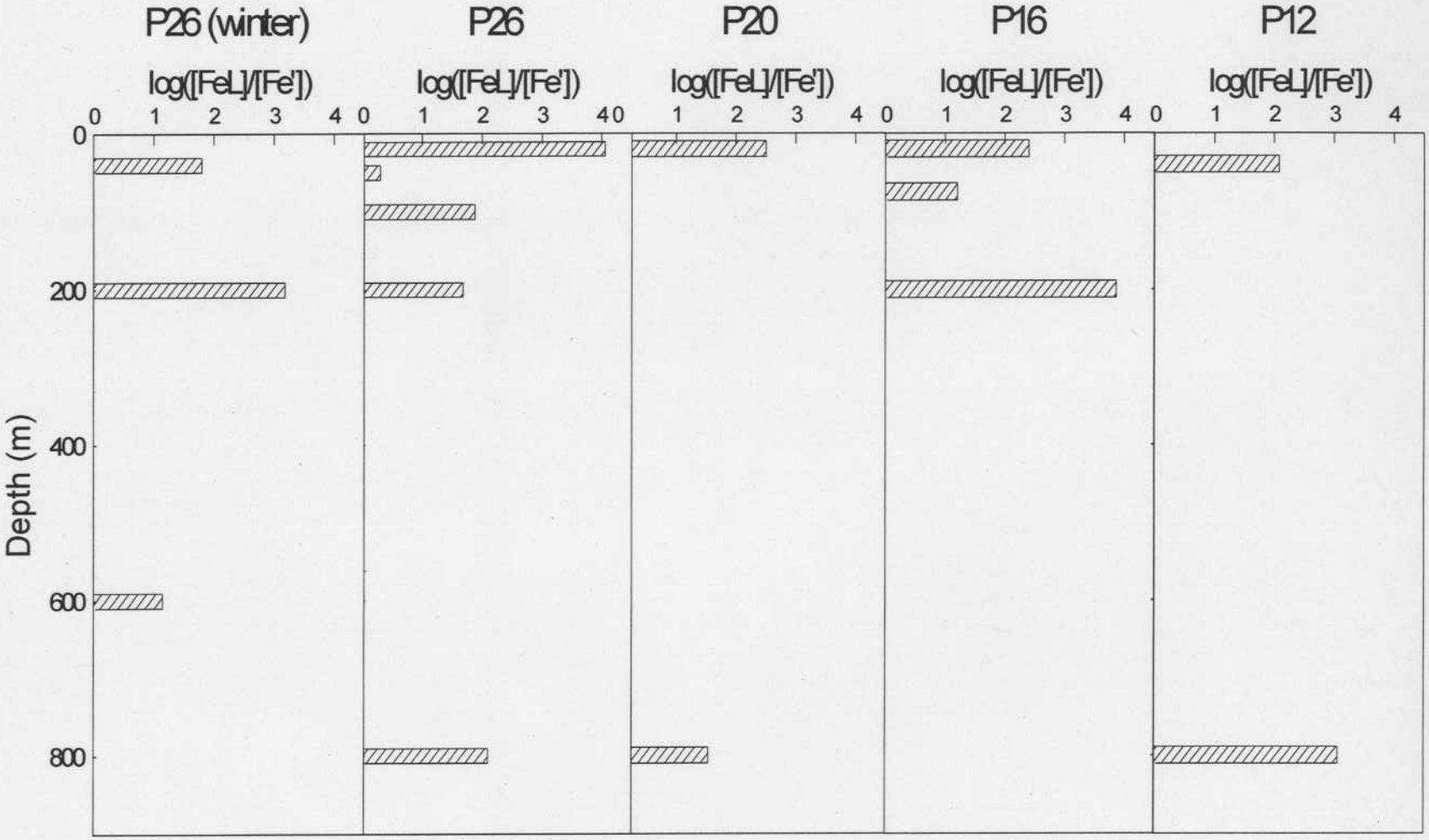

Figure 17. Ratio of organically bound Fe to total inorganic Fe from P12 (closest to coast) to P26 (furthest offshore) during August. The plot at the far left is of station P26 in February. Note the log scale along the x-axis.

suggesting that organically complexed Fe may be less reactive and has a longer residence time in surface waters of the subarctic Pacific.

Similar work performed in the both the Pacific and Atlantic Oceans demonstrates conditional stability constants for the Fe-ligand complexes of 10^{11} to 10^{14} with respect to Fe' (Gledhill and van den Berg, 1994; Powell and Donat, 2001; van den Berg, 1995; Wu and Luther III, 1995). Like this study, ligand concentrations were found to consistently exceed that of dissolved Fe. In addition, Rue and Bruland (1995) detected the presence of two ligand classes in surface waters of the central north Pacific. The average conditional stability constant with respect to *Fe'* of the stronger ligand was calculated to be $1.2 \times 10^{13} M^{-1}$, which is very close to our value of 1.4×10^{13} M^{-1}.

3.5.3 Biological availability of iron along Line P

The concentration of free inorganic Fe (Fe^{3+}) in seawater is not sufficient to meet the metabolic needs of phytoplankton (Maldonado and Price, 1999). It seems probable that the release of organic Fe chelators by organisms is a survival strategy to increase the dissolved Fe pool but the current data on whether the organically bound Fe is available for acquisition by phytoplankton is quite limited. Maldonado and Price (1999) investigated the utilization of Fe-siderophore complexes by autotrophic and heterotrophic plankton along Line P and found, surprisingly, that Fe uptake rates during the summer were consistently representative of Fe-stress across the transect, suggesting that Fe limitation occurs even in coastal waters where dissolved Fe concentrations are high. In our study, the proportion of organically bound Fe versus inorganic Fe, as well as total ligand concentration, were both found to increase seawards, coincident with increasing

levels of Fe-limitation. One explanation that may reconcile these ostensibly conflicting results is the role of size fractionation in dictating the availability of Fe for both biological consumption and ligand exchange. Colloidal Fe is much less readily taken up by phytoplankton than soluble Fe due to diameter-dependent limitations on the diffusion of large particles to cell surfaces (Wu et al., 2001) and the colloidal size class of Fe is known to be greatest in the coastal stations P4 and P12 along Line P (Nishioka et al., 2001), which suggests that size fractionation may restrict the availability of Fe to phytoplankton in coastal waters. Recent CLE-CSV experiments conducted on Atlantic seawater samples indicate 40 to 100% of colloidal Fe is present in the form of complexes, such as Fe oxides, that are inert to ligand exchange (Cullen et al., 2005). Thus despite high concentrations of total dissolved Fe and Fe' inshore, if a large portion of the Fe is in an inert, colloidal form, then it is feasible that phytoplankton may indeed experience Fe-stress in the coastal stations of Line P. Future work investigating thermodynamic partitioning of soluble and colloidal Fe along Line P will be invaluable towards understanding the bioavailability of Fe in this region.

3.5.4 Sources and sinks of naturally occurring ligands

Although the structure and identity of these organic Fe-binding ligands is still unknown, their conditional stability constants with respect to Fe', are very similar to those of siderophores. A variety of siderophores have been documented to be released by bacterioplankton under Fe deficient conditions (Gledhill et al., 2004) with conditional stability constants for inorganic Fe complexes of $10^{10.7}$ for Alterobactin A (Reid et al., 1993) to $10^{16.5}$ for desferal (Rue and Bruland, 1995) which are similar to the range of

values that have been calculated for FeL complexes detected by CLE-CSV in seawater. Studies have also shown potential ligand sources from photochemically mediated reactions in surface waters (Barbeau et al., 2001) and the potential for atmospheric deposition to provide Fe-binding ligands has yet to be explored. All these mechanisms by which organic Fe chelators may be introduced to the oceans occur within the upper water column and the presence of ligands along Line P below surface waters at concentrations less than the corresponding concentrations of Fe suggests that the occurrence of these ligands at depth is not facilitated by the same method of production in surface waters but instead originates from overlying waters. An Fe speciation study in the Arabian Sea (Witter et al., 2000) found that total ligand concentrations increased from the surface down to the oxygen minimum zone, pointing to organic matter degradation as a source of Fe-binding ligands. The deep ocean may then act as a source of organic Fe-binding ligands that may help to maintain dissolved Fe concentrations in the ocean interior that exceed thermodynamic solubility concentrations.

3.6.0 Conclusions

The concentrations and conditional stability constants of FeL complexes reported here from the subarctic northeast Pacific are similar to values reported by others across a range of ocean regimes. The ratio of [FeL]/[Fe'] increases offshore, indicating that Fe is more organically complexed in the HNLC waters. Whether or not this is the consequence of increased ligand production in response to Fe-stress by microbes is unclear but merits further study. Recent observations (Maldonado and Price, 1999) of Fe-stressed phytoplankton, even at the inshore P4 station indicates that while total

dissolved Fe and Fe' concentrations are higher some portion of these pools may be present in a less biologically available, perhaps colloidal, form. Results reported here help to support this observation insofar as total dissolved Fe and Fe' concentrations are higher but some portion of these pools may be present in a less biologically available, perhaps colloidal, form.

3.7.0 References

Anderson M. A. and Morel F. M. M. (1982) The influence of aqueous iron chemistry on the uptake of iron by the coastal diatom *Thalassiosira weissflogii*. *Limnology and Oceanography* **27**(5), 789-813.

Barbeau, K., Rue, E.L., Bruland, K.W., Butler, A. (2001) Photochemical cycling of iron in the surface ocean mediated by microbial iron(III)-binding ligands. *Nature* **413**, 409-413.

Borer P. M., Sulzberger B., Reichard P., and Kraemer S. M. (2005) Effect of siderophores on the light-induced dissolution of colloidal iron (III) hydroxides. *Marine Chemistry* **93**(2-4), 179-193.

Boyd P. W., Watson A. J., Law C. S., Edward R. A., Trull T., Murdoch R., Bakker D. C. E., Bowie A. R., Buesseler K. O., and Chang H. (2000) A mesoscale phytoplankton bloom in the polar Southern Ocean stimulated by iron fertilization. *Nature* **407**, 695-702.

Boye M. and van den Berg C. M. G. (2000) Iron availability and the release of iron-complexing ligands by Emiliania huxleyi. *Marine Chemistry* **70**, 277-287.

Bruland K. W. (1989) Complexation of zinc by natural organic ligands in the central North Pacific. *Limnology and Oceanography* **34**(2), 269-285.

Bruland K. W. (1992) Complexation of cadmium by natural organic ligands in the central North Pacific. *Limnology and Oceanography* **37**(5), 1008-1017.

Butler A. (1998) Acquisition and utilization of transition metal ions by marine organisms. *Science* **281**, 207-210.

Coale K. H. and Bruland K. W. (1988) Copper complexation in the Northeast Pacific. *Limnology and Oceanography* **33**(5), 1084-1101.

Coale K. H., et al. (1996) A massive phytoplankton bloom induced by an ecosystem-scale iron fertilization experiment in the equatorial Pacific Ocean. *Nature* **383**, 495-501.

Croot P. L. and Johansson M. (2000) Determination of iron speciation by cathodic stripping voltammetry in seawater using the competing ligand 2-(2-Thiazolylazo)-p-cresol (TAC). *Electroanalysis* **12**(8), 565-576.

Cullen J. T., Bergquist B. A., and Moffett J. W. (2005) Thermodynamic characterization of the partitioning of iron between soluble and colloidal species in the Atlantic Ocean. *Marine Chemistry* **98**(2-4), 295-303..

Duce R. A. and Tindale N. W. (1991) Atmospheric transport of iron and its deposition in the ocean. *Limnology and Oceanography* **36**(8), 1715-1726.

Gledhill M., McCormack P., Ussher S., Achterberg E. P., Mantoura R. F. C., and Worsfold P. J. (2004) Production of siderophore type chelates by mixed bacterioplankton populations in nutrient enriched seawater incubations. *Marine Chemistry* **88**, 75-83.

Gledhill M. and van den Berg C. M. G. (1994) Determination of complexation of iron(III) with natural organic complexing ligands in seawater using cathodic stripping voltammetry. *Marine Chemistry* **47**, 41-54.

Hutchins D. A., Franck V. M., Brzezinski M. A., and Bruland K. W. (1999a) Inducing phytoplankton iron limitation in iron-replete coastal waters with a strong chelating ligand. *Limnology and Oceanography* **44**, 1009-1018.

Hutchins D. A., Witter A. E., Butler A., and Luther G. W. I. (1999b) Competition among marine phytoplankton for different chelated iron species. *Nature* **400**, 858-861.

Johnson W. K., Miller L. A., Sutherland N. E., and Wong C. S. (2004) Iron transport by mesoscale Haida eddies in the Gulf of Alaska. *Deep-Sea Research Part II* **52**(7-8), 933-953.

Kuma K., Nishioka J., and Matsunaga K. (1996) Controls on iron (III) hydroxide solubility in seawater: The influence of pH and natural organic chelators. *Limnology and Oceanography* **41**(3), 396-407.

LaRoche, J., P. W. Boyd, R. M. L. McKay, and R. J. Geider. 1996. Flavodoxin as a *in situ* marker for iron stress in phytoplankton. *Nature* **382,** 802-805.

Maldonado M. T. and Price N. M. (1999) Utilization of iron bound to strong organic ligands by plankton communities in the subarctic Pacific Ocean. *Deep-Sea Research II* **46**, 2447-2473.

Martin J. H., et al. (1994) Testing the iron hypothesis in ecosystems of the equatorial Pacific Ocean. *Nature* **371**, 123-129.

Martin J. H. and Gordon R. M. (1988) Northeast Pacific iron distributions in relation to phytoplankton productivity. *Deep-Sea Research* **35**(2), 177-196.

Martin J. H., Gordon R. M., Fitzwater S., and Broenkow W. W. (1989) VERTEX: phytoplankton/iron studies in the Gulf of Alaska. *Deep-Sea Research* **36**(5), 649-680.

Moffett J. W. (2001) Transformations among different forms of iron in the ocean. In *The Biogeochemistry of Iron in Seawater* (ed. D. R. Turner and K. A. Hunter), pp. 343-369. John Wiley & Sons Ltd.

Nishioka J., Takeda S., Wong C. S., and Johnson W. K. (2001) Size-fractionated iron concentrations in the northeast Pacific Ocean: distribution of soluble and small colloidal iron. *Marine Chemistry* **74**, 157-179.

Obata H. and van den Berg C. M. G. (2001) Determination of picomolar levels of iron in seawater using catalytic cathodic stripping voltammetry. *Analytical Chemistry* **73**, 2522-2528.

Powell R. T. and Donat J. R. (2001) Organic complexation and speciation of iron in the South and Equatorial Atlantic. *Deep-Sea Research II* **48**, 2877-2893.

Reid R. T. and Butler A. (1991) Investigation of the mechanism of iron acquisition by the marine bacterium Alteromonas luteoviolaceus: Characterization of siderophore production. *Limnology and Oceanography* **36**(8), 1783-1792.

Reid R. T., Live D. H., Faulkner D. J., and Butler A. (1993) A siderophore from a marine bacterium with an exceptional ferric ion stability constant. *Nature* **366**, 455-457.

Rich H. W. and Morel F. M. M. (1990) Availability of well-defined iron colloids to the marine diatom.

Rue E. L. and Bruland K. W. (1995) Complexation of iron(III) by natural organic ligands in the Central North Pacific as determined by a new competitive ligand equiligration/adsorptive cathodic stripping voltammetric method. *Marine Chemistry* **50**, 117-138.

Ruzic I. (1982) Theoretical aspects of the direct titration of natural waters and its information yield for trace metal speciation. *Analytica Chimica Acta* **140**, 99-113.

Trick C. G., Anderson R. J., Price N. M., Gillam A., and Harrison P. J. (1983) Examination of hydroxamate-siderophore production by neritic eukaryotic marine phytoplankton. *Marine Biology* **75**, 9-17.

Tsuda A., Takeda S., Saito H., Nishioka J., Nojiri Y., Kudo I., Kiyosawa H., Shiomoto A., Imai K., Ono t., Shimamoto A., Tsumune D., Yoshimura T., Aono T., Hinuma A., Kinugasa M., Suzuki K., Shorin Y., Noiri Y., Tani H., Deguchi Y., Tsurushima N., Ogawa H., Fukami K., Kuma K., and Saino T. (2003) A mesoscale iron enrichment in the western subarctic Pacific induces a large centric diatom bloom. *Science* **300**, 958-961.

van den Berg C. M. G. (1995) Evidence for organic complexation of iron in seawater. *Marine Chemistry* **50**, 139-157.

van den Berg C. M. G. and Kramer J. R. (1979) Determination of complexing capacities of ligands in natural waters and conditional stability constants of the copper complexes by means of manganese dioxide. *Analytica Chimica Acta* **106**, 113-120.

Whitney F. A. and Robert M. (2002) Structure of Haida eddies and their transport of nutrient from coastal margins into the NE Pacific Ocean. *Journal of Oceanography* **58**, 715-723.

Witter A. E., Lewis B. L., and Luther G. W. I. (2000) Iron speciation in the Arabian Sea. *Deep-Sea Research II* **47**, 1517-1539.

Wu J., Boyle E., Sunda W., and Wen L.-S. (2001) Soluble and colloidal iron in the oligotrophic North Atlantic and North Pacific. *Science* **293**(5531), 847-849.

Wu J. and Luther III G. W. (1995) Complexation of Fe(III) by natural organic ligands in the Northwest Atlantic Ocean by a competitive ligand equilibration method and a kinetic approach. *Marine Chemistry* **50**, 159-177.

4.0 CHAPTER 4

Concluding Remarks

It is by no means a simple task to collect and measure dissolved Fe in seawater. The high risk of contamination associated with sample handling and analytical procedures as well as Fe's complex marine chemistry has certainly been a deterrent towards obtaining a high resolution data set of Fe distribution in the world ocean. Nevertheless, the implementation of Fe fertilization experiments has revealed Fe limitation in remote, but spatially expansive regions of the world ocean. Our understanding of marine Fe cycling has since progressed significantly owing in part to the development of standardized trace metal-clean techniques and improved ability to detect exceptionally low Fe concentrations in seawater.

There are still questions about the marine chemistry of Fe that remain unanswered or only partially resolved. The chemical speciation of Fe in seawater and which of these forms are accessible by organisms is poorly understood. While it is recognized that Fe is bound by naturally occurring organic ligands across a variety of oceanic regimes, the data is still sparse and the origins and structures of these chelators are not clear. In addition to its speciation, processes which supply Fe to the open ocean are poorly understood and their magnitudes are not well constrained. We have addressed the issues of Fe speciation and coastal distribution in the subarctic northeast Pacific by measuring dissolved Fe in both the Queen Charlotte Sound and out to the Gulf of Alaska and by determining the complexation of Fe by naturally occurring ligands along Line P.

4.1 Distribution of dissolved iron in Queen Charlotte Sound

Dissolved Fe in the benthic layer above continental shelf sediments is exceptionally high, up to 5.3±0.3 nM, and this Fe-rich layer of water is transported

offshore, remaining evident even in stations 40-50 km seaward of the shelf-slope break. The onshore-offshore gradient in Fe concentration confirms that waters within Queen Charlotte Sound have elevated levels of dissolved Fe relative to concentrations typical of the open ocean. The vertical profiles of dissolved Fe suggest the role of shelf sediments as the predominant source of Fe to this basin which enrich overlying waters by sediment resuspension (Johnson et al., 1999) or porewater diffusion (Elrod et al., 2004). The presence of an exceptionally broad continental shelf allows for large sediment loads to be deposited and confined within Queen Charlotte Sound.

The unique bathymetry and circulation of Queen Charlotte Sound draws attention to several different mechanisms that may aid in the offshore flow of this Fe-rich benthic layer. Tidal forcing may generate turbulent mixing of the bottom boundary layer in shelf waters. Depending on the direction of currents at depth along the shelf edge, this well-mixed layer may be transported downslope as a consequence of Ekman dynamics, or by wind-driven upwelling/downwelling along the coast. The annual formation of Haida eddies may also be an important path for the offshore advection of Fe (Johnson et al., 2005). The combined effects of these physical processes in Queen Charlotte Sound could present a more substantial supply of Fe to the HNLC Northeast Pacific than by eolian transport alone, perhaps serving to partially alleviate the Fe-stress typically experienced by resident phytoplankton populations (Maldonado and Price, 1999).

4.2 Iron speciation along Line P

Naturally occurring Fe-binding ligands were detected at 4 of the 5 sampled stations along Line P, exhibiting surface total ligand concentrations consistently in excess

of total dissolved Fe. The change from a nitrate to Fe-limiting regime is evident by the increasing offshore gradient in nitrate concentration and decrease in both total dissolved Fe and inorganic Fe along Line P. A comparison of surface ligand concentration and [FeL]/[Fe'] between winter and summer suggests a biological source of these chelators and the order of magnitude increase in the surface [FeL]/[Fe'] in the summer at P26 suggests a higher degree of organic complexation in HNLC, Fe-limited waters. While the sources and sinks of these ligands and the degree to which their Fe complexes are bioavailable remains uncertain, the similarity of the calculated conditional stability constants for the FeL complexes to those of known Fe-siderophore complexes indicates possible microbial ligand production under Fe-stress. Results from Maldonado and Price's (1999) examination of the biological uptake of organically complexed Fe along Line P may point to the presence of a fraction of the dissolved Fe associated with coastal waters existing in a less bioavailable form, perhaps as inert colloid species.

4.3 Future work

The conclusions drawn from both these studies are based on small data sets, and as a consequence, the trends observed from these measurements need to be confirmed by higher water column and spatial resolution. In Queen Charlotte Sound, little is known about the underlying physics and quantitative measurements of the circulation and cross-shelf advection in this region is needed. As well, tracking the flow of the benthic layer over the continental shelf and beyond the shelf-slope break will provide insight into how far offshore the high Fe concentrations carried by this water mass may persist. A continuation of CLE-CSV studies with a focus on variations in speciation from inshore to

offshore waters along continental shelf margins will help to identify the role of high affinity Fe-chelators in maintaining coastally derived Fe in a soluble, bioavailable form. Further investigations into the partitioning of naturally occurring organic ligands into colloidal and truly dissolved size classes in the subarctic northeast Pacific and the utilization of these size fractions by phytoplankton will greatly enhance our understanding of the marine biogeochemistry of Fe.

4.4 *References*

Boyle, E.A., Bergquist, B.A., Kayser, R.A. and Mahowald, N., 2004. Iron, manganese, and lead at Hawaii Ocean Time-series station ALOHA: Temporal variability and an intermediate water hydrothermal plume. Geochimica et Cosmochimica Acta, 69(4): 933-952.

Elrod, V.A., Berelson, W.M., Coale, K. and Johnson, K.S., 2004. The flux of iron from continental shelf sediments: A missing source for global budgets. Geophysical Research Letters, 31(L12307).

Johnson, K.S., Chavez, F.P. and Friederich, G.E., 1999. Continental-shelf sediment as a primary source of iron for coastal phytoplankton. Nature, 398: 697-700.

Johnson, W.K., Miller, L.A., Sutherland, N.E. and Wong, C.S., 2005. Iron transport by mesoscale Haida eddies in the Gulf of Alaska. Deep-Sea Research Part II, 52(7-8): 933-953.

Maldonado, M.T. and Price, N.M., 1999. Utilization of iron bound to strong organic ligands by plankton communities in the subarctic Pacific Ocean. Deep-Sea Research II, 46: 2447-2473.

Appendix A. Line P nutrient data.

Depth (m)	Nitrate (uM)	Phosphate (uM)	Silicate (uM)	Depth	Nitrate (uM)	Phosphate (uM)	Silicate (uM)
Winter:							
P4				**P26**			
5.4	13.7	1.29	22.5	4.7	14.4	1.38	18.5
10.7	13.7	1.29	22.5	11.6	14.4	1.37	18.5
24.4	12.9	1.23	20.4	25.7	14.4	1.38	18.5
49.8	9.6	1.03	13.1	50.6	14.4	1.38	18.5
77.4	12.3	1.22	17.3	74.7	14.4	1.38	18.7
103.6	18.6	1.64	25.7	98.5	14.6	1.39	18.6
123	26.6	2.08	32.4	123.5	24.1	1.92	35.1
153.9	29.3	2.2	37.3	149.2	30.5	2.27	48.3
176.1	30.5	2.27	40.7	175	33.2	2.44	55.2
200.9	30.8	2.24	43.6	202.8	35.7	2.61	62.5
247.5				250.9	39.1	2.81	71.6
299.8	35.9	2.6	58.4	300.6	41.9	2.97	80.1
398.6	39.3	2.87	73.3	402.6	43.5	3.14	94.6
599	43.4	3.14	99.2	598.9	44.6	3.24	115.6
802.4	44.5	3.32	117.3	828	45	3.28	134
801.5	44.7	3.32	117	999.9	45.4	3.29	145.7
997.8	44.9	3.32	134.7	1248.5	45.5	3.27	157.8
999.2	44.7	3.31	134.8	1500.7	45.1	3.24	167.1
1303.8	44.6	3.35	152.8	2001.5	43.2	3.1	174.3
				2499.9	41.5	2.96	176.4
				2998.5	39.9	2.83	175.1
				3501.1	38.7	2.75	173.5
				3999.7	37.9	2.7	173.4
				4310.6	37.8	2.67	174.5

Depth (m)	Nitrate (uM)	Phosphate (uM)	Silicate (uM)	Depth (m)	Nitrate (uM)	Phosphate (uM)	Silicate (uM)
Summer:							
P4				**P12**			
1.8	0	0.35	2.4	4.4	0.1	0.35	0.7
4.8	0	0.36	2.6	9.9	0.1	0.35	0.9
9.9	0	0.37	2	25	0.5	0.41	1.5
14.2	0.1	0.44	1.5	49.4	6.9	0.91	9.3
20.2	1.7	0.65	3.7	75.2	11.8	1.18	12.4
25.5	2.1	0.72	4.9	100.8	21	1.66	23.2
29.6	2.9	0.8	6.4	125	24.2	1.82	29.4
39.8	5.3	0.93	8.4	149.5	26.2	1.91	35
49.8	12.2	1.26	14	174.5	28.1	2.03	39.6
75.1	20	1.64	22	199.6	29.5	2.12	43.8
100.6	24.6	1.87	27.3	252.7	34	2.41	54.9
175.1	30.4	2.23	40.1	300.2	36.8	2.61	61.4
199.9	32.5	2.38	46.7	401.5	40.8	2.91	76.2
201	33.6	2.47	48.3	599.6	44.3	3.17	101.1
249.5	37	2.7	60.1	799.6	45.6	3.27	122.2
299.1	39.1	2.84	68	1000.3	46	3.31	137.3
399.6	41.1	3.02	80	1250.3	46	3.28	152.7
603.6	43.9	3.25	103.6	1250.6	46.2	3.29	152.9
799.3	44.7	3.31	117.6	1498.6	45.5	3.23	162.4
799.2	44.7	3.31	117.8	2001.7	43.5	3.08	174.6
1000.7	45	3.32	132.5	2502.2	42.1	2.95	177.7
1248.8	44.8	3.28	146.9	3001.7	40.8	2.88	178.6
1321.1	44.6	3.26	152.4	3256.4	40.8	2.88	178.9

Depth (m)	Nitrate (uM)	Phosphate (uM)	Silicate (uM)	Depth	Nitrate (uM)	Phosphate (uM)	Silicate (uM)
P16				**P20**			
3.9	1.2	0.52	3.2	4	4.2	0.66	2.9
10.2	1.3	0.53	3.2	9.9	4.1	0.65	2.9
24.5	3.3	0.66	8.3	25.3	3.8	0.57	1.6
50.5	8	0.99	11.3	50.1	10.7	1.18	11.6
75.5	12	1.2	13.2	74.8	14	1.35	15.8
99	18.2	1.55	21.5	100.5	17.1	1.52	21.4
124.1	25.2	1.92	33.6	125.5	22.5	1.8	31.9
149.9	27.1	2.01	38.9	150.1	26.1	1.96	39.5
175.2	28.4	2.1	43.5	174.8	30.2	2.22	50.1
201.1	30.7	2.24	50.6	199.5	32.7	2.37	57.1
249.6	36	2.58	63.5	249.2	36.6	2.64	68.3
301.1	39.3	2.81	72.9	301	4.3	0.66	2.9
400.5	41.7	2.97	86.5	400.3	42.3	3.01	92.3
599.1	44.2	3.18	109.1	599.5	4.3	0.67	3.1
799.2	45.1	3.25	129.4	799.9	44.7	3.21	132.1
1000.7	45.2	3.27	143.2	999.1	45.4	3.25	144.8
1249.6	45.6	3.26	156.2	1251	45.4	3.23	157.4
1499.5	45.2	3.21	164.9	1499.3	45.3	3.2	165.6
2000.8	43.2	3.06	174	2000.5	43.2	3.06	173.6
2499.6	41.6	2.94	176.3	2000.4	43.3	3.06	173.2
2499.9	41.5	2.94	176.5	2499.5	41.4	2.93	174.8
3001.5	40.2	2.84	175.9	2999.7	39.9	2.81	173.8
3501.2	39.2	2.77	176.7	3500.4	38.9	2.74	173.1
3674.4	39.4	2.77	177.4	4009.6	38.5	2.7	176.9

Depth (m)	Nitrate (uM)	Phosphate (uM)	Silicate (uM)	Depth	Nitrate (uM)	Phosphate (uM)	Silicate (uM)
P26							
4.9	6.8	0.88	8.7				
9.6	6.8	0.88	8.7				
24.4	6.9	0.88	11.4				
49.6	11.7	1.23	15.8				
73.4	13.4	1.31	16.9				
99.8	18.7	1.6	24.7				
124.3	25.6	1.98	38				
149	31.4	2.3	49.8				
174.9	33.5	2.43	57.3				
199.5	34.6	2.49	62.7				
248.7	38.4	2.74	74.5				
300.8	41	2.9	83.3				
399.9	43.4	3.09	97.1				
599.9	44.4	3.15	116				
798.2	45	3.21	131.9				
999.7	45.3	3.23	144.7				
1249.6	45.8	3.24	156.5				
1498.7	45.2	3.2	164.5				
2000.5	43.5	3.07	172.9				
2497.8	41.7	2.94	174.2				
3001.5	40	2.81	172.8				
3498	38.8	2.72	170.7				
3999.3	38.2	2.66	171				
4308.6	38.1	2.66	172.6				

Appendix B. Titration data

Cup	[Fe](nM) added	FeT (nM)	i (nA)	[FeTAC](nM)	[FeTAC] (corrected)	[Fe'](nM)	[FeL](nM)	[FeL]/[Fe']	[Fe']/[FeL]
P12 Summer									
40 m									
1	0	0.1	0.72	0.09	0.05	0.00041	0.049	120	0.0083
2	0.5	0.6	1.2	0.16	0.12	0.00095	0.48	509	0.0020
3	1	1.1	4.3	0.55	0.51	0.0040	0.59	146	0.0068
4	2	2.1	11.0	1.41	1.37	0.011	0.72	66	0.015
5	3	3.1	17.8	2.27	2.23	0.018	0.85	48	0.021
6	4	4.1	26.0	3.32	3.28	0.026	0.79	30	0.033
7	5	5.1	35.2	4.50	4.46	0.036	0.61	17	0.059
8	6	6.1	39.2	5.01	4.97	0.040	1.09	28	0.036
9	7	7.1	52.7	6.74	6.70	0.053	0.35	7	0.15
10	8	8.1	59.1	7.55	7.51	0.060	0.53	9	0.11
800 m									
1	0	0.5	0.53	0.08	0.04	0.00036	0.42	1173	0.00085
2	0.5	1.0	0.95	0.15	0.11	0.00090	0.85	943	0.0011
3	1	1.5	3.0	0.48	0.44	0.0035	1.02	288	0.0035
4	2	2.5	7.3	1.18	1.14	0.0091	1.31	144	0.0069
5	3	3.5	14.2	2.29	2.25	0.018	1.19	66	0.015
6	4	4.5	18.5	2.99	2.95	0.024	1.49	63	0.016
7	5	5.5	26.8	4.33	4.29	0.034	1.14	33	0.030
8	6	6.5	34.0	5.49	5.45	0.044	0.97	22	0.045
9	7	7.5	37.8	6.11	6.07	0.048	1.35	28	0.036
10	8	8.5	44.5	7.19	7.15	0.057	1.26	22	0.045

Cup	[Fe](nM) added	FeT (nM)	i (nA)	[FeTAC](nM)	[FeTAC] (corrected)	[Fe'](nM)	[FeL](nM)	[FeL]/[Fe']	[Fe']/[FeL]
P16 Summer									
20 m									
1	0	0.2	1.1	0.11	0.07	0.00053	0.13	252	0.0040
2	0.5	0.7	4.3	0.42	0.38	0.0030	0.32	105	0.0096
4	2	2.2	15.0	1.46	1.42	0.011	0.77	68	0.015
5	3	3.2	18.8	1.83	1.79	0.014	1.4	98	0.010
6	4	4.2	38.5	3.75	3.71	0.030	0.46	16	0.065
7	5	5.2	43.7	4.26	4.22	0.034	0.95	28	0.036
8	6	6.2	55.3	5.39	5.35	0.043	0.81	19	0.053
9	7	7.2	63.9	6.23	6.19	0.049	0.96	20	0.051
10	8	8.2	71.9	7.01	6.97	0.056	1.18	21	0.047
75 m									
1	0	0.1	1.4	0.14	0.10	0.0011	0.02	16	0.062
2	0.5	0.6	4.6	0.44	0.40	0.0035	0.21	61	0.016
3	1	1.1	8.9	0.86	0.82	0.0068	0.29	43	0.023
4	2	2.1	18.8	1.82	1.78	0.014	0.33	22	0.044
5	3	3.1	25.3	2.44	2.40	0.020	0.69	36	0.028
6	4	4.1	38.3	3.70	3.66	0.030	0.43	14	0.069
7	5	5.1	46.4	4.48	4.44	0.036	0.64	18	0.056
8	6	6.1	60.0	5.80	5.76	0.046	0.31	7	0.15
9	7	7.1	68.7	6.64	6.60	0.053	0.47	9	0.11
10	8	8.1	77.4	7.48	7.44	0.060	0.62	10	0.10
200 m									
1	0	0.3	0.45	0.04	0.004	0.00003	0.25	7344	0.0001

Cup	[Fe](nM) added	FeT (nM)	i (nA)	[FeTAC](nM)	[FeTAC] (corrected)	[Fe'](nM)	[FeL](nM)	[FeL]/[Fe']	[Fe']/[FeL]
2	0.5	0.8	3.1	0.31	0.27	0.0021	0.48	228	0.0044
3	1	1.3	6.25	0.62	0.58	0.0046	0.67	146	0.0068
4	2	2.3	15.1	1.49	1.45	0.012	0.79	69	0.015
5	3	3.3	24.7	2.43	2.39	0.019	0.84	44	0.023
6	4	4.3	33.8	3.33	3.29	0.026	0.94	36	0.028
7	5	5.3	45.5	4.48	4.44	0.035	0.78	22	0.046
8	6	6.3	52.8	5.20	5.16	0.041	1.05	26	0.039
9	7	7.3	66	6.50	6.46	0.052	0.74	14	0.069
10	8	8.3	73.9	7.27	7.23	0.058	0.96	17	0.060
P20 Summer									
20 m									
1	0	0.1	0.74	0.07	0.03	0.00027	0.09	319	0.0031
2	0.5	0.6	2.58	0.26	0.22	0.0018	0.40	228	0.0044
3	1	1.1	6.42	0.65	0.61	0.0048	0.51	106	0.0095
4	1.5	1.6	11.5	1.16	1.12	0.0089	0.50	56	0.018
5	2	2.1	14.6	1.47	1.43	0.011	0.68	60	0.017
6	3	3.1	25.2	2.54	2.50	0.020	0.61	30	0.033
7	4	4.1	35.3	3.55	3.51	0.028	0.58	21	0.048
8	5	5.1	43.6	4.39	4.35	0.035	0.74	21	0.047
9	6	6.1	55.1	5.54	5.50	0.044	0.57	13	0.077
10	8	8.1	71.6	7.20	7.16	0.057	0.90	16	0.063
800 m									
1	0	0.3	1.85	0.39	0.35	0.0028	-0.06	-21	-0.048
2	0.5	0.8	3.13	0.65	0.61	0.0049	0.17	35	0.028
3	1	1.3	4.48	0.94	0.90	0.0071	0.39	54	0.018

Cup	[Fe](nM) added	FeT (nM)	i (nA)	[FeTAC](nM)	[FeTAC] (corrected)	[Fe'](nM)	[FeL](nM)	[FeL]/[Fe']	[Fe']/[FeL]
4	1.5	1.8	7.02	1.47	1.43	0.011	0.35	31	0.032
5	2	2.3	8.5	1.77	1.73	0.014	0.54	39	0.026
6	3	3.3	11.8	2.46	2.42	0.019	0.85	44	0.023
7	4	4.3	17.4	3.63	3.59	0.029	0.67	23	0.043
8	5	5.3	22.5	4.70	4.66	0.037	0.60	16	0.062
9	6	6.3	27.1	5.66	5.62	0.045	0.63	14	0.071
10	8	8.3	30.2	6.30	6.26	0.050	1.98	40	0.025
P26 Summer									
20 m									
1	0	0.1	0.43	0.03	0.00	0.000009	0.11	11437	0.00009
2	0.5	0.6	3.38	0.24	0.21	0.0017	0.39	228	0.0044
3	1	1.1	7.9	0.57	0.54	0.0043	0.56	129	0.0077
4	1.5	1.6	11.8	0.86	0.83	0.0066	0.78	118	0.0085
5	2	2.1	16.8	1.22	1.19	0.0095	0.91	96	0.010
6	3	3.1	30.1	2.18	2.15	0.017	0.94	55	0.018
7	4	4.1	41.2	2.99	2.96	0.024	1.13	48	0.021
8	5	5.1	52.8	3.83	3.80	0.030	1.28	42	0.024
9	6	6.1	62.2	4.51	4.48	0.036	1.59	45	0.022
10	8	8.1	89.8	6.51	6.48	0.052	1.58	31	0.033
50 m									
1	0	0.1	1.8	0.13	0.08	0.0006	0.0013	2	0.49
2	0.5	0.6	4.7	0.32	0.27	0.0022	0.30	138	0.0072
3	1	1.1	9.8	0.68	0.63	0.0050	0.44	88	0.011
4	1.5	1.6	15.0	1.04	0.99	0.0079	0.58	74	0.014

Cup	[Fe](nM) added	FeT (nM)	i (nA)	[FeTAC](nM)	[FeTAC] (corrected)	[Fe'](nM)	[FeL](nM)	[FeL]/[Fe']	[Fe']/[FeL]
5	2	2.1	22.0	1.52	1.47	0.012	0.59	50	0.020
6	3	3.1	30.7	2.13	2.08	0.017	0.99	60	0.017
7	4	4.1	44.5	3.08	3.03	0.024	1.02	42	0.024
8	5	5.1	59.9	4.15	4.10	0.033	0.95	29	0.035
9	6	6.1	73.7	5.10	5.05	0.040	0.98	24	0.041
10	8	8.1	92.0	6.37	6.32	0.050	1.71	34	0.030
100 m									
1	0	0.2	2.8	0.25	0.21	0.002	-0.05	-31	-0.032
2	0.5	0.7	5.1	0.45	0.41	0.003	0.25	75	0.013
3	1	1.2	10.2	0.90	0.86	0.007	0.29	42	0.024
4	1.5	1.7	14.8	1.31	1.27	0.010	0.38	37	0.027
5	2	2.2	16.8	1.49	1.45	0.012	0.70	61	0.017
6	3	3.2	29.9	2.65	2.61	0.021	0.53	26	0.039
7	4	4.2	41.2	3.65	3.61	0.029	0.52	18	0.055
8	5	5.2	51.3	4.54	4.50	0.036	0.62	17	0.058
9	6	6.2	62.6	5.54	5.50	0.044	0.61	14	0.071
10	8	8.2	84.3	7.46	7.42	0.059	0.68	11	0.087
200 m									
1	0	0.4	2.2	0.30	0.26	0.0021	0.10	48	0.021
2	0.5	0.9	4.1	0.57	0.53	0.0042	0.34	80	0.013
3	1	1.4	7.6	1.05	1.01	0.0081	0.34	43	0.023
4	1.5	1.9	10.9	1.51	1.47	0.012	0.39	33	0.030
5	2	2.4	13.9	1.92	1.88	0.015	0.47	31	0.032
6	3	3.4	21.7	3.00	2.96	0.024	0.38	16	0.062
8	5	5.4	35.4	4.89	4.85	0.039	0.47	12	0.082

Cup	[Fe](nM) added	FeT (nM)	i (nA)	[FeTAC](nM)	[FeTAC] (corrected)	[Fe'](nM)	[FeL](nM)	[FeL]/[Fe']	[Fe']/[FeL]
9	6	6.4	42	5.81	5.77	0.046	0.55	12	0.083
10	8	8.4	58.0	8.02	7.98	0.064	0.33	5	0.20
800 m									
1	0	0.4	1.1	0.48	0.44	0.0035	-0.01	-4	-0.28
2	0.5	0.9	1.2	0.50	0.46	0.0037	0.46	126	0.0080
3	1	1.4	2.2	0.93	0.89	0.0071	0.53	75	0.013
4	1.5	1.9	2.9	1.20	1.16	0.0092	0.76	82	0.012
5	2	2.4	3.9	1.64	1.60	0.013	0.82	64	0.016
6	3	3.4	7.5	3.12	3.08	0.025	0.32	13	0.077
7	4	4.4	9.4	3.91	3.87	0.031	0.53	17	0.058
8	5	5.4	11.4	4.76	4.72	0.038	0.67	18	0.056
9	6	6.4	14.2	5.93	5.89	0.047	0.49	11	0.095
10	8	8.4	18.7	7.80	7.76	0.062	0.60	10	0.10
P26 Winter									
40 m									
1	0	0.1	25.8	0.45	0.13	0.0010	-0.06	-58	-0.017
3	1.1	1.1	59.5	1.03	0.71	0.0056	0.36	63	0.016
4	1.5	1.6	74.4	1.29	0.97	0.0078	0.59	76	0.013
5	2	2.1	86.2	1.50	1.18	0.0094	0.88	94	0.011
6	3	3.1	180	3.12	2.80	0.022	0.24	11	0.092
7	4	4.1	205	3.56	3.24	0.026	0.81	31	0.032
8	5	5.1	292	5.07	4.75	0.038	0.29	8	0.133
9	6	6.1	284	4.93	4.61	0.037	1.43	39	0.026
10	8	8.1	432	7.50	7.18	0.057	0.84	15	0.068

Cup	[Fe](nM) added	FeT (nM)	i (nA)	[FeTAC](nM)	[FeTAC] (corrected)	[Fe'](nM)	[FeL](nM)	[FeL]/[Fe']	[Fe']/[FeL]
200 m									
1	0	0.3	21.3	0.34	0.02	0.0002	0.27	1533	0.0007
2	0.5	0.8	42.8	0.69	0.37	0.0029	0.42	143	0.0070
3	1	1.3	80.9	1.30	0.98	0.0078	0.30	39	0.026
4	1.5	1.8	86.6	1.39	1.07	0.0085	0.71	83	0.012
5	2	2.3	119	1.91	1.59	0.013	0.69	54	0.018
6	3	3.3	161	2.58	2.26	0.018	1.01	56	0.018
7	4	4.3	221	3.55	3.23	0.026	1.04	40	0.025
8	5	5.3	256	4.11	3.79	0.030	1.47	49	0.021
9	6	6.3	322	5.17	4.85	0.039	1.40	36	0.028
10	8	8.3	517	8.30	7.98	0.064	0.25	4	0.26
600m									
1	0	0.6	47	0.87	0.55	0.0044	0.06	14	0.073
2	0.5	1.1	58.3	1.08	0.76	0.0061	0.35	57	0.017
3	1	1.6	61.3	1.14	0.82	0.0066	0.79	121	0.0083
4	1.5	2.1	98.3	1.83	1.51	0.012	0.60	50	0.020
5	2	2.6	111	2.07	1.75	0.014	0.86	62	0.016
6	3	3.6	151	2.81	2.49	0.020	1.11	56	0.018
7	4	4.6	173	3.22	2.90	0.023	1.70	73	0.014
8	5	5.6	275	5.12	4.80	0.038	0.78	20	0.049
9	6	6.6	330	6.14	5.82	0.047	0.75	16	0.062
10	8	8.6	412	7.67	7.35	0.059	1.21	21	0.048